Delft University of Technology

Technical and economic feasibility assessment of a Car Park as Power Plant offering frequency reserves

M.J. Poorte

TU Delft

Technical and economic feasibility assessment of a Car Park as Power Plant offering frequency reserves

by

M.J. Poorte

to obtain the degree of

Master of Science
in Mechanical Engineering

at the Delft University of Technology,
to be defended publicly on 26 October, 2017 at 14.00.

Student number:	4100778	
Project duration:	February 9, 2017 – October 26, 2017	
Thesis committee:	Prof. Dr. A. J. M. van Wijk	TU Delft, The Green Village
	Dr. C. B. Robledo	TU Delft, 3mE
	Dr. ir. R. A. C. van der Veen	TU Delft, TBM
	H.H.M. Mathijssen	TenneT
	Prof. ir. M. A. M. M. van der Meijden	TU Delft, TenneT

THE GREEN VILLAGE TU Delft TenneT Taking power further

“Life is like riding a bicycle. To keep your balance, you must keep moving.”

- Albert Einstein -

Preface

Before you lies the culmination of my thesis project. Eight months of research have led to this report and the results presented in it. I'm proud of presenting what I have done and want to thank all the people I have worked with over the past years for their implicit contribution to this research.

The story of this thesis project starts a little over one year ago. I had scheduled an appointment with professor van Wijk to discuss the possibility of doing research about future energy systems. After considering several topics and an optional collaboration with a research institute abroad, I came across an article about the need for new technologies that can offer reserves for frequency control. I thought: "If a car park of FCEV can operate as a power plant, can it also offer these reserves?". Professor van Wijk encouraged me to continue in this direction. Two weeks later, I had an appointment with Henrie Mathijssen, the manager of the department of system services at TenneT, and another two weeks later I started my graduation internship.

At the offset of the project, I immediately knew that this was a perfect fit although a complex and challenging research. My TBM graduate knowledge allowed me to quickly understand the mechanisms of the balancing market. The mechanical engineering master track has given me the tools and ability to understand the technical features of the system and come up with reasonable insights and solutions.

I would like to thank Ad for stimulating me to think about the bigger picture. Analysing future energy systems is not an easy task as it requires not only endless knowledge, but also courage to keep believing in your own ideas. I would like to thank Henrie, who forced me to evaluate my graduation process step by step and reflect not only on the content but also on how I experienced it as a person.

I would truly like to thank my supervisors at the TU Delft, Carla and Reinier, as well as my musketeers at TenneT, Jeroen, Samuel and Walter. They all gave me the freedom to develop my own research but were always prepared to discuss my findings and give feedback on my thesis. Their profound knowledge of the system, each approaching it from another perspective, gave me a solid backup when I needed it. Thank you!

Finally I would like to thank everyone else who helped me during the past months. It was a joyful and incredible learning experience. It was a period in which I met a lot of new and interesting people with whom I could discuss about the future energy systems but also about all the other systems in this world. Thanks for inspiring me and making this graduation period more fun.

M.J. (Michelle) Poorte
Delft, October 2017

Abstract

In the Netherlands the main sources of electricity are currently coal and gas fired power plants. Due to the increasing share of electricity that is produced from renewable energy sources, the operational hours of these conventional power plants are decreasing. However, these power plants are also the main source of frequency reserves, which are required to guarantee the stability of the electricity grid. Stability is maintained if there is a real time balance between the electricity production and consumption.

Due to the decreasing availability of conventional power plants, the possibility to offer frequency reserves with other power sources must be explored. A possible provider is the Car Park as Power Plant (CPPP). This is an aggregation of Fuel Cell Electric Vehicles (FCEV) parked in a car park and operating in Vehicle to Grid (V2G) mode. This thesis contains a technical and economic feasibility assessment of a Car Park as Power Plant offering frequency reserves in a future power system with a low share of conventional power plants.

The dynamics of the frequency was analysed considering the reduction of the operational hours of the conventional power plants. This causes the inertia in the system to decrease. As a consequence, this increases the rate of change of frequency (RoCoF). A high RoCoF makes the frequency react faster which will make it more feasible that the maximum instantaneous frequency deviation will be reached. When this maximum deviation is reached, the system enters the alert state, which could endanger the global security of the system.

To prevent the frequency from reaching the maximum instantaneous frequency deviation under conditions of a high RoCoF, the full activation time (FAT) of the frequency reserves could be reduced. The FAT is the maximum time between the moment that the signal for a change in power output is given and the actual moment that the required power output is reached. Reserves with a reduced FAT are referred to as fast frequency reserves.

By measuring the FAT of the FCEV in V2G mode with an experimental setup, it was tested if the FCEV could offer the fast frequency reserves. The FCEV appeared to be a suitable power source to offer fast frequency reserves. When the power output of the battery and the fuel cell are combined, an even higher power gradient and thus a shorter full activation time, can be obtained. However, improvements must be implemented in the V2G discharge unit and the energy management system of the FCEV to optimise the operation in V2G mode.

The economic feasibility of the CPPP as provider of frequency reserves was then analysed. The factor that has the highest impact, is the position of the CPPP on the bid ladder. Only when the price for frequency reserves is relatively high, the reserves of the CPPP will be activated. This is caused by the high price for hydrogen, which is the dominant factor in the marginal costs of the CPPP. Most of the time the prices for frequency reserves and for electricity sold on the spot market are lower than the marginal costs of the CPPP.

From a technical point of view the CPPP is a suitable power source to offer fast frequency reserve. The profitability of the CPPP is, however, strongly related to the occupation pattern of the car park and the price for frequency reserves. The occupation pattern can be influenced by the aggregator by giving incentives to the car owners, combining different car parks with deviating occupation patterns or by operating company car parks with, for example, autonomous driving cars. The price for frequency reserves is dependent on the quickly evolving market and can not be influenced by the aggregator of the

CPPP. The aggregator can influence the marginal costs of the CPPP. By adding relevant components to the system, like hydrogen production units or storage facilities, the aggregator can offer reserves with different power sources, which will have different marginal costs.

From the point of view of the transmission system operator, it could be possible to add an extra product for fast frequency reserves instead of changing the requirements of the existing reserves. This could have a positive effect on the profitability of the CPPP. The specific requirements such as the minimum bid size, validity period and payment mechanism for this product should be evaluated in further studies.

Contents

List of Figures

List of Tables

Nomenclature

Abbreviations

AC	**A**lternating **C**urrent
ACE	**A**rea **C**ontrol **E**rror
ACER	**A**gency for the **C**ooperation of **E**nergy **R**egulators
ACM	**A**utoriteit **C**onsument & **M**arkt
aFRR	**a**utomatic **F**requency **R**estoration **R**eserves
AS	**A**ncillary **S**ervices
BE	**B**ritish **E**urope
BL GL	**Bal**ancing **G**uide**l**ine
BOP	**B**alance **O**f **P**lant
BRP	**B**alance **R**esponsible **P**arties
BSP	**B**alancing **S**ervice **P**roviders
CaPP	**C**ar **a**s **P**ower **P**lant
CBS	**C**entraal **B**ureau **S**tatistiek
CE	**C**ontinental **E**urope
CHP	**C**ombined **H**eat and **P**ower
CPPP	**C**ar **P**ark as **P**ower **P**lant
CSD	**C**old **S**hut **D**own
DC	**D**irect **C**urrent
DoF	**D**egree **o**f **F**reedom
DSO	**D**istributed **S**ystem **O**perator
E-program	**E**nergy **program**
EMS	**E**nergy **M**anagement **S**ystem
ENTSO-e	**E**uropean **N**etwork of **T**ransmission **S**ystem **O**perators for **e**lectricity
EV	**E**lectric **V**ehicle
FAT	**F**ull **A**ctivation **T**ime
FC	**F**uel **C**ell

FCEV	**F**uel **C**ell **E**lectric **V**ehicle
FCR	**F**requency **C**ontainment **R**eserves
FRR	**F**requency **R**estoration **R**eserves
HHV	**H**igher **H**eating **V**alue
HVDC	**H**igh **V**tage **D**irect **C**urrent
IGCC	**I**nternational **G**rid **C**ooperation and **C**ontrol
IOP	**I**nformatie **O**verdracht **P**unt
IRE	**Ir**ish **E**urope
ISP	**I**mbalance **S**ettlement **P**eriod
LFC	**L**oad **F**requency **C**ontrol
LFC Area	**L**oad **F**requency **C**ontrol **Area**
LFC Block	**L**oad **F**requency **C**ontrol **Block**
LHV	**L**ower **H**eating **V**alue
mFRR	**m**anual **F**requency **R**estoration **R**eserves
NE	**N**orthern **E**urope
NPV	**N**et **P**resent **V**alue
PEMFC	**P**roton **E**exchange **M**embrane **F**uel **C**ell
RES	**R**enewable **E**nergy **S**ources
RoCoF	**R**ate **o**f **C**hange **o**f **F**reuqency
RR	**R**eplacement **R**eserves
RTU	**R**emote **T**erminal **U**nit
SA	**S**ynchronous **A**rea
SEP	**S**amenwerkende **E**lektriciteits-**P**roducenten
SO GL	**S**ystem **O**peration **G**uide**l**ine
SoC	**S**tate **o**f **C**harge
SRL	**S**elf-**R**eguating **L**oad
SS	**S**ystem **S**ervices
TSO	**T**ransmission **S**ystem **O**perator
TTW	**T**ank-**T**o-**W**heel
V2G	**V**ehicle to **G**rid
VRES	**V**ariable **R**enewable **E**nergy **S**ources

Symbols

$P_{FCR,ISP}$	Power output setting for FCR for a specific ISP
Δf	Frequency deviation
ΔP_{NL}	Power deviation in the Netherlands
$\eta_{CPPP,ISP}$	Efficiency of the car park for a specific ISP
λ_{Add}	Frequency bias by additional observed reaction
λ_{Auto}	Frequency bias by autocontrol of production
λ_{CE}	Frequency bias constant for Continental Europe
λ_{FCR}	Frequency bias caused by frequency containment reserves
λ_{NL}	Frequency bias constant for the Netherlands
λ_{SRL}	Frequency bias caused by self regulating load
π	Number phi
a, b	Empirically determined constants in the root equation
ACE_{NL}	Area control error in the Netherlands
C_{CPPP}	Yearly costs of the car park related to operations as power plant
$C_{d,ISP}$	Degradation costs for a specific ISP
C_{FC}	Capital costs per kW of the FC system of the car
C_{ic}	Investment costs
C_{NL}	Contribution coefficient of the Netherlands
$C_{oc,ISP}$	Operational costs for a specific ISP
$C_{pe,ISP}$	Costs of purchased energy for a specific ISP
CC_i	Capital costs of component i
CF_{year}	Yearly cash flow
$E_{\mathrm{H_2},ISP}$	Total amount of hydrogen required for a specific ISP
$E_{aFRR\downarrow,ISP}$	Maximum amount of electricity produced for delivery of aFRR down for a specific ISP
$E_{aFRR\uparrow,ISP}$	Maximum amount of electricity produced for delivery of aFRR up for a specific ISP
$E_{BL,ISP}$	Electricity produced as baseload for a specific ISP
$E_{FCR,ISP}$	Electricity produced for delivery of FCR for a specific ISP
E_{kin}	Kinetic energy
E_{NL}	Electricity production in the Netherlands
E_{SA}	Electricity production in the Synchronous Area

$E_{V2G,ISP}$	Total amount of electricity produced by the FCEV in V2G mode for a specific ISP
f_m	Rotating frequency
H	Inertia constant
H_{aFRR}	Transfer function of submodel of the automated frequency restoration reserves
H_{FCR}	Transfer function of submodel of the load frequency control
$H_{inertia}$	Effect of inertia
H_{SRL}	Transfer function of submodel of the self regulating load
$HHV_{\mathrm{H_2}}$	Higher heating value of hydrogen
$L_{h,driving}$	Lifetime of the FC system in driving mode
L_{peak}	Maximum system peak load
M	Total inertial response of the system
$m_{\mathrm{H_2},ISP}$	Hydrogen mass required for a specific ISP
$m_{\mathrm{H_2}}$	Hydrogen mass
$p_{\mathrm{H_2}}$	Hydrogen price
$p_{aFRR\downarrow,ISP}$	Price of aFRR down per ISP
$p_{aFRR\uparrow,ISP}$	Price of aFRR up per ISP
P_{aFRR}	Power required for aFRR
$P_{BL,ISP}$	Power output setting for the baseload for a specific ISP
P_{BL}	Power offered as baseload
$p_{e,ISP}$	Price of electricity per ISP of the spot market
$P_{FCEV,ISP}$	Average power output of a FCEV for a specific ISP
$p_{FCR,ISP}$	Price of FCR per ISP
$p_{FCR,ISP}$	Price of FCR per ISP
P_{FCR}	Power required for FCR
P_{idling}	Power output when FCEV is in idling condition
P_{ref}	Power of the reference incident
$P_{V2G,max}$	Maximum power output of the FCEV in V2G condition
P_{V2G}	Total power output of the FCEV in V2G condition
$R_{aFRR,ISP}$	Revenues for a specific ISP received by offering aFRR
$R_{aFRR,year}$	Yearly revenues received by offering aFRR
$R_{BL,ISP}$	Revenues for a specific ISP received by offering a baseload

$R_{BL,year}$	Yearly revenues received by offering a baseload
R_{CPPP}	Yearly revenues of the car park related to operations as power plant
$R_{FCR,ISP}$	Revenues for a specific ISP received by offering FCR
$R_{FCR,year}$	Yearly revenues received by offering FCR
S_B	Rated power
t_{ISP}	Time of one ISP
t_{PB}	Payback time

Units

ω	Rotational speed	[rad/s] or [rpm]
E	Energy	[Wh] or [J]
f	Frequency	[Hz]
J	Moment of inertia	[kg·m^2]
P	Power	[W]
t	Time	[s]

1

Introduction

When electricity was discovered, it was seen as nothing more than a scientific curiosity. It was experienced for the first time by rubbing fur on amber, which caused electricity by means of attraction [1]. It was only after the scientific revolution, more than 1000 years later, that scientists actually started constructing machines to create electricity and conduct simple experiments. The vast series of inventions and discoveries, such as Volta's Pile in 1800, the complete mathematical theory of electricity of Ohm in 1827, the demonstration of electromagnetic induction by Faraday in 1831, the invention of the direct current (DC) electric generator by Edison in 1870 and the alternating current (AC) motor by Tesla in 1880, made it possible to construct the vast public electricity supply chain that is known today [2].

Large share of the world's population can make use of electricity because of the presence of the electricity network. In developed countries, not only do end-users want to use electricity, they also demand that it is available at all times [3]. Moments of blackouts are not tolerated and the cost of electricity also needs to stay within acceptable margins [4]. The Transmission System Operator (TSO), which for the Netherlands is TenneT, is the operator of the electricity network and has the task to make sure that the required level of quality is maintained [5].

The services aimed at maintaining the desired quality of the electricity within the network are called system services (SS). These services are considered part of the electricity system and guarantee that all the users of the network can make use of a stable electricity flow. By users, not only consumers are intended, but all the utilities connected to the network. Some users can also contribute to the quality of the electricity and offer certain services. These services are ancillary to the operation of the electricity network. For this reason they are called ancillary services (AS) [6]. In Figure 1.1 the relation between the described services is shown. The arrows indicate the direction of the delivery of the service [7].

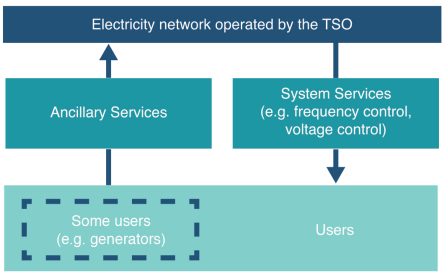

Figure 1.1: Some users can offer ancillary services that are bought by the TSO, who offers system services to all the users of the electricity network [6].

1.1. Problem statement

One of the requirements for a reliable electricity system, is the need for the production and consumption of power in the transmission network to be in balance at every point in time. The AS related to this task will be referred to as balancing services. The current market parties in the Netherlands that offer balancing services, called balancing service providers (BSP), are mostly conventional electricity producers or large consumers that can ramp up or down their production or consumption of electricity to restore the balance.

The electricity sector has however been characterised by fast changes and developments in the past years. Only a couple of decades ago, the concept of “Limits to Growth” was introduced by the Club of Rome [8]. This club announced the depletion of resources by 2100 in relation to the economic and population growth. At that time, the production portfolio for electricity was almost only constituted by conventional power plants, which released large amounts of greenhouse gasses in the atmosphere during operation. The limited availability, in combination with the polluting character of these conventional resources, was an incentive for many parties to take action.

In the following years, the awareness of the need for clean technologies to provide electricity has increased enormously. Nowadays, many countries are adopting policies that try to reduce the negative impact of conventional power plants and stimulate the development of renewable energy sources (RES) [9]. By signing the Paris agreement, also the Dutch government has announced the ambition to gradually reduce the amount of CO_2 emissions with 80-95% in 2050 compared to 1990 [10, 11]. This implies, amongst others, a shift in the methods used to produce electricity. The amount of emitted CO_2 must decrease which means that the emitted greenhouse gasses of conventional power plants must be reduced or their use will have to diminish significantly to reach the target. The current gas and coal fired power plants can not remain the main source of electricity production.

However, these power plants are also the main sources of balancing services. The market conditions already force them to frequently operate under must-run conditions, which leads to increasing costs of balancing services [12, 13]. Therefore, balancing services can no longer rely solely on conventional power plants. The decrease of operational hours of conventional power plants is accompanied by the increase of different renewable energy technologies that have less impact on the environment. There is a need to investigate their potential to contribute as BSP to guarantee the stability of the power system in the future.

1.2. Frequency control of the national electricity network

1.2.1. Stability of the power system

Power system stability is “the ability of an electric power system to remain in a state of operating equilibrium under normal operating conditions, and to regain a state of equilibrium after being subjected to a disturbance” [14]. This means that, in order to remain stable, the system must adjust itself to changing conditions. Due to the high complexity and interdependency of stability problems, any form of instability may not occur in its pure form [15, 16]. This makes it difficult to understand and deal with instability phenomena. For the ease of comprehension and analysis, three main categories of stability phenomena can be identified: voltage stability, rotor angle stability and frequency stability [17–20]. In this research the containment of frequency stability will be the main focus.

1.2.2. Frequency quality parameter

The frequency is a direct indicator for the balance between the generation and the demand of the total active power in the system and must remain within a predefined range around the nominal frequency

of 50 Hz. Frequency deviations outside this range can trigger an automatic protection mechanism, which could lead to a complete blackout [21]. If the active power generation exceeds the active power consumption, the system frequency will rise. If the active power consumption exceeds the active power generation, the frequency will fall [18]. The difference between active power generation and consumption is commonly referred to as imbalance. The larger the imbalance, the larger the frequency deviation will be.

The most relevant frequency parameters and targets have been identified by the European Network of Transmission System Operators for Electricity (ENTSO-e) to stimulate harmonisation and integration of the European electricity market, and to guarantee a secure power system. Specific values have been attributed to these parameters based on characteristics of the power system. These quality parameters are being bound in formal EU regulation by the EU network codes called the System Operation Guideline (SO GL).

Figure 1.2 depicts the dynamic behaviour of the frequency after a power generation outage. At the moment of power outage, a decrease of the frequency can be noticed. The maximum allowed deviation occurring after an incident is called the maximum instantaneous frequency deviation or frequency nadir which is equal to a deviation of 800 mHz compared to the nominal frequency. The maximum steady state frequency deviation is the extremity that the frequency can reach without bringing the stability of the system in danger. This frequency range is between 50.2 and 49.8 Hz. The time to restore frequency indicates the maximum duration of a deviation until the frequency is restored to the standard frequency range and is equal to 15 minutes. To bring the frequency back within the standard frequency range, in which it must operate under normal operation, a set of control mechanism called Load Frequency Control (LFC), is established.

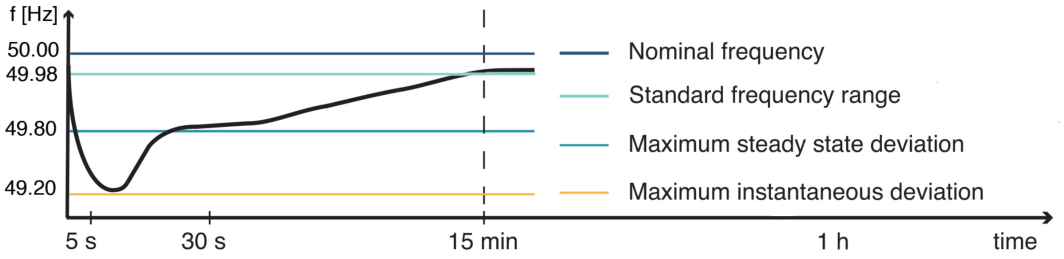

Figure 1.2: Dynamic behaviour of the frequency after an imbalance with the frequency parameters indicated.

1.2.3. Load frequency control

The mechanism of LFC is a system that can activate power reserves in case of an imbalance. If there is a shortage of power, the reserves can ramp up and if there is an abundance, the reserves can ramp down. In the European system, there are mainly three types of reserves that contribute to the stabilisation of the frequency: frequency containment reserves (FCR), frequency restoration reserves (FRR) and replacement reserves (RR). The RR are not used in the Dutch system and will therefore not be considered in this research.

When a disturbance takes place, first the FCR is activated. Once these reserves are activated, the deviation of the frequency stops and stabilises at a value that differs from the nominal value. Then, FRR is activated to bring the frequency back to its nominal value. The time required to ramp up or down the reserves influences the time it takes to stabilise the frequency. Currently the full activation time (FAT), which is the time to activate all the reserves, is 30 seconds for FCR. The FRR must be activated within 15 minutes. The FATs are shown in Figure 1.3.

The amount of FCR required per TSO is calculated each year based on the share of electricity that is produced and consumed within the operation area of that TSO and the total synchronous area (SA). A SA is an electrically connected region in which the frequency is the only common parameter. The SA in which the Dutch grid is located is Continental Europe (CE), the largest in the world that supplies over 400 million customers in 24 countries [22]. For TenneT, in the past years, the amount of FCR has been approximately 100 MW. This reserve must be offered symmetrically, meaning that if 10 MW of FCR is offered, the power source must be able to scale up and down 10 MW.

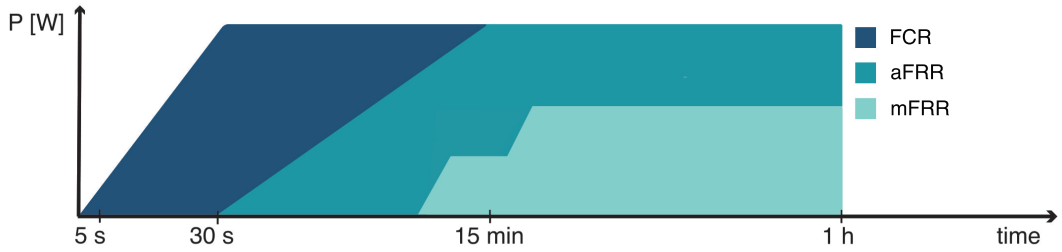

Figure 1.3: Graphical representation of the full activation time of FCR and FRR according to the requirements of the Dutch market for frequency reserves.

The FRR is used to balance the power to its scheduled value. This process involves automatically instructed services (aFRR) , previously known as secondary reserves, and manually instructed services (mFRR), known as tertiary reserves [23]. Currently the required amount of available aFRR in the Netherlands is 340 MW upward and 340 MW downward. These reserves are contracted separately.

In this research mFRR, used for large-scale and expected long-lasting imbalances, will not be taken into consideration, as these reserves are subject to long term contracts and are sporadically used. This makes it less interesting for the small scale renewable technologies to participate in this market.

1.2.4. Responsibilities

To manage the activation of the frequency reserves, a cascade of responsibilities, that starts at European level, has been established in the SO GL, which is drafted by ENTSO-e and since 14 September 2017 official EU regulation [24]. Within the ENTSO-e network there are five SAs: Continental (CE), Nordic (NE), Baltic, British (BE), and Irish (IRE) Europe. A SA is build up on one or more Load Frequency Control Blocks (LFC Block). Each LFC Block is operated by one or more TSOs who are responsible for operating a specific LFC Area. One LFC Block can consist of one or more LFC Areas.

The Dutch system is a LFC Block with only one LFC Area operated by one TSO. The task of a TSO can be divided in mainly three stages, namely system planning, system operation and system settlement. The planning stage entails all the tasks completed before the actual transaction of electricity. This needs to be done to identify possible network constrains or violations. The operation stage is about maintaining the continuous balance of supply and demand. The settlement stage consists of the arrangements that need to be made to settle deviations that occur during the system operation stage.

To be able to balance supply and demand, the Dutch law attributes the administrative responsibility of forecasting generation and demand to the balance responsible parties (BRP). During the planning phase, the BRP provides energy-programs (E-program) to the TSO a day before the day of delivery [25]. An E-program contains the transactions of energy during an imbalance settlement period (ISP). After gate closure time, the BRP has the responsibility to accept the imbalance price in case of a deviation of the E-program [26].

The last relevant actors for the balancing mechanism are the balancing service providers (BSP). This is the actor that offers the reserves required for balancing. The BSP offers its capacity for a certain price on the specific markets for frequency reserves. For the different frequency reserves there are different activation mechanisms.

The distribution system operator (DSO) and the regulators are not specifically mentioned in this cascade of responsibilities. Nowadays the DSOs are, from a frequency control point of view, not directly involved in the balancing process. They have to communicate the transported amounts of electricity for the settlement of aFRR, but this does not have a direct influence on the balancing mechanism. As a monopolist, the TSOs as well as the DSOs, are regulated. The regulators monitor and verify the correct functioning of the market. In the Netherlands the Autoriteit Consument & Markt (ACM) guards the compliance of entities with the Dutch Electricity law. The Agency for the Cooperation of Energy Regulators (ACER) complements and coordinates the work of national energy regulators at the European level. In reference [27] a more extensive explanation can be found about the different responsibilities of the relevant parties within the Dutch balancing market.

1.3. Research question

If the running hours of conventional power plants decrease, balancing services must be offered by different resources [28]. New BSP will have to enter the balancing market in order to be able to offer system services for frequency restoration. According to recent studies, the integration of the transport and electricity supply chain could provide an interesting solution to contribute to the stability of the electricity grid [29]. In literature, the symbiosis between electric vehicles (EV) and the electricity grid, in which EVs offer services to the grid, is called Vehicle to Grid (V2G).

Personal vehicles are utilised only 5% of the time for transportation, making them potentially available the remaining 95% of the time for a secondary function like offering frequency reserves [30, 31]. However, the individual participation of single EVs is not possible for mainly two reasons. The individual capacity is too small to participate in power system markets. Furthermore, the availability of one single EV is unpredictable from the power system's perspective as its main purpose is transportation. A larger fleet of vehicles could provide the solution by delivering a significant amount of reserves to the power system, while being statistically more reliable. Such a mechanism to form clusters of smaller single units, that together could offer services, is called aggregation and is administered by the aggregator [32]. An aggregator acts as a mediator between the system operator and small scale customers, enabling mutually beneficial coordination for EV owners and the power system [33]. The key role of the aggregator is to present the available capacity of the aggregation as a single entity to the system operator.

Within the context of the Green Village, a platform that helps innovations get to a large-scale application, an interesting concept that considers such an aggregation was developed by Ad van Wijk: Car as Power Plant (CaPP). This concept is extensively described in reference [31]. With CaPP, a new idea is introduced where an aggregation of hydrogen Fuel Cell Electrical Vehicles (FCEV) can offer power. When parked, these cars can produce electricity in a clean and efficient way with only water and heat as reaction product.

The CaPP concept can be implemented in different settings and applications. For example, the vehicles that are parked at residential locations or cars that are all parked at the same location. Within this research it is chosen to consider the application of a clustered fleet of FCEVs parked in a car park, which has the required infrastructure available to deliver both power to the grid as fuel to the cars. This specific concept is referred to as Car Park as Power Plant (CPPP). It is expected that a fleet of vehicles aggregated at the same location is more beneficial to operate as a power plant with respect

to a fleet that is spread out over a wide area and parked at autonomous parking places. This is mainly because of the scale effects of the required infrastructure to offer the frequency reserves. Limiting this infrastructure to the area of the car park will reduce the overall costs [34, 35].

The aggregator of the CPPP could be a suitable candidate to operate as a BSP. It could offer FCR and aFRR to contribute to the stability of the electricity system in the future. The aggregator will be financially compensated for the services delivered but there are also costs related to the delivery these services. Considering the aforementioned developments, the following research question is formulated:

What is the technical and economic feasibility of a Car Park as Power Plant offering frequency reserves in a future power system with a low share of conventional power plants?

1.4. Research approach

To answer the main research question three research areas needed to be explored. An overview of these areas, which are referred to as parts, can be found in Figure 1.4. First, the changes in the electricity production portfolio and the impact on the frequency stability are examined. Based on the effect of these changes, the contribution of a FCEV on the frequency stability is identified. Then, the contribution of an individual FCEV regarding the frequency stability is tested by performing measurements in V2G connection. Finally, the aggregation of multiple FCEVs in a car park that offers frequency reserves is analysed from a financial point of view. These steps result into four subquestions, of which two are answered in the first part and the other two in the second and third part.

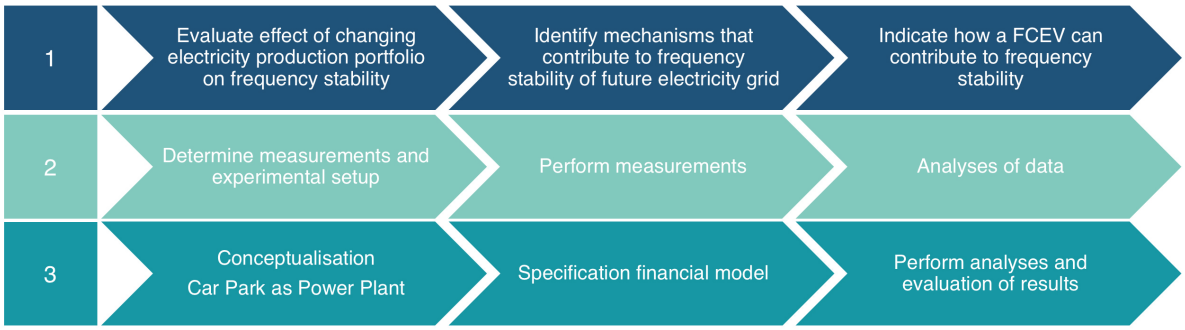

Figure 1.4: Overview of the research steps taken to answer the main research question.

Currently there are still enough conventional power plants that offer FCR and aFRR. If this share will decrease in the future, it will have an impact on the frequency stability. To be able to evaluate the contribution of the CPPP to the stability of the electricity grid, first, the effect of the ongoing changes in the electricity production portfolio on the frequency stability, need to be evaluated.

This information is gathered by carrying out a literature review and data analysis. The identified changes are simulated in a LFC model [36]. This model is a tool made in MATLAB and Simulink that mimics the behaviour of the frequency under different conditions. This approach has been chosen because the results of the LFC model display a suitable level of detail for the scope of this research by simulating the frequency as a result of one aggregated system. With this analysis the following subquestion can be answered: **1. How does the changing electricity production portfolio affect the frequency stability of the electricity grid?**

Once the effect on the frequency stability is identified, the possible contribution of the FCEV is evaluated. From literature, the main control mechanisms that contribute to the frequency stability are identified. In this thesis control mechanisms are referred to as the adaptations or extensions of the existing LFC framework. The most suitable control mechanism for the FCEV to contribute to the stabilisation of the frequency, is selected. By using the LFC model, the effect of this control mechanism is evaluated. This analysis answers the following subquestion: **2. How can the FCEV contribute to the frequency stability of the electricity grid?**

The first two subquestions constitute the first part indicated in Figure 1.4. The second part contains the evaluation of the capability of the FCEV to offer frequency reserves according to the control mechanisms proposed in the first part. An experiment is carried out to test whether the FCEV is qualified to offer the frequency reserves. Besides this experiment, also the findings of pilots for frequency reserves executed by TenneT and other TSOs and BSP, are included in the evaluation of the FCEV as balancing resource. With this analysis the following subquestion is answered: **3. Is the FCEV capable of offering frequency reserves to the future electricity grid?**

The final aspect to examine, is the the economic value that the aggregator could create by offering frequency reserves. First, a conceptual design of the car park is made to determine the technologies required to operate as a power plant. Second, by using MATLAB, a model is developed to estimate the financial potential of the CPPP when it offers frequency reserves. Several analyses are performed to understand the relation between the power that could be offered by the CPPP and boundaries that are encountered on the market for frequency reserves. With this analysis an answer to the following subquestion can be formulated: **4. What is the economic feasibility of the CPPP that offers frequency reserves?**

The first three subquestions give an answer to the question if the FCEV, and thus the CPPP, is technical feasible to offer frequency reserves in a future where the share of conventional power plants is reduced. The answer to the fourth subquestion gives an insight in the economic feasibility of the CPPP concept. All four subquestions contribute to the formulation of a founded answer to the main research question.

1.5. Scientific contribution

Extended research is done on the changing dynamics of the frequency and possible solutions to retain the stability of the electricity grid [37]. Other research has focussed on the suitability of balancing markets for new entries and only a few have actually entered the market [38, 39]. Current initiatives with e-boilers, second life batteries and EVs are tested in pilots launched by TenneT, other TSO's and BRP, to experimentally evaluate and examine which changes need to be implemented to make the market more flexible and accessible for new entrants.

This research aims to integrate the existing knowledge of the individual research fields by evaluating the technical and economic performance of a car park for FCEVs that could offer frequency reserves. The investigated capability of the FCEVs to offer frequency reserves, considering the changing dynamics of the power system, has not been tested before. The aggregation of FCEVs as CPPP has not yet been analysed for the purpose of balance service provision. From the pilots initiated by TenneT, a lot of information about the difficulties that new entries encounter is collected. All this information will be used to evaluate the potential of the CPPP as aggregator to participate in the market. The combination of these factors, shown in Figure 1.5, constitutes the backbone of this research.

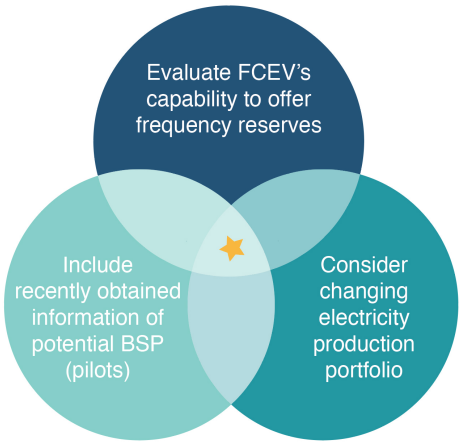

Figure 1.5: Identification of the scientific contribution of this research.

1.6. Structure of the report

The core of this thesis can be divided in three parts according to the indicated research parts. In the first part the first two subquestions are answered. The second part, Chapter 3, deals with the third subquestion. In the third part, Chapter 4, 5 and 6, an answer to the fourth subquestion is elaborated. In Chapter 7 the final discussion, conclusion and recommendations can be found which elaborate on the main research question.

Part

2

Effect of changing electricity production portfolio on frequency stability

The electricity sector has experienced many changes in the past and will continue to undergo many more changes in the future. In Europe, the past decennia have been characterised by the liberalisation of the sector and the rise of the competitive electricity market. A vast set of regulations has been established to guarantee the availability, affordability and acceptability of electricity, fair participation for market parties and an integrated European electricity market [40, 41]. One global trend is related to the decrease of operational hours of the conventional power plants and the increase of RES such as, wind, solar photovoltaic, biomass and hydropower [42]. Due to this trend, new challenges are emerging that require changes to the electric utility business model and regulatory policies to ensure a secure and reliable power system.

In this chapter the changes that influence the dynamic behaviour of the frequency and the methods to guarantee the stability, are examined. First, a detailed explanation of the system is given, which elaborates on the frequency reserves considered and the LFC model used. Then, the results are described and a brief discussion about the findings can be found. Finally, the conclusion, which contains the answer to the first two subquestions, is provided.

2.1. Analysis of frequency dynamics

To answer the first two subquestions, simulations are executed with the LFC model to determine, first, what the effect on the frequency dynamics is of the decreasing share of conventional power plants and, second, what the adaptations of the current requirements for frequency reserves are to improve the stability considering the changing frequency dynamics.

2.1.1. Reserves for frequency control

Frequency containment reserves (FCR) A difference between the power generation and demand will cause a system frequency deviation. The FCR controller of reserve providing units will automatically react ensuring that the system frequency is maintained within defined limits [43]. The proportional controllers start increasing or decreasing the power output of the reserve providing units as long as the system frequency continues to change. When the balance is re-established, the system frequency stabilises and remains at a quasi steady-state value. This new stable value will differ from the nominal frequency [43].

Frequency containment reserves can only be contracted in a symmetrical way. Not every single unit within the portfolio of the BSP needs to be symmetrical, but the total cluster of units must offer it symmetrically. For example, if a power plant has a maximum power output of 200 MW and the operator wants to offer FCR, then the power plant can not operate at full capacity because it cannot ramp up. If it wants to offer 10 MW FCR, it can use a maximum of 190 MW for other purposes.

The full amount of contracted FCR needs to be activated at a deviation of 200 mHz. The contracted reserves must be able to support the frequency control for a week. This period is referred to as validity period. In case of limited resources, the supplier must be able to deliver reserves for at least 15 minutes at the maximum deviation of 200 mHz or a partial delivery during a proportionally smaller frequency deviation. Once the 15 minutes are past and the resource would be exhausted in either way, the supplier must restore the reserves within 2 hours from the moment the standard frequency range is reached. Limited resources are for example EVs with a limited energy storage capacity.

The frequency containment process is a collectively organised process, to which each LFC Area within the synchronous area contributes. The sum of the FCR within continental Europe is equal to the reference incident of 3000 MW (P_{ref}). The reference incident covers the maximum instantaneous power deviation due to loss of load or loss of generation capacity which in continental Europe is equal to the tripping of two of the largest generating facilities, each 1500 MW, connected to the same busbar [44, 45]. The minimum quantity required for primary contributions per TSO is evaluated annually. This quantity is based on the share of electricity that is produced within the LFC Area (E_{NL}) compared to the total amount of electricity produced within the SA (E_{SA}). This share is referred to as the contribution coefficient (C_{NL}) for a TSO. The minimal power required for FCR that the TSO has to provide is then calculated according to Equation 2.1.

$$P_{FCR} = C_{NL} \cdot P_{ref} = \frac{E_{NL}}{E_{SA}} \cdot P_{ref} \tag{2.1}$$

Table 2.1 gives the values of FCR required within the Netherlands of the past years. For instance, in 2014, the contribution coefficient corresponded to 3,4 % for the Dutch LFC Area. The rounded value of FCR that TenneT needed to have available was 101 MW. The table shows also the aFRR that was required from 2012 until 2017. The next section will discuss this value.

Table 2.1: FCR and aFRR required by the Netherlands over the past years including the contribution coefficient and the frequency bias contribution for each year.

Year	C_{NL} [%]	P_{FCR} [MW]	λ_{NL} [MW/Hz]	P_{aFRR} [MW]
2012	3,9	117	1074	300
2013	3,8	114	1020	300
2014	3,4	101	911	300
2015	3,2	96	885	300
2016	3,4	102	913	340
2017	3,6	107	961	340

Automated frequency restoration reserves (aFRR) The aFRR is activated by the TSO if the programmed active power deviates from the actual delivered active power. A signal, called delta-setpoint, is send to the BSP that has committed itself to deliver aFRR. The delta-setpoint is calculated based on the import and export within a LFC Area. This calculated value is referred to as area control error (ACE) and indicates if the imbalance originates from a specific LFC Area. If this value is not equal to zero including a tolerance range, aFRR will be activated.

To calculate the ACE, shown in Equation 2.2, the contribution from the frequency containment process must be taken into consideration. This is done by introducing a frequency bias constant that describes how the system reacts to a frequency deviation. The frequency bias factor of the Netherlands (λ_{NL}) is calculated by multiplying the bias constant of continental Europe (λ_{CE}) with the contribution coefficient. This is shown in Equation 2.3. The frequency bias factor of continental Europe is based on the characteristic behaviour of the frequency that contains, for example, the effect of FCR and aFRR. The ACE becomes the sum of the deviation from the planned power flow (ΔP) and the product of the frequency bias constant (λ_{NL}) with the frequency deviation (Δf) [27].

$$ACE_{NL} = \Delta P_{NL} + \Delta f \cdot \lambda_{NL} \tag{2.2}$$

$$\lambda_{NL} = C_{NL} \cdot \lambda_{CE} \tag{2.3}$$

Additional mechanisms like virtual tie lines or the international grid cooperation and control (IGCC) also contribute to the calculation of the ACE. These will not be further discussed in this research. An overview of the frequency bias factors for the Dutch LFC Area is given in Table 2.1. The value of λ_{CE} is an administrative value agreed upon by the European system operators. Deviations from this values like non-delivery of FCR will automatically be accounted for in the ACE [27].

The minimum quantity required for aFRR is annually determined per TSO. A by ENTSO-e recommended value for aFRR is determined from Equation 2.4 with a = 10 and b = 150. L_{peak} is the maximal system peak load. The values of the past years are shown in Table 2.1 .

$$P_{aFRR} = \sqrt{a \cdot L_{peak} + b^2} - b \tag{2.4}$$

The full activation time is equal to 15 minutes, thus the reserves must increase or decrease the power output with 7% per minute of the total offered capacity. The delta-setpoint, which is given every 4 seconds, can be smaller than the total offered capacity and is rounded to integer numbers. After 15 minutes the imbalance must be smaller than 100 MW, otherwise mFRR is added.

2.1.2. Load-frequency control model

To evaluate the effect of changing system characteristics on power balancing, a model of the power system is developed by [46] and later improved by [36] and [37]. The model is based on the foundations explained in [18]. In this section a brief explanation of the model is given. More details about the model can be found in [46], [36] and [37].

A power system can be defined as the ensemble of all electrically connected grid components, plus all generators, loads and control centers associated with them. Three basic assumptions have been made. First it is assumed that the frequency in the SA is equal and that inter-area oscillations in the network are absent. The second assumption is that the mechanical and electrical rotational speeds are always identical in all generators. A third assumption is that voltage control is completely decoupled from frequency control which is valid under normal operating conditions.

A simplified block diagram of the relevant part of the model for this research, can be seen in Figure 2.1. The transfer function, shown in Equation 2.5, presents the frequency response as a function of the power imbalance. Decreasing the transfer function leads to a decreased sensitivity of the power system to disturbances. The frequency deviations have to be minimised to guarantee the stability of the grid. In [46] the complete derivation of the transfer function can be found.

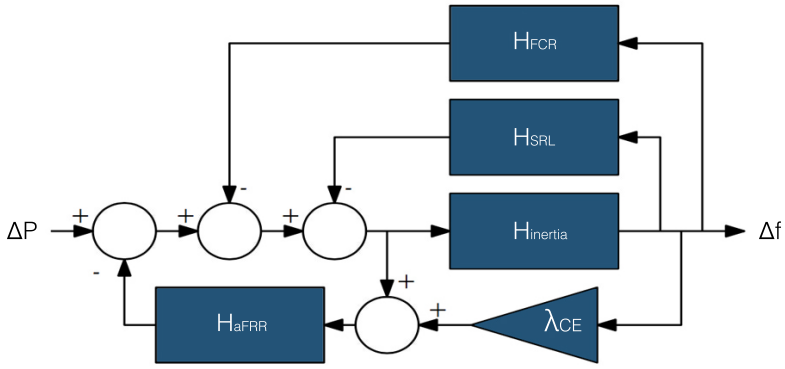

Figure 2.1: Simplified block diagram of the LFC model [46].

$$\frac{\Delta f}{\Delta P} = \frac{H_{inertia}}{H_{inertia}[H_{SRL} + H_{FCR} + \lambda_{CE} \cdot H_{aFRR}] + 1} \tag{2.5}$$

In this model the effect of FCR (H_{FCR}), aFRR (H_{aFRR}) and two intrinsic mechanisms of the system (H_{SRL} and $H_{inertia}$), the effect of which will be extensively explained in the results, are included. The multiplication constant (λ_{CE}) represents the frequency bias constant as explained in Section 2.1.1. All the input variables of the system correspond to the actual or expected values of continental Europe.

2.1.3. Analysis

To determine which parameters needed to be adapted during the simulations, a literature review and data analysis is executed. With the information gained from literature and data, the factors that influence the dynamics of the frequency are identified. Once these factors are known, the corresponding parameters in the LFC model are adapted to simulate the effect of those changing factors. The control mechanisms that could influence the stability of the frequency under the changing conditions are evaluated. The possible control mechanisms are examined in the light of the capabilities of the FCEV. Also in this case, the corresponding parameters in the LFC model are adjusted to analyse the effect on the frequency stability.

2.2. Changing frequency dynamics

The response of the frequency depends on two main mechanisms of which one is driven by the physical properties of the system and the second depends on the LFC. The decrease of the operational hours of conventional power plants and the parallel increase of RES have a large impact on the physical properties of the system.

2.2.1. Increase of variable renewable energy sources

The electric power industry has shifted from a vertically integrated system, where a single utility owned and operated the generation, transmission and distribution systems and provided power at regulated rates, to a decentralised system, where competitive companies sell unbundled power on a market [47]. In the vertically integrated system the Samenwerkende Elektriciteits-Producenten (SEP) could control the generation plants they owned to balance the load [48]. Nowadays, the generation as well as the load are much more variable.

The variety of technologies that can produce electricity on a large scale has increased enormously over the years. Not only conventional power plants can offer the required amount of power but also a vast share of RES contributes to the production of electricity [49]. The share of electricity that is produced with RES has increased over the years and will increase even more [11]. This trend can be identified in Figure 2.2. In the Netherlands, the share of electricity produced by RES has increased from circa 3 % to 13 % in 15 years [50, 51]. In countries where the amount of RES has reached even higher levels, the frequency deviation is higher for larger share of the time [52].

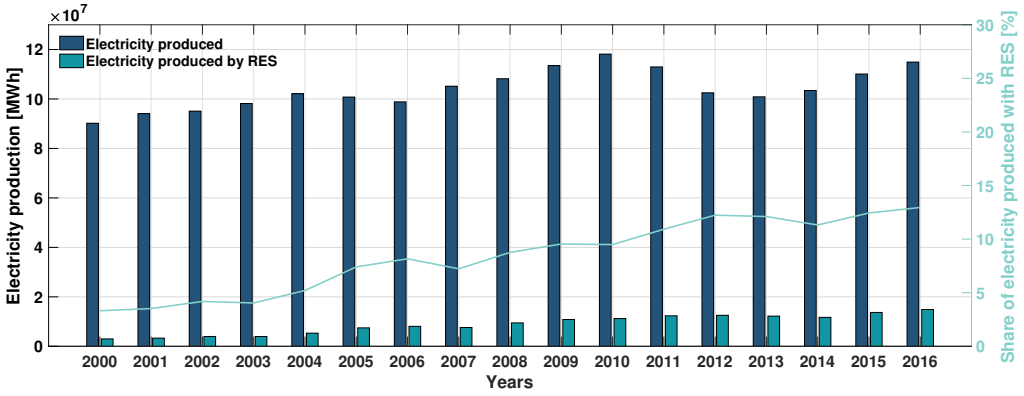

Figure 2.2: Total electricity production and share produced by RES in the Netherland.

The largest growth of RES is caused by the expansion of wind and solar power. These RES are also called variable RES (VRES). The difficulty of VRES is the predictability and availability. Unlike bio- or conventional fuels, the power source is not always available and depends on geographical and climatological conditions. Prediction models are used to estimate the available amount of power but even if the accuracy of prediction models is increasing rapidly, the forecast of VRES will never be 100% accurate.

The variation in solar energy output during the day and year is highly predictable because of the cycle of the sun. What makes it less predictable, is the presence of clouds. Clouds can cause a very rapid change in output of individual photovoltaic systems, however, the impact on the total power system is minimised if the panels are geographically spread over a vast area. The variation of wind is strongly related to daily and seasonal changes. A storm creates moments of more wind, which can impose challenges to the system. Considering the amount of offshore parks that is planned to be built in the North Sea, there will be moments in which the cut off speed is reached and a large share of the wind turbines will be shut down [13]. The positive side of VRES in a vast interconnected area as continental Europe, is that fluctuations of individual components will be smoothened [53].

Flexibility will play an important role as the variations in supply and demand grow to levels far beyond what is seen today [54]. The VRES have a high level of technical flexibility potential as they can ramp up faster than most conventional units. However, they do not have the capability to store large shares of energy. The VRES reduce also the conventional source of flexibility, because the traditional suppliers, conventional power plants, are being forced to shut down at moments of overflow of sun and wind. This gap of energy flexibility needs to be covered by new resources or smart use of the current ones [55].

2.2.2. Decreasing rotational inertia in the power system

The previously mentioned increase of VRES pushes the conventional power plants out of the market. On the one hand this is a desirable effect because of the lower impact on the environment, but on the

other hand it brings along the necessary challenges to maintain the desired grid stability.

A decrease of operational hours of conventional power plants causes a decrease of inertia in the total power system. Inertia is considered to be the kinetic energy stored in the system due to the rotational motion of the conventional synchronous generators, which have been the backbone of the power system for decades. This energy stored in the rotating mass of the system, referred to as inertia, operates as a buffer. The larger the inertia, the more time the system has to restore a frequency deviation [15].

If the frequency decreases, the rotational speed of the synchronous machine decreases, kinetic energy is released and converted into additional electrical energy, which is fed into the grid. If the frequency increases, the opposite happens [56]. The kinetic energy (E_{kin}) of a single synchronous machine is given in Equation 2.6 with J as the moment of inertia and f_m the rotating speed of the machine. The inertia constant of a synchronous machine, indicated by H in Equation 2.7, denotes the time duration in which the machine can supply its rated power solely with its stored kinetic energy [57]. To obtain the inertia constant, the kinetic energy is divided by the rated power (S_B). Typical values of the inertia constant of synchronous machines are between 5 and 10 s.

$$E_{kin} = \frac{1}{2} J \, \omega_m^2 = \frac{1}{2} J \, (2 \, \pi \, f_m)^2 \tag{2.6}$$

$$H = \frac{E_{kin}}{S_B} = \frac{J \, \omega_m^2}{2 \, S_B} \tag{2.7}$$

Currently the amount of synchronous machines are still sufficient to provide inertia to the system. The inertia is already considered at a dangerously low level in conditions of system split [45]. For this reason the development of new operational practices and control methods of other power suppliers is required to ensure a stable system operation in times of low inertia [58].

2.2.3. Decreasing self-regulating load

Another mechanism of the system is the self-regulating load (SRL). This is the effect of the load that in analogy with synchronous machines represents the energy that the load can exchange with the system due to frequency deviation. A change in frequency leads to a proportional change in power consumption of the load which stabilises the system frequency [45].

Currently the share of load that is self-regulating is circa 1 to 2 %/Hz. This means that 1 to 2% of the load increases if the frequency increases with 1 Hz. The SRL has a damping effect on frequency changes as it responds proportionally to the frequency deviation like primary control. Therefore, the SRL helps to minimise the frequency deviation after a disturbance [36, 46].

Most of the SRL is provided by mechanically and electrically coupled machines. A number of developments cause the self-regulating effect of the loads to decrease. Power electronics are used as a controller decoupling these machines from the frequency. This improves their efficiency but reduces the SRL available.

2.2.4. Increasing rate of change of frequency

The rotational inertia and SRL are considered intrinsic mechanisms of the system which together form the inertial response. The inertial response determines the first reaction of the frequency after an imbalance. This reaction is referred to as the rate of change of frequency (RoCoF), which is expressed

as the deviation of the frequency in a certain time step shown in Equation 2.8. The derivation of this relation can be found in Appendix A.

$$\frac{df}{dt} = \frac{\Delta P}{4\pi^2 J f_m} = \frac{\Delta P}{M} \tag{2.8}$$

This change of frequency is caused by a power imbalance (ΔP), which is the difference between the load and generation. The way the frequency changes depends on the size of this power imbalance and on the inertial response, which is represented by the factor in the denominator of Equation 2.8. In this equation J represents the systems inertia which includes both the rotational inertia as the SRL. The change of the frequency is smaller if the inertial response is higher because the inertial response damps the change of the frequency. It is expected that the RoCoF will increase due to the decrease of inertial response [37, 54].

The model simulates the behaviour of the frequency in CE after a power shortage equal to the reference incident. In Figure 2.3 the behaviour of the frequency in the first 15 seconds after an imbalance is shown. In Figure 2.4 the total time span from the moment of the imbalance until the frequency has reached the standard operation range is represented.

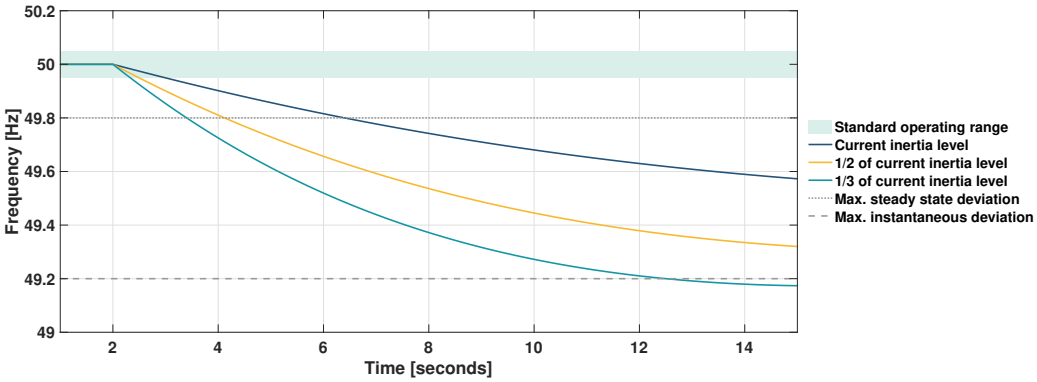

Figure 2.3: First 15 seconds of the frequency response after an imbalance for different values of the inertia in the system.

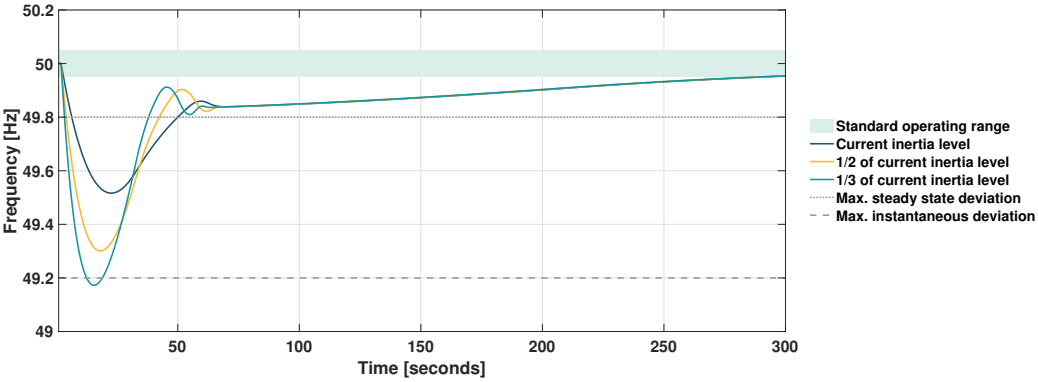

Figure 2.4: Complete reaction time of the frequency response after an imbalance for different values of the inertia in the system.

In the model the inertia is based on the residual load, which is the remaining load after the subtraction of the share produced by VRES. If the residual load is small, also the inertia in the system is small. Based on scenario's the level of residual load and thus the inertia in the future system can be estimated. In 2011 the residual load was approximately 145 MW and the average inertial constant (H) of conventional

power plants is assumed 5. This gives an aggregated moment of inertia of 58,000 MWs/Hz [37]. This corresponds to a share of 73.3% of power that still needs to be covered by conventional power plants.

Three different values for the inertia of the system are evaluated. The first one indicates a moment of inertia where 73.3% of the power is produced by conventional power plants. The second and third value indicate a potential future level of inertia with respectively half and one third of the first value. This corresponds to 36.7% and 24.7% of the power that is produced by conventional power plants.

In the figures it can be seen that for lower levels of inertia, the frequency tends to be more volatile. When the first state of inertia is considered, the frequency passes the maximum steady state deviation value but does not create a threat to the system. The third value does create a significant danger for the system as it passes the maximum instantaneous deviation. Considering future scenarios where nearly 0% of the electricity will be generated by conventional power plants, the inertia will be even lower than the values used in the simulation. The maximum instantaneous deviation of frequency will be reached if no measures are taken. New mechanisms and technologies are required to guarantee the stability of the frequency in the future [37, 57].

In Figure 2.4 it can be noticed that from 60 seconds onwards, the frequency for the different inertia values, is identical. This is because the inertial response of the system is a mechanism that is taken into account with the calculation of the ACE, which determines the amount of aFRR needed. The amount of aFRR needed is therefore automatically adjusted to guarantee the stability of the frequency. The decreasing inertia in the power system creates the largest threat in the first seconds after the power imbalance.

2.3. Influence of control mechanisms on frequency stability

There are two options to avoid the frequency from crossing the threshold of maximum instantaneous frequency deviation in the first seconds after an imbalance. One is to make sure that the RoCoF remains at a reasonable level. The second option is to make sure that the impact of the frequency reserves is large enough to keep the frequency from reaching the maximum instantaneous deviation. The first method is considered a proactive mechanism while the second is considered a reactive mechanism.

2.3.1. Limiting the rate of change of frequency

Currently, the inertial response is provided by conventional inertia. This is the inertia provided implicitly by the synchronous generators in the power system. This is however, not the only option to keep the RoCoF on an acceptable level. Alternatively to conventional inertia, the inertial response can be provided by non-conventional technologies. This type of inertia is explicitly added to the power system [37].

There are mainly three possibilities to provide inertia with alternative mechanisms: synchronous condensers, synthetic inertia on wind turbines and synthetic inertia on HVDC. Synchronous condensers are a well-established technology, while the synthetic inertia is a modern concept based on controls of power electronics and is still developing. Synthetic inertia is achieved by reprogramming power inverters attached to, for example wind turbines, so that they emulate the behaviour of synchronised spinning masses. The speed of converter controlled wind turbines is most of the time still asynchronous and thus decoupled from the grid frequency, which implies that they do not possess an intrinsic response to frequency deviations [59]. With the development of control mechanisms, the options to couple wind turbines to the frequency is explored and analysed but not yet widely implemented [60–63].

The FCEV power electronics could be adapted in such a way that it could offer synthetic inertia as well. In recently published research about EVs, the application of synthetic inertia shows limited improvements regarding the maximum instantaneous frequency deviation and the frequency slope. A

smaller deadband improved these two characteristics but worsened the RoCoF [64]. The increase of power electronic has, however, also resulted in power quality challenges as evidenced by harmonic distortions, voltage sags and other disturbances. More research should be done to evaluate the effect of power electronics on the stability of the power system and the possibilities of FCEV to offer synthetic inertia. As this is a solution that focusses specifically on control mechanisms of power electronics, this option will not be considered in this research.

2.3.2. Increasing the effect of frequency reserves

The second method to keep the frequency within the security range besides limiting the RoCoF, is to make sure that the effect of the activation of frequency reserves is large enough to keep the frequency from reaching the maximum instantaneous deviation. In this case the current requirements for frequency reserves need to be considered. There are two options: increase the amount of activated reserves or increase the speed of activation.

Increasing the amount of activated reserves requires an adaptation of the current calculation method for the delta-setpoints. The amount of reserves that are activated is based on thorough deterministic calculations. The required amount of FCR is based on the reference incident, the activated amount of aFRR is based on the amount of activated FCR, SRL and inertia. If the SRL and the inertia changes, also the activated amount of aFRR should change. The values assumed to calculate the amount of activated aFRR, should be updated considering the system changes. This could be an option but is not specifically related to the capabilities of the FCEV.

Increasing the speed of activation is a solution that allows to exploit the capabilities of FCEVs as batteries and fuel cells (FC) are considered fast responding technologies [64]. Faster response could be implemented by creating a completely new market for fast frequency reserves or by adapting the current requirements for the existing frequency reserves. An example of a new market is the Enhanced Frequency Control in Great Britain [65]. An amount of 200 MW of enhanced frequency response has been reserved through a tendering exercise held in July 2016. This consists in a service that achieves 100% active power output at 1 second (or less) after registering a frequency deviation.

This new product is the result of a new market that the system regulator has created. This is a solution that is not considered in the scope of this research. In this research, it is examined if the stability of the frequency can be improved without developing a new market. Within the existing framework of LFC in the Netherlands, the current requirements are examined in the light of new technologies, to see if an adjustment of the requirements, could also make sure that the frequency stays within the required ranges. For this reason it is chosen to focus on the adaptation of the requirements of the current existing frequency reserves.

Over the past years, the requirements for the FAT have been fixed to a constant value while the flexibility of the technologies for power generation has improved a lot in this period. Studies have shown that by changing the requirements for frequency reserves, the stability of the frequency can be improved [32]. Current technologies like batteries, flywheels and FCs have a much faster response time compared to the large conventional power plants. By decreasing the FAT, the reserves will react faster and could prevent the frequency from reaching the maximum instantaneous deviation. The RoCoF would remain the same but it is expected that the deviation will be stopped earlier.

With the LFC Simulink model, different settings for the activation time were simulated to evaluate the effect on the frequency. The low inertia level is considered, which is approximately equal to one third of the current inertia of the power system. First the activation time for FCR was decreased from 30 s to 15 s and 5 s. In Figure 2.5 the behaviour of the frequency is shown for the first 15 seconds. It can be seen that when the FAT requirement for FCR stays equal to 30 seconds, the maximum instantaneous deviation will be exceeded. When the FAT is decreased to 5 seconds, the frequency reaches the

steady state deviation bandwidth faster. This can be seen in Figure 2.6, where the first 5 minutes after the imbalance are shown. In case of the 5 seconds requirement for FCR, the frequency passes the maximum steady state deviation after 13.5 seconds. In case of the 15 and 30 seconds requirement, this is respectively after 25.5 and 38 seconds. A shorter FAT for FCR implies a faster return to a stable situation.

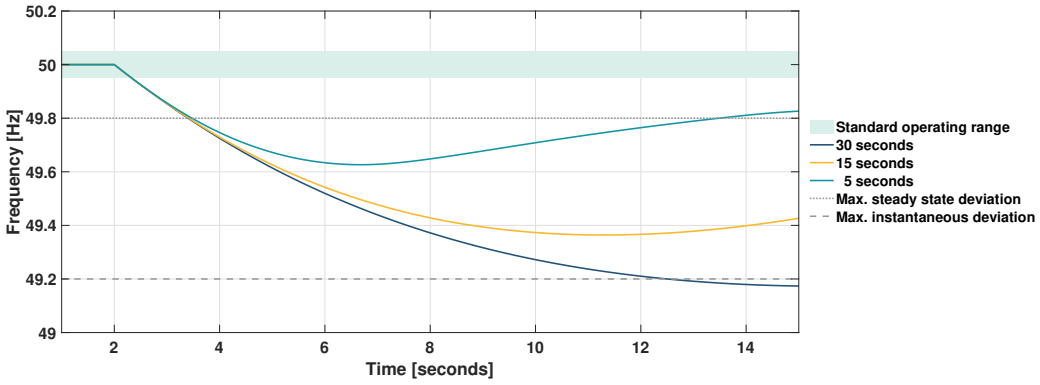

Figure 2.5: First 15 seconds of the frequency response after an imbalance for different full activation time requirements for FCR.

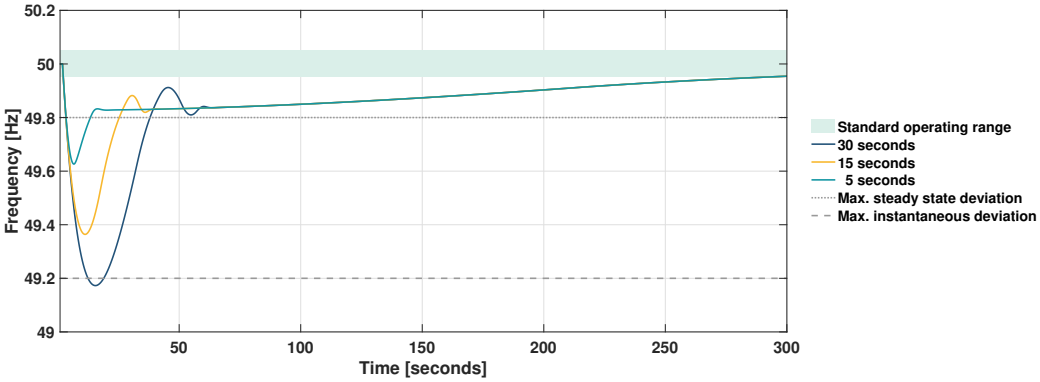

Figure 2.6: Complete reaction time of the frequency response after an imbalance for different full activation time requirements for FCR.

From Figure 2.6 it can also be seen that from the moment that the frequency reaches the maximum steady state deviation, the dynamic behaviour is the same regardless of the requirements for FCR. As mentioned before, this is due to the fact that the amount of aFRR required is adjusted accordingly to the calculated ACE which includes the effect of FCR.

In the previous simulation, the FAT of aFRR is kept constant. By decreasing the FAT of aFRR, the time that the frequency needs to return to the standart operating range could become even shorter. The requirements of aFRR are expressed as a percentage of the maximum aFRR activation. It is 7% per minute. In the model, the requirements for aFRR are expressed as a power gradient in MW per second. The setting used in the model of [37] is equal to 15 MW/s. The effect of faster aFRR is tested for 30 MW/s and 100 MW/s. The value of 100 MW/s is high as it would require, for example, 10,000 FCEVs to ramp from 0 to 10 kW in one second. It does, however, give an idea of the effect of such a change of requirements. The amount of inertia is kept at one third of the current value. The requirements for FCR are set one time to 30 seconds and one time to 5 seconds to evaluate the difference between the two settings. The results are depicted respectively in Figure 2.7 and in Figure 2.8.

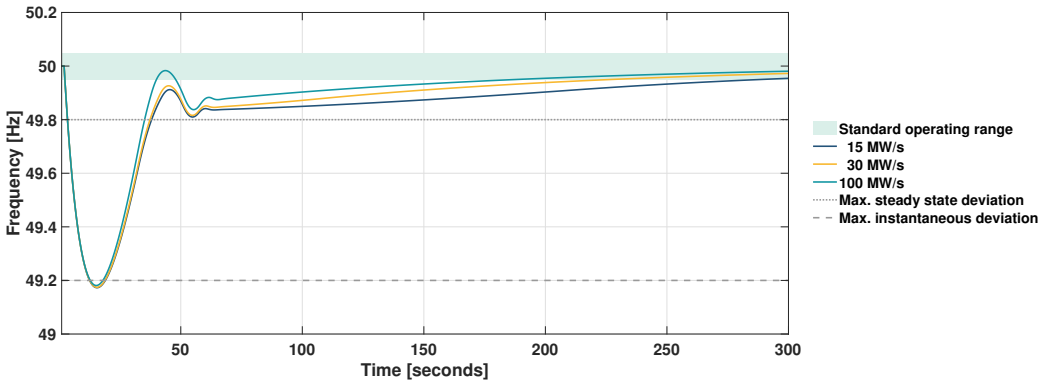

Figure 2.7: The frequency response after an imbalance for different FAT requirements for aFRR with the requirement for FCR set to 30 seconds.

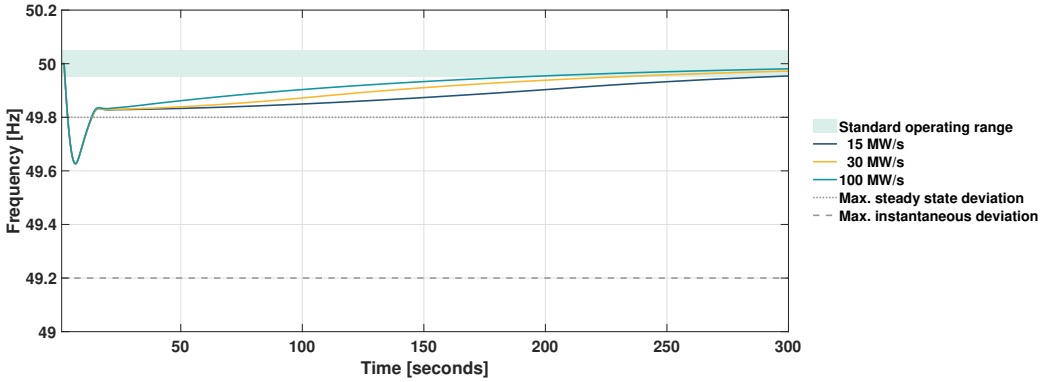

Figure 2.8: The frequency response after an imbalance for different FAT requirements for aFRR with the requirement for FCR set to 5 seconds.

It can be seen that higher power gradients for aFRR will decrease the time that the frequency needs to return to the standard operating range. There is no difference in the time that the frequency needs to return to the standard operating range when comparing the 30 seconds (2.7) and 5 seconds (2.8) FAT for FCR. It can also be deduced from the figures that the difference between the 30 MW/s and 100 MW/s ramp is rather small. This could imply that ramps of 100 MW/s are exorbitant and that an optimum needs to be identified. In the case of the FAT of 30 seconds for FCR, an overshoot can be identified in all three cases. This is not visible in case of a 5 seconds requirement for FCR. This implies that if an adjustment is done in the requirement for one type of frequency reserve, the effect on the dynamics of the other frequency reserves should be taken into consideration. A more detailed analysis about the stability of the system should be done to determine the reciprocal effect between the FAT of FCR and aFRR.

It should be mentioned that during the simulations all the frequency reserves are assumed to have the same reaction speed. In reality this is not the case. Different reserves have different settings. The variety of reaction speed contributes to the stability of the system. If all reserves would react at the same speed, overreaction could occur. The fact that the requirement for aFRR is expressed in a percentage of the maximum power output, is a mechanism for the reserves to react with different speeds and safeguard the stability of the system. Also the droop setting of the proportional controller for FCR makes sure that the reaction is spread out over the entire system.

If adaptations of the FAT are considered, this effect should be taken into consideration. Not all reserves need to react with the minimum possible FAT as this would influence the stability of the system as well. Another effect of short FATs is that large share of the current BSP are pushed out of the market. On one hand, this could be desirable as it could obstruct conventional power plants to participate in this market. On the other, if there are no new BSP that could take over this task, it could be dangerous for the stability of the system. If the FAT is set to a very low value which can be offered only by a very narrow set of BSP, the prices for frequency reserves could increase, which is an undesirable side effect.

2.4. Conclusion

The first two subquestions concern the impact of the increase of variable renewable energy sources on the frequency stability, and what the contribution of FCEVs could be to stabilise the frequency. The subquestions and answers are elaborated below.

Subquestion 1: How does the changing electricity production portfolio affect the frequency stability of the electricity grid?

In the electricity production portfolio there is a shift from conventional production methods towards renewable production methods. While the conventional fuels are available 24/7, large share of the renewable production methods relies on intermittent sources called variable renewable energy sources. The effect of the increase of these sources is twofold.

Firstly, it reduces the operational hours of the conventional power plants. This causes the inertia in the power system to decrease. The inertia is essential as it determines the rate of change of the frequency. This rate of change is an indicator for the time the system has to respond to a power imbalance. A power imbalance causes the frequency to deviate from its nominal value which is undesirable. If the inertia reduces, the rate of change of frequency will increase, which makes it more probable that the frequency will exceed the maximum instantaneous frequency deviation.

This could happen if 75.6% of the electricity would be produced by renewable energy sources. In Germany there already have been moments that 62% of the electricity was produced by solar and wind [66, 67]. In the Netherlands this has not happened yet but if the sustainability goal of 2023 is achieved, a total of 4500 MW and 6000 MW windpower respectively off- and onshore and 9000 MW of solar panels, will be installed. The total of 19,500 MW installed variable renewable energy sources is circa 55.4% of the total electric capacity that is currently installed in the Netherlands [68–70]. Under the right weather conditions and low electricity demand, there will be moments that a significant share of the electricity is produced by variable renewable energy sources. Considering that the goals of 2023 are just one step in the right direction and not the end goal, it is assumable that even larger shares of variable renewable energy sources will be operational around mid century and thus the low level of inertia will become a threat for the stability of the power system if no adequate measures are taken [71].

The second effect of the increase of variable renewable energy sources is that the availability of frequency reserves is reduced due to the diminishing operational hours of conventional power plants. Sustainable resources could replace the conventional power plants. This could be done by offering synthetic inertia, to keep the rate of change of frequency at an acceptable level, or by offering frequency reserves, to restore the frequency to its nominal value. Renewable energy sources like wind power could offer inertia or frequency reserves but because of the variable availability this could not be sufficient to guarantee the stability of the grid.

Subquestion 2: How can the FCEV contribute to the frequency stability of the electricity grid?

The decreasing inertia in the system will increase the rate of change of the frequency. Faster frequency dynamics raise the question whether the current frequency control system will remain sufficient for containing and restoring the frequency. There are multiple options to make sure that the stability of the frequency is guaranteed, considering the changing dynamics of the frequency. As mentioned above, synthetic inertia is one of the options to keep the rate of change of frequency within acceptable margins. This solution does, however, not exploit directly the capability of the FCEV.

Another solution that suits the capabilities of the FCEV better, is increasing the deployment and performance of existing frequency reserves. This can be done by increasing the amount of activated reserves or by increasing the reaction speed. This second option is the most interesting from the point of view of the capabilities of the FCEV as the power sources in the vehicle, are considered fast responding technologies. Increasing the reaction speed, which implies a reduction of the full activation time, could contribute to the stability of the frequency by avoiding it to reach the maximum instantaneous frequency deviation.

II

Part

3

Experimental measurements of the full activation time of a FCEV

As established in the previous chapter, if no other mechanisms are implemented to replace the inertia in the system, the RoCoF will increase. The maximum instantaneous frequency deviations could be reached, which is not desirable for the stability of the system. One of the solutions to keep the frequency from reaching the maximum instantaneous frequency deviation is to increase the activation speed of frequency reserves.

Vehicles are designed to have large and frequent power fluctuations, since that is in the nature of roadway driving. Due to this characteristic of vehicles, the largest contribution to frequency stability can be delivered by responding quickly to frequency deviations [30]. A faster frequency response implies that the FAT should be reduced. The FAT of the FCEV in V2G mode is still unknown.

In this chapter it is explained how the FCEV is tested to be able to evaluate the FAT in V2G mode and assess the capability of the car to deliver fast frequency reserves. To understand the results of the experiment, some background information about the internal mechanism of the vehicle is given. Then, the experiment is described which explains how the third subquestion is answered. The results of the experiment are presented and, finally, a conclusion is formulated.

3.1. Mechanism of a FCEV

The FCEV is a specific type of EV that as a main power source uses a FC stack. The FC stack contains layers of individual FCs that combine hydrogen and oxygen to produce a voltage. The FC of the examined vehicle is the low temperature proton exchange membrane fuel cell (PEMFC). The cells are stacked together in series to multiply the voltage and generate electricity, which is used to drive the electric traction motor [72][1].

The electricity is generated by a electrochemical reactions, shown in Equation 3.1 and 3.2. A FC consists of an anode (3.1), where the hydrogen is split into positively charged ions and electrons, a cathode (3.2), where the protons and electrons recombine with oxygen to form water and heat, which are the products of the process, and an electrolyte, where ions carry the current between the electrodes. Some of the water is recirculated to the humidifier and excess water is extracted out of the tailpipe.

[1] In this research when referring to FC, the total FC stack is intended.

Anode:

$$H_2 \longrightarrow 2\,H^+ + 2\,e^- \tag{3.1}$$

Cathode:

$$\frac{1}{2}O_2 + 2\,H^+ + 2\,e^- \longrightarrow H_2O \tag{3.2}$$

Every FCEV has different specifications [73–75]. For this experiment a Hyundai ix35 Fuel Cell vehicle is used, which has a 100 kW FC stack installed and generates over 400 V when operating. In Figure 3.1, which represents the internal energy system of a FCEV, it can be noticed that there is also a battery that operates as an additional power source.

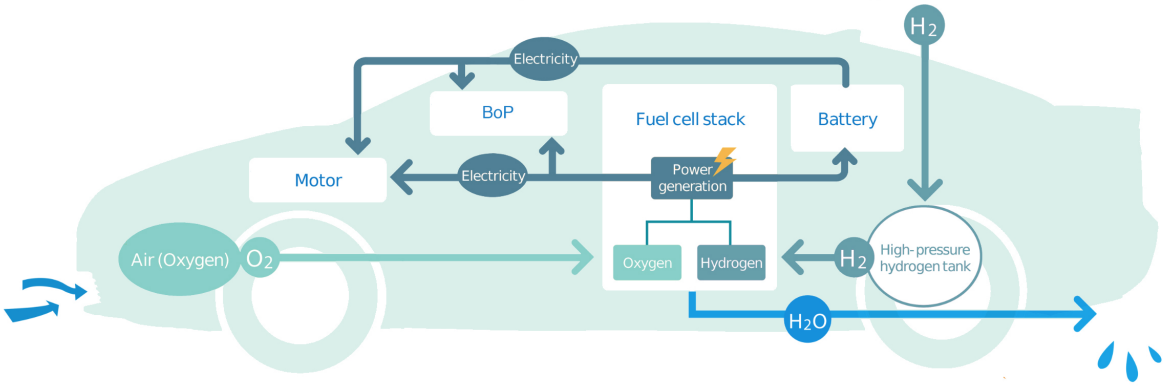

Figure 3.1: General overview of the internal energy system of a FCEV.

In the Hyundai ix35 the additional power source is a high voltage lithium-ion polymer battery that operates at a nominal voltage of 180 V. The battery stores electrical energy which comes from both the FC stack and the electric traction motor when the vehicle is decelerating. The process of recovery of electrical energy is called regenerative braking. The battery provides extra current to the traction motor during acceleration. It has an energy capacity of 0.95 kWh and a maximum power output and input of 24 kW. Besides the high voltage battery, there is an auxiliary battery of 12 V, which is used to initiate the fuel cell stack during startup. This battery is also used to supply power to the headlamps, the audio system, and other low voltage electrical components in the vehicle [72].

When considering the internal energy system of a FCEV, it is important to mention the balance of plant (BOP). The BOP is the set of activities that is required to keep the system operational and consumes electricity. The alteration between the power sources is determined by the energy management system (EMS) of the vehicle. This is a system that is significantly different for each type of FCEV.

3.2. Experiment

The FCEV needs to measure up to the requirements for delivering frequency reserves and preferably react even faster than the current requirements. The FAT stands for the time the balancing resource needs to ramp up from zero to the maximum power output. The two frequency reserves taken into consideration are FCR and aFRR. Considering that the FAT for FCR is shorter than that for aFRR, if the FCEV satisfies the requirements of the first, it will also satisfy the latter.

Several interviews were done to examine the FAT of other technologies which are experimenting with the delivery of frequency reserves. From these interviews it was deduced that the FAT can be split up in two parts. The first part is the time related to the data communication, referred to as reaction

delay. This is measured from the moment that a signal is send until the moment that the balancing resource actually reacts. The second part of the FAT is the time that the balancing resource actually adjusts the power output and reaches the point of full activation. This will be referred to as activation time. The requirement for the maximum allowed reaction delay for FCR is 2 seconds.

$$\text{FAT} = \text{Reaction Delay} + \text{Activation Time} \tag{3.3}$$

As no actual aggregation, control mechanism and communication system is yet available for the CPPP concept, the reaction delay of this aggregation could not be measured. During the experiment only the activation time of the balancing resource was measured.

3.2.1. Experimental setup

At the Green Village a commercial Hyundai ix35 has been modified to operate in V2G mode while maintaining road access permits [76, 77]. A DC outlet was added to the right front corner of the vehicle with a type 1 SAE J1772 socket shown in Figure 3.2. The modification also included a software update and dashboard activation button which activates the cold shut down procedure (CSD) which is needed to prevent the exhaust water from freezing in case of low ambient temperatures [78]. The FC and battery operating voltage, current, and other power system related parameters are logged with a frequency of 5 Hz by a data logger.

With a type 1 cable and plug the DC socket in the car can be connected to the DC-AC discharge unit, which is the white container in Figure 3.2. This discharge unit transforms the DC power from the FCEV into 3 phase AC Power at 380 V, which is delivered to the grid. Power discharge settings can be manually defined in the discharge unit for a fixed amount. This implies that the FCEV can deliver only a constant power to the grid and can be switched on and off.

To deliver power to the grid the current in the discharge unit must be synchronised with the 50 Hz of the electricity grid. On activation of the start and shutdown button on the discharge unit, the inverter is started and the electricity begins to synchronise. Once it is synchronised, the FCEV starts delivering power. To stop delivering power to the grid, the AC load has to be switched off first, in this case by switching off the inverter. More technical details and safety measures about the adaptations of the FCEV and the experimental setup can be found in reference [76].

Figure 3.2: Experimental setup of the FCEV operating in V2G mode.

3.2.2. Measurements

The activation time is the time that the FCEV needs to ramp from zero to the maximum power output. The maximum power output of the FCEV in V2G mode is limited to 10 kW. This limitation is caused by the heat produced by the FC during the generation of electricity. The FCEV is equipped with a large radiator and cooling fan to maintain the temperature at a desirable operating level. In stationary mode the FCEV has less cooling capacity and can not operate at the maximum power of 100 kW. For this reason the power output in stationary mode is reduced to a value that enables the on-board utilities of the FCEV to regulate the fuel cell's temperature [35]. This implies that the delivered power can scale between 0 and 10 kW.

To determine the activation time of the FCEV connected to the grid, the power output of the FCEV is measured while the discharge unit is switched on and off. This is done for two different settings. The first setting is for a power output of 10 kW and the second setting is a power output of 5 kW. For each setting, a cycle is repeated 10 times to improve the reliability of the measurements. The cycle consists of 2 minutes of idling conditions, then the discharge unit is switched on for 5 minutes, after which it is switched off again and a new cycle starts. Each activation of the FCEV represents one measurement of the activation time. This implies that for each setting there are 10 measurements, which gives a total of 20 measurements. The average of these measurements gives an indication of the activation time of the FCEV.

The total input signal for both settings is shown in Figure 3.3. In total, one cycle takes approximately 7 minutes, one whole experiment takes approximately 70 minutes. With the current and voltage output of the FC and the battery the power of both components was calculated. The total DC power output of the FCEV is equal to the sum of the FC and the battery DC power output.

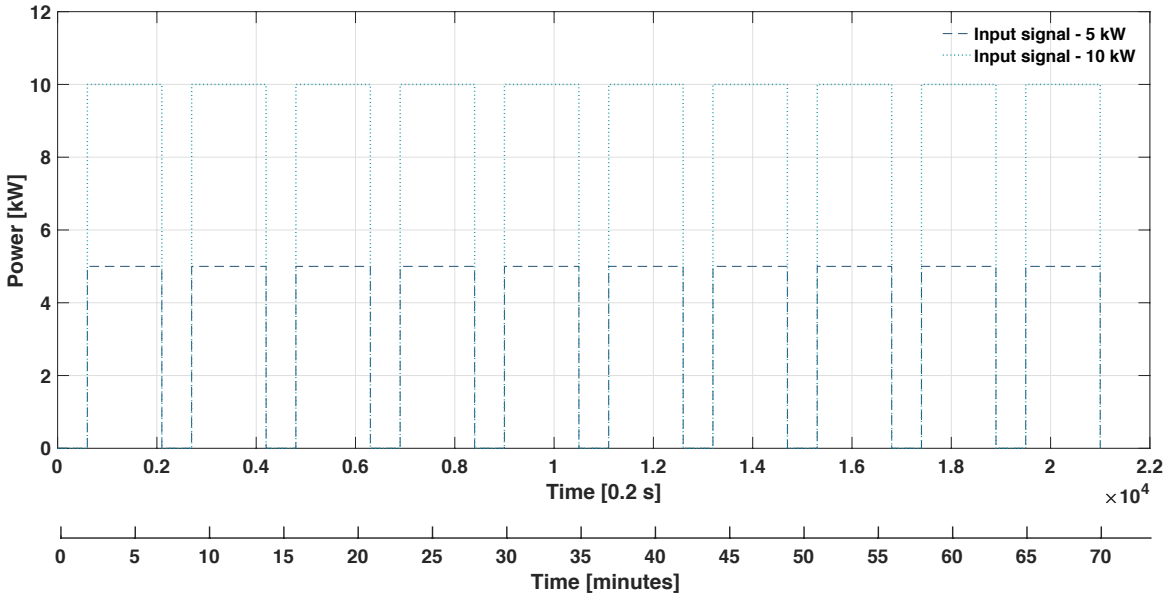

Figure 3.3: FCEV input signals for the experimental setting of 5 kW and 10 kW.

To carry out the experiments, first the power output of the discharge unit is set to the right value, for the first experiment to 10 kW and for the second experiment to 5 kW. After setting the power output, the FCEV is connected properly to the discharge unit and switched on. When the FCEV is switched on but the discharge unit is switched off, the FCEV remains in idling condition. It does not actively deliver power to the grid but there is a power output which is internally used by the FCEV. Once the discharge

unit is switched on, the FCEV actively starts delivering power. By switching on and off the discharge unit, the FCEV gets activated (ramp up) and deactivated (ramp down).

The timing was done with a chronometer and the on/off switching of the discharge unit was done manually. Due to these factors, inaccuracies are present in the timing of the measurements. This can be seen in Figure 3.4 where the power output of the FCEV is represented. It can be noticed that the measurements of the 5 kW and 10 kW experiment start being out of phase when the time proceeds. It does however, not affect the ability to estimate the activation time of the FCEV as the point of activation can be identified in the data set by the steep ramps.

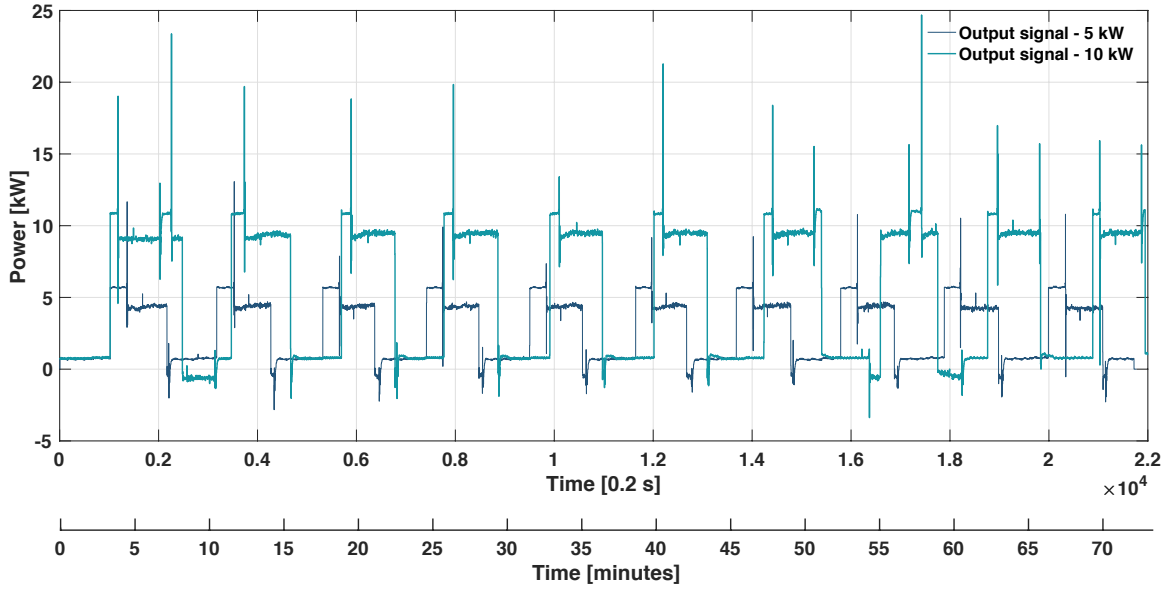

Figure 3.4: Power output of the FCEV for the experimental setting of 5 kW and 10 kW.

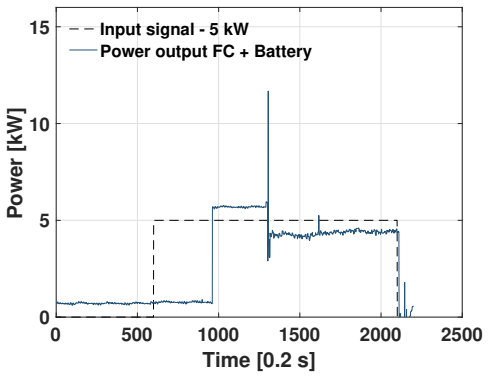

Figure 3.5: Representation of the input signal of the 5 kW power output experiment with the corresponding reaction of the FCEV.

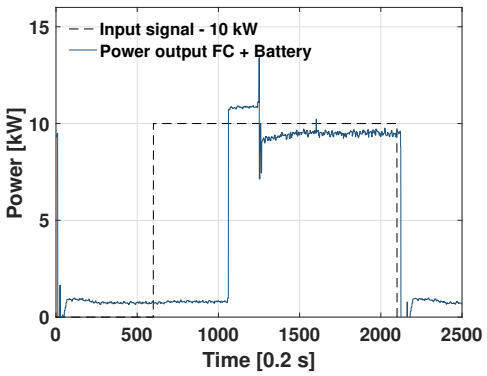

Figure 3.6: Representation of the signal input of the 10 kW power output experiment with the corresponding reaction of the FCEV.

The signal given for one cycle and the reaction of the power output of the FCEV is indicated in the Figures 3.5 and 3.6. The exact time the discharge unit needs to synchronise with the grid is not measured accurately but can be approximated with by analysing the data. The time to synchronise is around 60-80 seconds. This is the time between the moment that the discharge unit is switched on and the FCEV actually starts delivering power. This time will be referred to as synchronising time. This delay in

power output can be reduced to approximately zero by switching on the FCEV after the synchronisation of the discharge unit. For this reason the delay caused by synchronisation of the discharge unit will not be considered when evaluating the FAT.

3.2.3. Analysis

To evaluate the full activation time of the FCEV, the power gradient is calculated. This is the difference in the power output of the FCEV per second. It is calculated by subtracting the power output at time t from the power output of time $t+1$ as can be seen in Equation 3.4.

$$\frac{\Delta P}{\Delta t} = \frac{P_{(t+1)} - P_{(t)}}{t_{log}} = (P_{(t+1)} - P_{(t)}) \cdot f_{log} \tag{3.4}$$

The t_{log} is equal to 0.2 seconds as the logging frequency (f_{log}) is set to 5 Hz. The power gradient of the individual components will be evaluated because of the higher level of detail that can be obtained. Once the power gradient is know, the activation time can be calculated and summed up to the estimation of the reaction delay, to obtain the FAT.

3.3. Results and discussion

3.3.1. Power output

The total DC power output of the FCEV is considered as the sum of the DC power output of the FC and of the battery. The individual power outputs are calculated by multiplying the respective current and voltage output. The sum of the power outputs does, however, not correspond precisely to the V2G input signal defined in the discharge unit. This can be seen by comparing the Figures 3.3 and 3.4. It can be noticed that sometimes the power output is higher than the V2G input signal and other times the power output becomes negative. The reason for this behaviour is the EMS of the FCEV.

In general, the EMS appears to be mainly driven by the SoC of the battery. During both experiments the SoC of the battery always stayed between 42% and 57%. This was also indicated by previous research with the FCEV in V2G mode [76]. The SoC of the battery is shown in Figure 3.7. Due to the fact that the SoC is logged with a frequency of 1 Hz, the power output data, which is logged with a frequency of 5 Hz, is adjusted to an equal logging frequency by taking the average value of the 5 consecutive measurements. This is done only for the graphical representations when considering the SoC. When calculating the power gradient and the full activation time the actual measured values are considered.

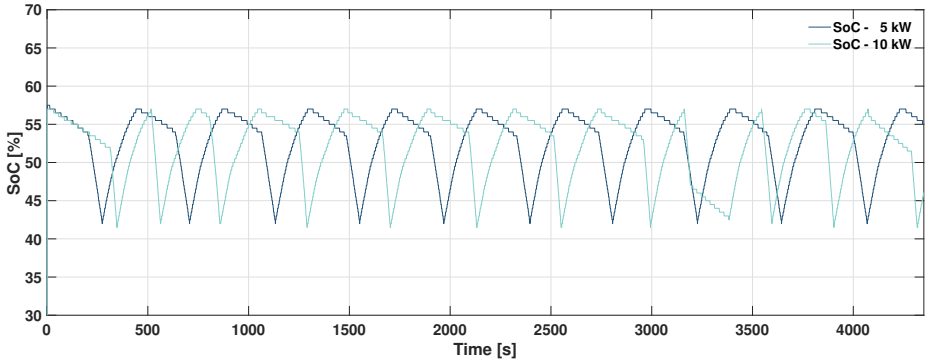

Figure 3.7: State of charge of the battery in the FCEV for both experiments.

To maintain the SoC of the battery within this range, the FC is used to charge the battery. This causes the individual power output of the FC to be higher than the V2G setting. This can be seen in Figure 3.8, which shows a detailled time frame of the 5 kW experiment. Power peaks of 10 kW are reached even if the V2G setting is 5 kW. It can also be noticed that during the idling conditions, when there is no power request from the grid, the battery is the main power source. Negative power values of the battery correspond to periods that the battery is being charged.

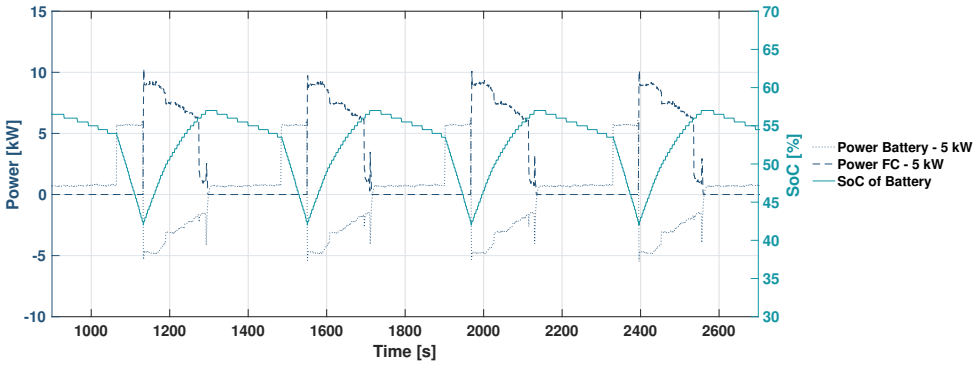

Figure 3.8: Detail of the battery power, FC power and SoC in a limited time frame of the 5 kW experiment.

When the battery is being charged during shut down of the discharge unit, the FC will continue to charge the battery until it reaches 57%. Then the battery will take over the power request for the BOP in idling condition. This can be seen in Figure 3.9 in the time frame between 3600 and 3750 seconds. It can also be noticed that when the discharge unit is switched on, just before 3400 seconds, when the discharge unit is not yet synchronised with the grid, the FC starts charging the battery. When the grid is synchronised, indicated by the large power increase around 3425 seconds, the FC starts delivering extra power output. Contrary to the other results, where the battery always starts delivering power once the discharge unit is synchronised with the grid, the main power source in this case is the FC until the battery is full again. Then the FC is switched off and the battery delivers the power. The charging of the battery is never interrupted during a switch from power delivering mode to idling condition or vice versa. If the FC is charging the battery, the FC will not be completely switched off before the battery reaches its upper charge limit.

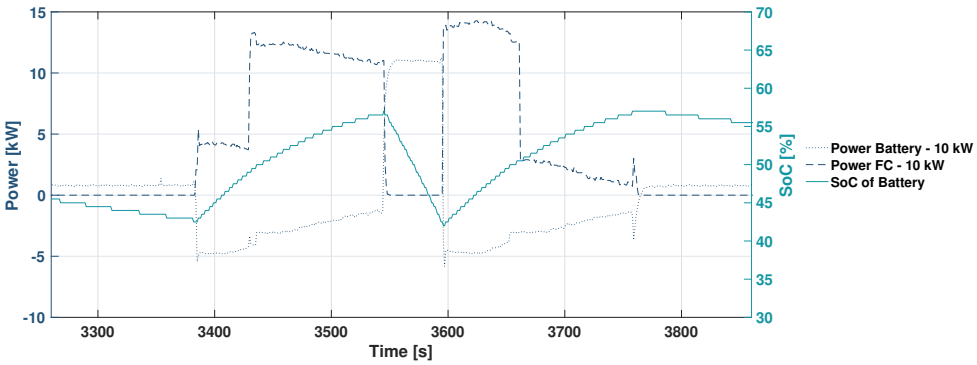

Figure 3.9: Detail of the battery power, FC power and SoC in a limited time frame of the 10 kW experiment.

The EMS is a crucial part of the FCEV. Every vehicle producer determines different settings in the EMS which strongly influence the performance of the vehicle. In general the strategy objective in a hybrid vehicle, which has fuel and a battery as energy source, is to minimise the fuel consumption. There is,

however, a difference between the EMS for driving and V2G mode.

The general constrains of the EMS in driving mode, are related to technical components, vehicle performance and driver comfort [79]. The governing objective functions in V2G mode seem to be related to the SoC of the battery and the minimisation of FC start and stops. Another relevant parameter in V2G mode is the temperature of the FC. To avoid excessive heating of the FC, the rotations per minute of the coolant pump are increased once the temperature reaches 66°C. Increasing the speed of the coolant makes sure that the temperature decreases and stays below 68°C. The rotational speed can vary between 1500 and 3000 rpm. This can be seen in Figure 3.10 and 3.11, which represent the outlet temperature of the coolant and rotations per minute of the coolant pump.

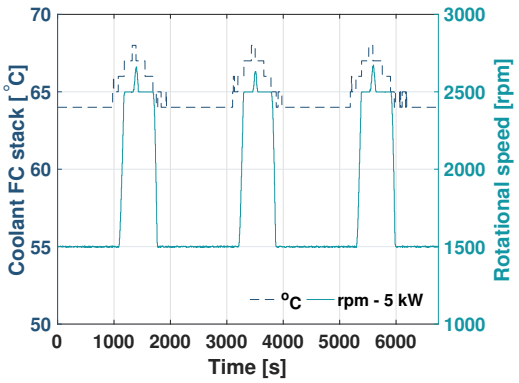

Figure 3.10: Detail of the outlet temperature of the coolant of the FC stack and rotations per minute of the coolant pump for the 5 kW experiment.

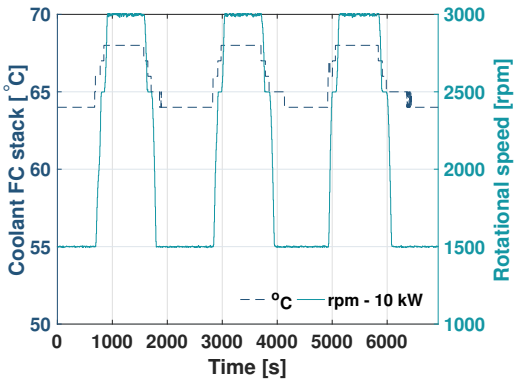

Figure 3.11: Detail of the outlet temperature of the coolant of the FC stack and rotations per minute of the coolant pump for the 10 kW experiment.

This behaviour of the temperature is in line with previous experiments done with the FCEV in V2G mode. According to those experiments the outlet temperature of the cooling fluid initially increases until 68°C and reaches a steady state after approximately 1.5 hours. The temperature at steady state fluctuates between 60 and 64°C. At that point the rotational speed of the pump is 1500 rpm [76].

In this experiment the discharge unit is switched on and off, which creates a fluctuating power output and short running periods. This impedes the system to reach a steady state. During operation of the FC, the temperature of the cooling fluid oscillates between 64 and 68°C. This is on average 4°C higher compared to the coolant temperature for stationary power delivery but still amply below the maximum allowed temperature. In Figure 3.11 it can be noticed that for the 10 kW power output the rotational speed is higher than the one for the 5 kW power output, shown in Figure 3.10. This implies that more work needs to be done to cool the FC when higher power output is delivered to the grid. The cooling of the FC stack can be considered well suited to operate under fluctuating power conditions in both cases.

3.3.2. Power gradient

The power gradient of the FC and the battery measured for the 5 kW and 10 kW experiment, are shown respectively in Figure 3.12 and 3.13. The average absolute power gradient, up- and downward, is calculated by taking the average of power gradients at the moments when the FC and battery switch on and off. This results into the values of Table 3.1. It can be seen, comparing the results of the two experiments, that for higher power settings of the FCEV, the absolute power gradient is higher. It can also be seen that the power gradient of the FC upward is higher than the power gradient of the battery upward. In case of the power gradient downward, it is exactly the contrary. The battery has a higher power gradient in that case. This applies for both the case of 5 kW as for 10 kW.

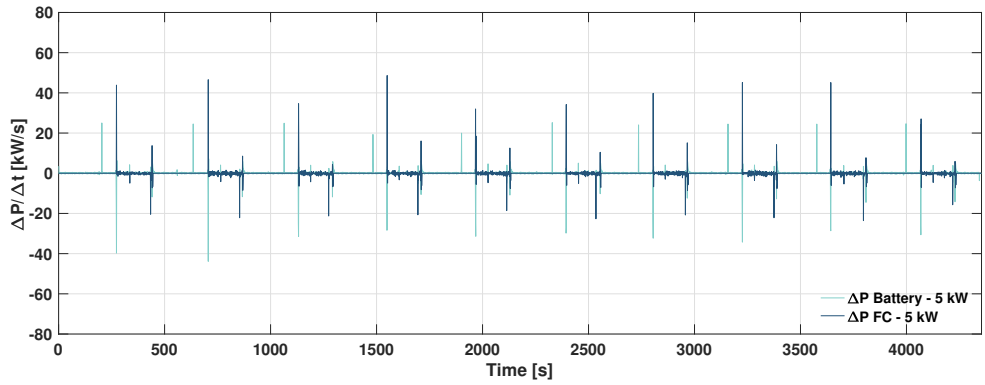

Figure 3.12: Power gradients of the 5 kW experiment.

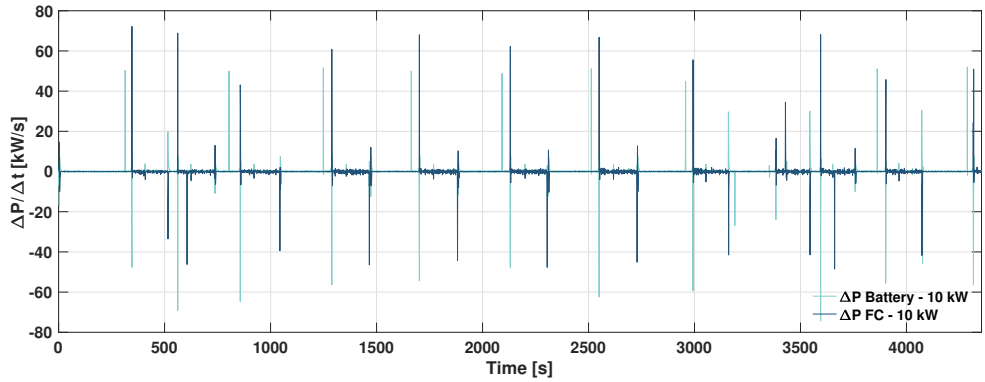

Figure 3.13: Power gradients of the 10 kW experiment.

Comparing these power gradients with previously done experiments with the FCEV in V2G mode, the results of this experiment are slightly lower except for the value of the battery upwards, which is slightly higher [76]. The difference between these results and previous results do however, not deviate significantly. The deviations are presumably caused by difference in ambient temperature, initial values of the FCEV and start-up conditions [80]. All these factors have a large impact on the performance of the power components.

Table 3.1: Absolute power gradients of the battery and the FC.

[kW/s]	FC ↑	Battery ↑	FC ↓	Battery ↓
5 kW	38.3	24.7	-21.7	-29.6
10 kW	60.2	50.0	-44.4	-57.2

Considering literature, it was expected that both for up- and downward regulation, the battery would have had a higher power gradient due to the higher responsiveness compared to FCs. This is also why FCEVs are equipped with an additional battery to guarantee the dynamic transients desired by vehicle consumers [81][82]. This difference is mainly caused by the fact that the FC requires a system that delivers the external reactants to the reaction sites. However, the time constant for both reactions, in the battery and in the FC, is in a range of 10^{-2}-10^{-4} seconds, which makes both components suitable for fast balancing response [83].

To evaluate this deviating result, the relative power gradients are calculated. The relative power gradient is expressed as fraction of the total V2G power output value (5 kW and 10 kW) and as fraction of the maximum power output of the individual components. This is 100 kW for the FC and 24 kW for the battery. Table 3.2 provides an overview of the power gradient of the FC and the battery in comparison with the maximum power output of the individual components. It can be seen that in this case the power gradient of the battery is higher for up- and downward regulation. It can also be seen that higher power gradients are reached if the V2G power output is set to a higher value. For the FC as well as for the battery, the 10 kW experiment has almost a double power gradient compared to the 5 kW setting.

Table 3.2: Relative power gradients of the battery and the FC compared to the maximum power output of the individual components.

[%/s]	**FC ↑**	**Battery ↑**	**FC ↓**	**Battery ↓**
5 kW	38.3	102.8	-21.7	-123.3
10 kW	60.2	208.2	-44.4	-238.6

These percentages are compared with the power gradient of a flywheel, which is also considered a suitable device for fast response [84]. The power gradient of an existing supplier of frequency reserves using flywheel energy storage is calculated to compare it with the power gradient of the FC and battery of the FCEV. The maximum power output of the individual flywheels is equal to 100 kW. The flywheels reach a full range response in 4 seconds. This implies that they have a relative power gradient of $25\frac{\%}{s}$ [85] [86]. This is in most cases a lower gradient than the battery and the FC of the Hyundai ix35. Only when the FC ramps down with a 5 kW V2G setting, it has a lower gradient which is equal to $21.7\frac{\%}{s}$. From these results it can be concluded that the FC and battery are at least as good as the flywheel to provide fast frequency response.

If the relative power output of the battery and the FC is compared with the V2G power input value, the FC is faster when ramping upward and the battery is faster when ramping downward. This is the same result found when considering the absolute power gradient. This is caused by the duality of the function of the FC. The FC is the main power source of the FCEV and charges also the battery. When the battery needs to be charged, the FC reaches higher power outputs than the V2G setting. For this reason, it reaches also higher power gradients compared to the battery when it ramps upwards and not when considering downward power gradients. These values are shown in Table 3.3. The different results compared to literature are caused by the sizing of the components. Due to the fact that the FC is the main power source and has a capacity of 100 kW it is able to reach higher power gradients compared to the maximum capacity of 24 kW of the battery.

Table 3.3: Relative power gradients of the battery and the FC compared to the maximum V2G input signal.

[%/s]	**FC ↑**	**Battery ↑**	**FC ↓**	**Battery ↓**
5 kW	765.8	493.3	-434.3	-591.8
10 kW	602.2	499.7	-444.1	-572.6

In the current EMS of the Hyundai ix35, the FC and the battery always alternate each other when operating in V2G mode. Even higher power gradients could be achieved if the FC and battery power are combined and activated or deactivated simultaneously. Additional information about the datasets of the experiments can be found in Appendix B.

3.3.3. Full activation time

The high power gradients result in an sub second activation time of the FCEV. For the fastest reaction (5 kW, FC, upward) it will take 0.13 seconds to ramp from idling condition to 5 kW power output. For the lowest power gradient (5 kW, FC, downward) it will take 0.23 seconds to reach -5 kW. The values are represented in Table 3.4.

Table 3.4: Activation time of the battery and the FC for the V2G setting of 5 kW and 10 kW.

[s]	**FC ↑**	**Battery ↑**	**FC ↓**	**Battery ↓**
5 kW	0.1306	0.2027	0.2302	0.1690
10 kW	0.1661	0.2001	0.2252	0.1746

To be able to approximate the FAT, the reaction delay needs to be summed up to the reaction time. To estimate a reaction delay, the FAT of similar pilots that are experimenting with frequency reserves, is taken into consideration. The pilots that are considered to evaluate the reaction delay also operate with aggregations of EVs. They offer frequency reserves by increasing or decreasing the charging speed of BEVs. This can be done adapting the software in the charging pole or in the EMS of the vehicle. A list of all the pilots with a brief description can be found in Appendix C.

The reaction delay of these pilots varies strongly depending on the type of aggregation and the used communication system. According to the estimations of the participating pilots, the delay is between 2 and 7 seconds. The maximum allowed reaction delay for FCR is, however, only 2 seconds. The ability to offer FCR is limited due to the relatively long reaction delay. For aFRR the current measured reaction delays are allowed.

While the reaction delay is in the order of magnitude of a couple of seconds, the activation time is an order of magnitude smaller. The decimals of the FAT depend strongly on the type of power source that is used while the reaction delay depends on the data communication system. If the reaction delay of the pilots would be used as an assumption for the reaction delay of the CPPP, the reaction delay is approximately 96% of the FAT. The FCEV is certainly able to offer the frequency reserves but the right communication system needs to be adapted to make sure that the reaction delay is small enough. This reaction delay is considered the bottleneck of the ability to offer frequency reserves. The large reaction delay emphasises the need for a fast communication system between the TSO, the BSP and the balancing resource.

It should, however, be kept in mind that the optimum FAT is not yet determined and depends on the RoCoF. Before considering new communication methods, an evaluation of what the time range for the FAT requirement, is needed. In this research the only dynamic characteristic considered is the RoCoF. It is not evaluated what the effect on other characteristics of the power grid is. Shorter FATs could, for example, cause systematic overshoots of the frequency. Further research should be done to evaluate the effect on the total power system dynamics.

3.3.4. Inaccuracy of the current sensor

In the results it can be seen that, when the FC is the main power source, the average DC power output is circa 0.5 kW lower than the requested AC power given as input signal in the discharge unit. When defining a power output signal of 5 kW, the FC power output is on average equal to 4.5 kW. For a power output signal of 10 kW, the output of the FCEV is equal to 9.5 kW. This can be seen in Figures 3.5 and 3.6 by comparing the values of the signal input and the power output. The first seconds the battery delivers the power, which results in a DC power output of a value slightly higher than the requested AC power. This is correct as the DC power still needs to be converted to AC power, which will cause a

loss of circa 97%. The second part the FC becomes the main power source and the DC power is lower than the requested level.

The offset of the FC is due to the inaccuracy of the current sensor in the car that measures the current form the FC. The maximum global offset current is ±3.5 A. On a total measuring range between -400 and 400 A this represents a small offset. This results, however, in a large inaccuracy of the measured DC FC current when it operates only from 0 to 45 A. A FC electric power inaccuracy of +/- 1.2 kW is possible, when multiplying the maximum global offset current with the average FC voltage of 350V during power production. The actual DC power output of the FC delivering 10 kW and 5 kW should be approximately 10.5 kW and 5.5 kW.

3.4. Conclusion

Subquestion 3: Is the FCEV capable of offering frequency reserves to the future electricity grid?

Considering the results of the experiments, it can be said that the FCEV is capable of offering frequency reserves that could contribute to the stability of the future electricity grid. The measured activation time for the Hyundai ix35 is between 0.13 and 0.23 seconds in the tested power range. If the reaction delay is below 2 seconds, it can be concluded that the FCEV is capable of offering FCR. The FCEV would already satisfy the requirements for aFRR with the assumption that the reaction delay is equal to the delay of the current pilots with BEVs. The hypothetical FAT of the FCEV is well below the current requirements for the FAT in the Netherlands. Even if the required FAT for FCR will be reduced by 80% to improve the frequency stability in a power system with a high RoCoF, the FCEV would be a suitable device to deliver frequency reserves. The FCEV also appears to be quicker compared to other technologies that are currently used as fast frequency reserves like flywheels and other pilots that are being evaluated.

The decimal values of the calculated FAT of the FCEV are strongly dependent on the power source and the EMS of the vehicle. A shorter FAT can be reached by simultaneously activating the FC and the battery. Besides a combined operation of the FC and the battery, the share of power delivered by the two sources could also be adjusted. The current power output of the FCEV is limited to 10 kW because of cooling limitations of the FC and the discharge unit. If the two power sources could deliver simultaneously, the total power output of the FCEV could be increased even further.

The current V2G EMS is not optimised for a high power gradient but focusses on the state of charge of the battery, the minimisation of start-up and shut down of the FC and the temperature of the FC. When considering the FCEV connected to the grid, other objectives and constrains, besides the ones used in driving mode, should be considered to optimise the functionality of the vehicle. In driving mode the EMSs objective is to minimise the fuel consumption. The underlaying assumption for this objective function is that the fuel is more expensive than the electricity used from the battery. This is not per definition the most economical and durable system for V2G operation. A different objective function could be evaluated for V2G operation that considers the technical as well as the financial incentives to switch between the battery and FC power output.

III

Part

4

Conceptualisation of a car park offering frequency reserves

In the previous chapters, it is indicated that a FCEV could contribute to the stability of the frequency by offering fast responding frequency reserves. However, the capacity of one FCEV is too small to participate in the market for frequency reserves. For this reason, an aggregation of multiple FCEVs needs to be considered. In this research the aggregation of FCEVs parked in a car park is evaluated.

Three main concepts needed to be considered to have a complete overview of the system: technical characteristics of the CPPP, relevant actors and market regulations. In this chapter these three aspects, in relation to the car park that offers frequency reserves, are explained. Several assumptions are made to be able to make the specifications of the model in the next chapter. All the assumptions are summarised in Appendix D.

4.1. Technical characteristics of the car park

Considering the results of a scenario analysis that can be found in Appendix E, it is expected that the concept of a car park with FCEVs that operates as a power plant, could become feasible around mid century. For this reason, assumptions needed to be made about the system design. An extensive trade off between different options was made and can be found in Appendix F. The key factors that were relevant for the trade off were the economical feasibility and efficiency of the system.

Figure 4.1 shows a simplified graphical representation of the assumed car park system design. From the national hydrogen grid the car park acquires the hydrogen. The local hydrogen distribution system, that continuously fuels the FCEVs, consists of a low pressure hydrogen distribution network. The vehicles are fuelled through a special socket that transports the hydrogen directly to the FC system in stead of being stored in the hydrogen tank. The FCEVs are plugged into the DC grid of the car park. The DC grid includes all the necessary converters to be able to deliver AC power at the right voltage to the national electricity grid. The vehicles adjust their power output according to the setpoints received from TenneT through the data communication system.

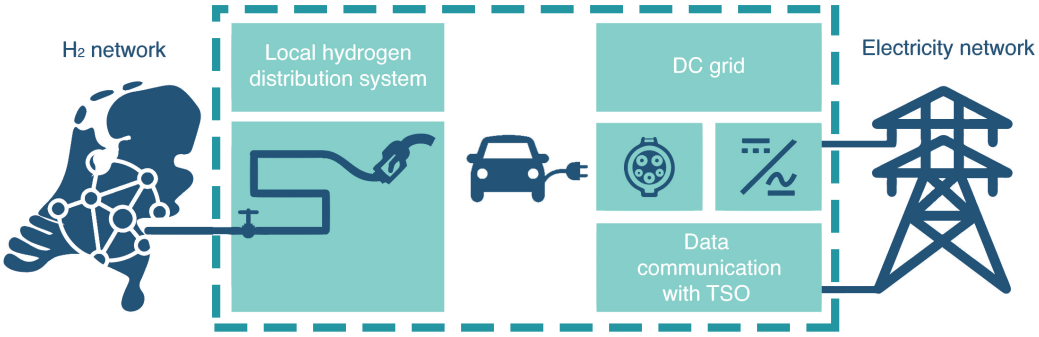

Figure 4.1: Overview of the technical additions required for the car park to deliver power to the grid: the local hydrogen distribution system, the DC grid including the conversion components and the communication system.

The total power that can be delivered by the CPPP depends on the capacity of the total aggregation of FCEVs. The number of available vehicles is determined assuming that all the vehicles in the car park are FCEVs. Two factors determine the amount of available cars in the car park: the size and the occupation pattern.

The size of the car park is determined by the amount of parking places. More parking places per car park implies more potential capacity to offer as balancing reserve. In the Netherlands there is a total of 210,000 parking places in car parks. This excludes the places near hospitals, parking territories and companies. These parking places are divided amongst circa 500 car parks [87]. This means that on average there are 420 parking places in one car park. This amount is considered as the maximum capacity of the car park under study. The location, opening hours of nearby companies and shops, seasonal fluctuations and other factors influence the size of a car park but will not be considered into detail in this research.

The occupation pattern has an influence on the amount of cars that are actually available at the car park. Several occupation patterns will be considered during the analysis but one is used as a base case. This is the occupation pattern of a city car park based on real data from 2016. To make this estimation, which can be considered as a stochastic power source, data from 7 car parks was collected [88]. This data contained the empty parking places in the car parks measured each 15 minutes. This time step was chosen for convenience because it is equal to the ISP of the electricity market and will be the time step in the financial model as well. The average occupation pattern of the 7 car parks of one week is shown in Figure 4.2. The average occupation pattern for one year is used in the financial model as an input variable.

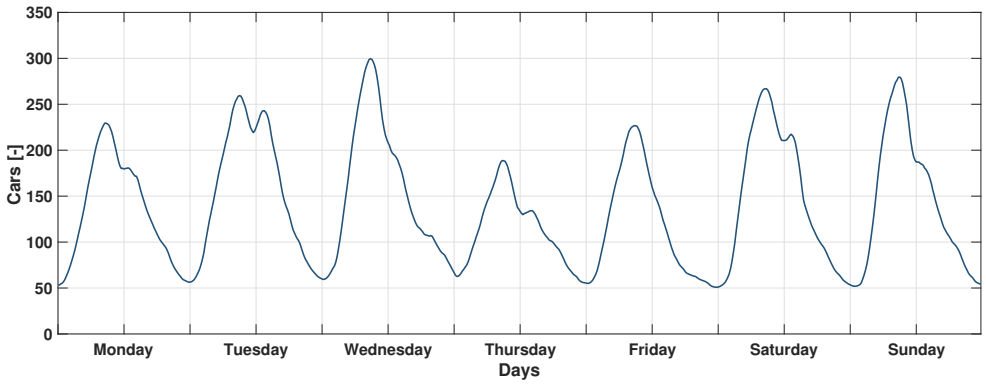

Figure 4.2: Average weekly occupation pattern in a car park with 420 parking places

A high level of accuracy can be reached in the estimation of the occupation of car parks [88]. The development of algorithms and machine learning improves the precision of the estimation. A potential error can be even further decreased by considering the occupation of neighbouring car parks. A smaller lead time can also improve the estimation [89]. For this reason, in the model the amount of available cars and thus the available power was considered as a given value.

4.2. Actors related to the car park

Within the CPPP system there are multiple actors involved. To understand the relevant cash flows that are required to determine the financial potential of the CPPP, the relations between these actors should be understood. The cash flows that result from the interaction between the different actors are indicated in Figure 4.3. The revenues and costs related to the main function, namely operating as a car park, are not considered. This implies that the cash flows described below are additional compared to normal operation of a car park.

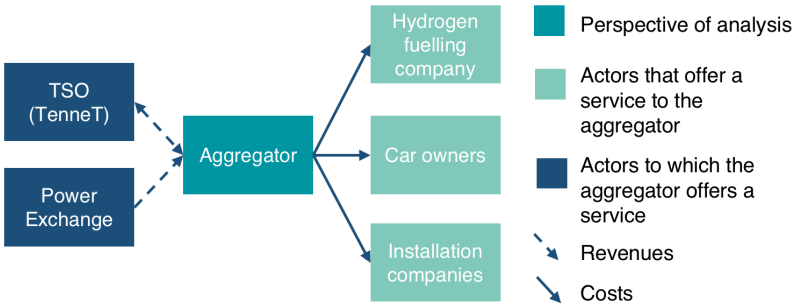

Figure 4.3: Overview of the main actors and the corresponding cash flows for the calculation of the profit of the aggregator.

Car park owner as aggregator The key actor is the aggregator represented as the central block in Figure 4.3. In this research it is assumed that the owner of the car park is also the aggregator. This is reasonable to assume because the owner is usually the actor that decides to invest in new components or services that can be delivered by the car park. The car park owner, which from now on will be referred to as aggregator, needs to adapt the car park to be able to deliver power to the grid.

Aggregator as BRP & BSP The frequency reserves that are considered in this research are FCR and aFRR. The FC of the vehicles is considered the main power source to deliver the reserves. This implies that if the aggregator wants to offer FCR, which has a symmetrical character, the aggregator should also offer a baseload to be able to ramp down. The baseload is the electricity sold on a specific electricity market. The aggregator also has to deliver a baseload if it wants to offer aFRR down. For this reason the combination of three products is considered: baseload, FCR and aFRR (up and down). Where the first is traded on the power exchange, the two latter must be offered on the respective single buyer market for FCR and aFRR. By selling these products the aggregator will receive a payment from TenneT. The specific mechanism of these markets is explained in Section 4.3.

If the aggregator operates as a power plant and offers a baseload, it has to have balancing responsibility and thus be a BRP. The BRP has to send an E-program with the planned transactions for each ISP. This is also required when offering aFRR because during the settlement, the activated reserves must be corrected on the energy balans of a BRP. When offering only FCR this is not appliable. In this research it is assumed that the aggregator does not create imbalance. This implies that the aggregator is not charged for causing imbalance.

Installation companies The aggregator will have to invest to be able to operate as a power plant. The required adaptations are done by the operators specialised for this function. The cost flow to this group of actors, represents the investment costs.

Owners of the cars An assumption is that the cars are not in possession of the aggregator. For this reason the owner of the car needs to be compensated for the degradation of the FC use caused by the aggregator. It is assumed that the cost of degradation represents the minimum price that the aggregator needs to pay to the car owner to compensate for the use. The degradation costs are variable costs of the aggregator.

Hydrogen fuelling company The main energy source of the system is the hydrogen which is used to produce electricity. The aggregator will have to pay the used fuel. The hydrogen costs are, as well as the degradation costs, considered variable costs of the aggregator. These costs are being payed to the hydrogen fuelling company.

4.3. Considered market regulations

The available capacity that the aggregator of the car park has at its disposal, needs to be offered on a market. The Dutch electricity market is a highly complex system that can be approached from many different perspectives. In this section a trade off is made on which electricity market the baseload is offered and a brief explanation is given about the markets for frequency reserves to emphasise the basic decision mechanisms that are considered in the model.

4.3.1. Baseload offered on the spot market

The electricity market can be divided in four submarkets. This subdivision is made based on the time until the actual electricity production and consumption takes place. An overview of these four markets, put in chronological order with respect to the moment of trade, is shown in Figure 4.4. On the forward market, also referred to as the long term market, the largest share of electricity is sold. This is done with contracts of years, quarters or months.

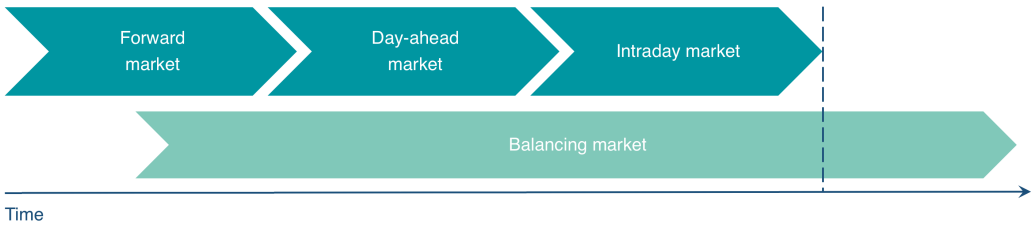

Figure 4.4: Electricity markets in chronological order with the moment of the electricity transmission indicated with the dotted line.

The day-ahead market is the market that takes place one day before the actual transmission of electricity. On this market expected changes in production or consumption can be adjusted. This trade takes place by means of an auction. Bids can be done 24 hours per day starting 45 days before the delivery day. The auction is open until 12.00 of the day before transmission. The auction is cleared and a price per hour is determined by the marginal price on the bid scale [90].

The intraday market opens when the operators of TenneT have checked the balance on the grid, which is usually around 17.00 of the day before the electricity transmission and closes 5 minutes before the actual delivery. This trade also takes place in the form of an auction in blocks of one hour [91].

The fourth market is the balancing market which is this “the entirety of institutional, commercial and operational arrangements that establish market-based management of balancing” [92]. This includes also the markets for frequency reserves. This market is spread over a larger time frame. FCR is traded before the electricity transmission. However for FRR, there is a bidding, activation and a settlement phase. The first phase takes place before the scheduled electricity is produced, the second phase takes place in real time and the settlement phase takes place after the electricity production. The dotted line in Figure 4.4 indicates the moment that the scheduled electricity is being produced.

If the CPPP delivers a baseload, it has to be sold on one of the electricity markets. Due to the variable available capacity of the CPPP, the forward market is not a reasonable option. The day-ahead and the intraday market, referred to as spot markets, offer enough flexibility for the aggregator to offer its capacity. Almost 90% of the electricity that is sold on the spot markets is sold on the day-ahead market and only 10% is sold on the intraday market [41, 93, 94]. The advantage of the intraday market is the short leap time of 5 minutes which gives the aggregator the advantage of being able to estimate more accurately its available capacity.

For most of the time the prices on the day-ahead and intraday market are similar. Only for the 10% cheapest and 10% most expensive hours they differ slightly [93]. A reasonable option for the CPPP aggregator to offer its baseload, would be on these spot markets because of the flexibility. Only the prices of the day-ahead market were available on the ENTSO-e transparency platform. These prices will be used to calculate the revenues obtained from the offered baseload. The minimum bid size of this market is 100 kW.

4.3.2. FCR delivered by the car park

Currently FCR is still contracted through a weekly auction on Tuesday of the week before the activation takes place. The BSP can offer a certain amount of capacity for one week at a certain price. The minimum bid size is 1 MW. The capacity is accepted based on merit order. If contracted, the BSP gets a capacity payment equal to the price of the bid. In the near future the FCR auction will be changed to daily auction and will have a validity period of 4 hours. This is expected to be operational halfway 2019.

The amount of FCR that could be offered by the car park is limited to the minimum capacity constantly available in a week. Looking at the average occupation trends of a car park established in the previous section, the minimum amount of cars is equal to approximately 10% of the maximum capacity. For a car park of 420 places that is equal to 42 vehicles. The maximum amount of FCR that could be offered by one CPPP is then equal to 210 kW. This value is derived by multiplying the number of cars available for FCR (42) times the maximum power output (10 kW) and dividing it by two because of the need of symmetry. This is not enough since the minimum bid size is 1 MW. With shorter validity periods, a higher number of cars available for FCR can be reached, which makes it possible for the CPPP to offer FCR.

When FCR is delivered, a deviation compared to the E-program will be noticed. In the Netherlands this deviation is not compensated because of the distribution of the frequency deviations. In continental Europe this is approximately a normal distribution around zero. The symmetrical character of the frequency will cause the use of FCR to be also symmetrical. That implies that the moments of more power output will be equal to the moments of less output with respect to the baseload. Furthermore the changes of the FCR contribution are measured and monitored by the aggregator. This makes it difficult for TenneT to make adequate settlements for energy compensation.

A difficulty regarding the measurements of the frequency and the activation of FCR is related to the location of measurements. It needs to be determined what the impact is of the FCR contribution of aggregators with assets located geographically in different areas. Depending on this impact, it needs

to be determined if a single frequency measurement point for the entire pool of assets is required or every single asset needs to measure the frequency independently to evaluate the FCR contribution per asset. This aspect of the market for FCR is not considered in this research but does constitute an important development that needs to be evaluated to create an accessible market in the future.

4.3.3. aFRR delivered by the car park

In the market for aFRR there is a capacity as well as an energy payment. There are three options to operate as a BSP on the market for aFRR. The first one regards all the power plants larger than 60 MW. They are obliged by law to offer what they have as FRR, automated or manual. If activated, these BSP get an energy payment for the delivered service. Then there are the BSP with whom TenneT has a capacity contract. Half of these contracts (170 MW) are sold on yearly basis and half on monthly basis. These BSP are obliged to bid in with at least the contracted capacity otherwise they will receive a financial penalty. These providers will get a capacity payment and an energy payment if their bid is activated. If their bid is not activated they will only receive the capacity payment. The third option is for BSP to bid on the auction on a voluntary basis if and to the extent that, they are in possession of power that can be ramped suitably and the technical means for control. These providers will receive only an energy payment if the bid is activated [95].

Contracted aFRR power has no priority over voluntarily offered regulating power; the bid ladder is determined on bid price only, as can be seen in Figure 4.5. The order of the bids determines also the order of activation. If the price of aFRR up is lower than the marginal bid, the bid is accepted. For aFRR down, it is exactly the opposite. The bidding phase closes one hour before the activation of the reserves can take place. The activation is based on the delta-setpoints that are sent by TenneT to the BSP. If the reserves are activated the amount of aFRR used and the corresponding price is calculated during the settlement of the transactions.

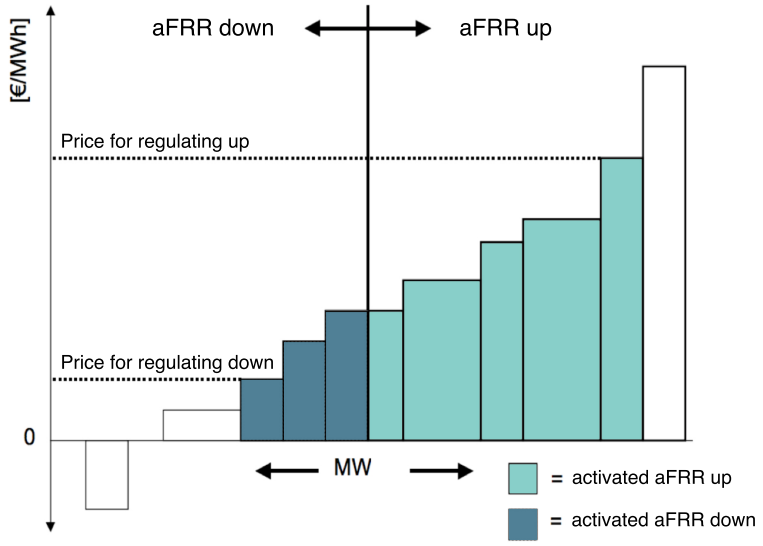

Figure 4.5: Graphical representation of the bid ladder mechanism of aFRR regulation.

The energy payment is in euro per kWh which differs for each ISP. If the price of aFRR up is positive, it implies that the BSP will receive a payment from TenneT to deliver electricity. If the price is negative, the BSP will pay TenneT to deliver electricity. For aFRR down it is exactly the other way around. If the price is positive, the BSP will pay TenneT to ramp its power output down. By ramping down, the BSP saves variable costs. For this reason the BSP is willing to pay to decrease the power output. If the

price for aFRR down is negative, TenneT pays the BSP.

The capacity payment is in euro per MW per year or month depending on the contract. This will not be taken into consideration in this research as the fixed available reserve of the CPPP is not large enough to guarantee the required amount for a yearly or monthly contract. For this reason only energy payments will be considered.

The minimum size of automated frequency restoration reserves that can be offered is 4 MW. TenneT has the intention to reduce the minimum size for aFRR to 1 MW to improve the accessibility of smaller providers on this frequency reserve market. For aFRR the power must be available for 15 minutes, equal to one ISP. This makes it possible to offer larger amounts of reserves at certain moments of the day for this balancing service. Considering the peak moments in the yearly pattern there are moments that the car park is completely filled. This means that 420 cars could operate at 10 kW which is equal to 4.2 MW.

4.3.4. Passive contribution to balance the system

A BRP can deviate from its E-program to help the TSO to stabilise the grid. This is called ”passive contribution” as there is no agreement set up before the transaction of electricity. TenneT publishes real-time the cumulative delta-setpoint that has been sent to all BSP every minute, on their website including the respective price. All BRPs can use this information to increase or decrease their production to help the TSO. If they react in the right direction, they will receive a financial compensation equal to the imbalance price. The risk is that the imbalance can change direction quickly which implies that there is a risk for the BRP that if it increases power output in one moment, in the next it is not required anymore. The BRP needs to pay for the imbalance costs if it deviates in the wrong direction. This mechanism is not implemented in the model.

5

Specification of the financial model

Based on the conceptual model described in the previous chapter, a financial model is developed to estimate what is the business case for the aggregator of a car park that offers frequency reserves. In Appendix E, it was concluded that the share of FCEVs will be large enough to develop a CPPP concept around mid century. For this reason, the parameters required to make the financial model of the car park as power plant are based on estimates for mid century.

5.1. Overal sequence of the model

The financial model is split up in two parts. In the first part the yearly cash flow of the CPPP is calculated. The available capacity of the CPPP serves as the main input variable together with the used frequency reserves and the prices of the offered products for each ISP. For each ISP the input data varies. For this reason, each ISP, the calculations of the revenues and the costs, which are required to calculate the yearly cashflow, need to be repeated. The overal sequence of the first part of the model is represented in Figure 5.1.

Figure 5.1: General mechanism of the first part of the financial model.

First, the amount of baseload, FCR and aFRR that could be offered, is calculated. Secondly, it is checked if the capacity that could be offered, satisfies the market requirements which means that it is checked if the available capacity per product is larger than the minimum bid size. Thirdly, the sold electricity and thus the revenues are calculated. As a fourth step the actual amount of electricity produced is calculated. Once this is done, the costs are determined. As a last step, the yearly cash flow is calculated by summing up all the revenues and costs over the entire year.

The second part of the model combines the yearly cash flow, which is the output of the first part, with the investments that need to be done to operate as a BSP. With these values the net present value and the payback time can be calculated to be able to evaluate the business case of the CPPP.

5.2. Objective function

The first part of the model optimises the yearly profit by setting the baseload and frequency reserves that the aggregator of the CPPP could offer. It calculates the yearly cash flow by subtracting the yearly costs (C_{CPPP}) from the yearly revenues (R_{CPPP}) for different settings of the baseload and amount of FCR offered. The objective function is shown in Equation 5.1.

$$\max_{P_{BL},P_{FCR}} (R_{CPPP} - C_{CPPP}) \tag{5.1}$$

The free variables of the fleet are the amount of baseload and FCR offered. These variables are referred to as degrees of freedom (DoF) or control variables. The baseload per vehicle ranges from 0 to 10 kW. The amount of FCR that can be offered is modelled as three different discrete values. These correspond to the maximum amount (100%), medium amount (50%) and minimum amount (0%) of FCR. The amount of aFRR that can be offered is a consequence of the settings of the control variables. The control variables can take different values independently but are subject to constraints.

5.3. Constraints

In Equation 5.2 the main constraint is shown. The total power output of the aggregation can vary between zero, which is equal to idling condition (P_{idling}), and the maximum amount ($P_{V2G,max}$) which is equal to 10 kW times the amount of vehicles available. As a consequence, also the individual products (baseload, FCR and aFRR) that can be offered by the aggregation, are bounded between these values as shown in Equation 5.3.

$$P_{idling} \leq \vec{P}_{V2G} \leq P_{V2G,max} \tag{5.2}$$

$$P_{idling} \leq \vec{P}_{BL}, \vec{P}_{FCR}, \vec{P}_{aFRR\uparrow}, \vec{P}_{aFRR\downarrow} \leq P_{V2G,max} \tag{5.3}$$

The actual power output of the total aggregation ($\vec{P}_{V2G}$), expressed by Equation 5.4, is equal to the sum of all the individual products. Additional relations are required to express the proportion between the products that can be offered. The offered capacity for FCR must be symmetrical. This does not mean that it must be offered symmetrically by the same car, only the total power output of the aggregation must be symmetrical. This constraint is shown in Equation 5.5. It represents the maximum amount of FCR that can be delivered, which is 100%. By multiplying this value with 0.5 and with 0, the other two options for the amount of FCR that can be offered, are calculated.

$$\vec{P}_{V2G} = \vec{P}_{BL} + \vec{P}_{FCR} + \vec{P}_{aFRR}\uparrow + \vec{P}_{aFRR}\downarrow \tag{5.4}$$

$$\vec{P}_{FCR,max} = min((\vec{P}_{BL} - 0), (P_{V2G,max} - \vec{P}_{BL})) \tag{5.5}$$

The amount of power that is available to deliver aFRR depends on the maximum power output of the aggregation ($\vec{P}_{V2G,max}$), the power delivered as baseload ($\vec{P}_{BL}$) and the power reserved for FCR ($\vec{P}_{FCR}$). For aFRR simultaneous bids can be done for up- and downwards regulation. The amount of aFRR up ($\vec{P}_{aFRR}\uparrow$) is the gap that is left between the maximum V2G power output of the aggregation and the sum of what is already offered. The amount of aFRR down ($\vec{P}_{aFRR}\downarrow$) is equal to the gap between what is

already offered and the idling status, so zero power output. These relations are expressed in Equation 5.6 and Equation 5.7.

$$\vec{P}_{aFRR}\uparrow = P_{V2G,max} - (\vec{P}_{BL} + \vec{P}_{FCR}) \tag{5.6}$$

$$\vec{P}_{aFRR}\downarrow = (\vec{P}_{BL} - \vec{P}_{FCR}) - P_{idling} \tag{5.7}$$

5.4. Yearly revenues (R_{CPPP})

The total yearly revenues are equal to the sum of the revenues obtained from the three different products: baseload, FCR and aFRR. The yearly profit for each product is equal to the summation over all the ISPs (N). This relation is shown in Equation 5.8. To be able to calculate the revenues for each ISP, it needs to be checked if the available capacity for a specific product satisfies the minimum bid size. If this is the case, the available amount is rounded down to the nearest possible bid size that can be offered. Then the payment can be calculated. Depending on the product offered, the specific payment is attributed.

$$R_{CPPP} = R_{BL,year} + R_{FCR,year} + R_{aFRR,year} = \sum_{1}^{N} R_{BL,ISP} + R_{FCR,ISP} + R_{aFRR,ISP} \tag{5.8}$$

The minimum bid size for the baseload is 100 kW and if the capacity satisfies this amount, the aggregator receives an energy payment for the amount of electricity produced. The power available as baseload ($P_{BL,ISP}$) is deployed to generate electricity ($E_{BL,ISP}$) by multiplying the power with the time of one ISP (t_{ISP}). The summation over the whole year constitutes the total yearly revenue for offering baseload, which is shown in Equation 5.9. It is assumed that the aggregator will sell any desired quantity of baseload.

$$R_{BL,year} = \sum_{1}^{N} E_{BL,ISP} \cdot p_{e,ISP} = \sum_{1}^{N} P_{BL,ISP} \cdot t_{ISP} \cdot p_{e,ISP} \tag{5.9}$$

For offering FCR the aggregator receives only a capacity payment. The capacity that can be offered for this product depends strongly on the validity period which is longer than one ISP. For each validity period, the amount of FCR that can be offered, needs to be recalculated. The amount that can be offered in an ISP ($P_{FCR,ISP}$) is equal to the minimum amount available for FCR in that validity period. In the model two different validity periods of 1 week and of 4 hours are considered because the first is the current requirement and the latter will be implemented in the near future. These two values are considered to evaluate the impact of the reduction of the validity period. For the validity period the current average price per week, 2000 euro per MW, is assumed and divided by the amount of ISPs in a week. This results in a payment of 2.98 euro per MW per ISP ($p_{FCR,ISP}$). To obtain the yearly revenues from selling FCR, the summation is done over the total amount of ISPs in a year (N), as shown in Equation 5.10.

$$R_{FCR,year} = \sum_{1}^{N} P_{FCR,ISP} \cdot p_{FCR,ISP} \tag{5.10}$$

For aFRR a distinction is made between aFRR up ($R_{aFRR\uparrow,year}$) and aFRR down ($R_{aFRR\downarrow,year}$) of which the sum composes the total revenues, represented in Equation 5.11. The revenues from aFRR up are

simply the summation over the year of the product between the energy delivered and the price per ISP ($p_{aFRR\uparrow,ISP}$, $p_{aFRR\downarrow,ISP}$). The summation over the year of aFRR down is indicated with a minus sign, because if the price is positive, the aggregator pays the TSO and thus the revenues are lower. If the price is negative, the TSO pays the aggregator to ramp down, and thus the revenues are higher.

Also in this case, the power that can be offered for this service ($P_{aFRR\uparrow,ISP}$, $P_{aFRR\downarrow,ISP}$), is multiplied with the time of one ISP (t_{ISP}) to obtain the amount of electricity produced ($E_{aFRR\uparrow,ISP}$, $E_{aFRR\downarrow,ISP}$). Due to the fact that not every ISP aFRR is required or the amount of aFRR required is smaller than the amount that can be offered by the aggregator, each ISP it must be checked if the amount of electricity that could be produced for this service, is actually needed. If not, the produced electricity for aFRR in that ISP is set to zero. This is done by comparing the electricity that could be produced for aFRR with the used amount of electricity for aFRR in 2016. This is an additional step compared to the capacity sold as baseload and FCR and represented in Figure 5.2.

As explained in Section 4.3 the current minimum bid size for aFRR is 4 MW but it will be changed to 1 MW. For this reason, both settings will be evaluated to analyse the effect of the reduction of the bid size.

$$\begin{aligned} R_{aFRR,year} &= R_{aFRR\uparrow,year} + R_{aFRR\downarrow,year} \\ &= \sum_{1}^{N} E_{aFRR\uparrow,ISP} \cdot p_{aFRR\uparrow,ISP} - \sum_{1}^{N} E_{aFRR\downarrow,ISP} \cdot p_{aFRR\downarrow,ISP} \\ &= \sum_{1}^{N} P_{aFRR\uparrow,ISP} \cdot t_{ISP} \cdot p_{aFRR\uparrow,ISP} - \sum_{1}^{N} P_{aFRR\downarrow,ISP} \cdot t_{ISP} \cdot p_{aFRR\downarrow,ISP} \end{aligned} \tag{5.11}$$

Figure 5.2: Detail of the calculation sequence of the revenues for aFRR.

The amount of aFRR actually activated is small compared to the total amount that a TSO has to have at its disposition. An analysis is done based on historical data from 2013 until 2016. This analysis shows that the probability of a cumulative setpoint being lower than 100 MW each minute, is circa 90%. The probability of being lower than 200 MW is circa 98%. This implies that the largest share of the time, from the 340 MW aFRR that needs to be available, only the lowest bids are activated. In Appendix G the data analysis that supports this analysis can be found. From this analysis it can be concluded that in reality the offered aFRR of the CPPP will be activated only if the reserves belong to the lowest 34% of the bid ladder.

Due to the fact that the position of the CPPP bids on the bidladder have a large impact on the actual activation of the aFRR and the competitiveness on the spot market, an additional check is added to the model. For each ISP it is evaluated, for the baseload and the aFRR, if the marginal costs of the CPPP are lower than the price for electricity on the spot market and aFRR up on the reserves market. For aFRR down it is checked if the marginal costs are higher than the price on the respective market. If this is the case, the bid is accepted and the revenues are attributed to the aggregator. Otherwise the energy produced in that specific ISP will be equal to zero as well as the revenues. This addition to the calculation sequence for the baseload and aFRR are respectively shown in Figure 5.3 and 5.4 with the turquoise blocks.

The marginal costs are assumed equal to the operational costs per kWh. The operational costs, which are explained in detail in the next section, are composed out of hydrogen and degradation costs. Due to the uncertainty about the hydrogen price, a best and worst case for the marginal costs of the CPPP are determined in Appendix H. The two cases are respectively 0.0524 and 0.226 euro per kWh of electricity and will be used during the analysis with the financial model.

Figure 5.3: Detail of the calculation sequence of the revenues for baseload.

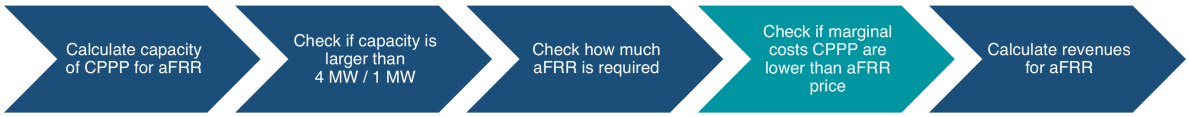

Figure 5.4: Detail of the calculation sequence of the revenues for aFRR.

5.5. Yearly costs (C_{CPPP})

The yearly costs for the CPPP are calculated using the approach of [30] and [96] as a guideline. The yearly costs are equal to the operational costs (C_{oc}) of the CPPP summed over the ISP periods of one year as shown in Equation 5.12. The operational costs consist of purchased energy costs ($C_{pe,ISP}$) and degradation costs ($C_{d,ISP}$).

$$C_{CPPP} = \sum_{1}^{N} C_{oc,ISP} = \sum_{1}^{N} C_{pe,ISP} + C_{d,ISP} \tag{5.12}$$

5.5.1. Costs of purchased energy

The costs of the purchased energy is equal to the price of hydrogen per kilogram (p_{H_2}) times the total amount of hydrogen required (m_{H_2}). This relation is shown in Equation 5.13. The price for hydrogen at a fuelling station is expected to be circa 2 to 4 dollars per kilogram around mid century which corresponds to 1.76 to 3.52 euro per kilogram with an exchange rate of 0.88 euro per dollar [97][98][99][100]. Considering a more hydrogen oriented economy and the assumption of a national hydrogen network, it should be possible to buy hydrogen on an industrial scale from the network. The current price for industrially reformed hydrogen from natural gas is around 1 euro per kilogram [101][102][103]. This value will be used for the financially most optimistic case. These values result is a range from 1 - 3.52 euro per kilogram hydrogen to calculate the variable costs related to the hydrogen consumption. These values represent respectively the best and worst situation considering the hydrogen price and will be used in further analysis.

$$C_{pe} = m_{\mathrm{H}_2} \cdot p_{\mathrm{H}_2} \tag{5.13}$$

The mass of hydrogen required needs to be calculated. For each ISP it is known how much energy is delivered to the gird as it is the sum of the individual products ($E_{V2G,ISP}$). In Equation 5.14 it can be seen that the relation between the electricity delivered to the grid and the required hydrogen depends

on the efficiency of the system ($\eta_{CPPP,ISP}$) and the higher heating value of hydrogen (HHV_{H_2}) which is a constant. The HHV represents the amount of energy contained in one kilogram of hydrogen and is equal to 39.41 kWh/kg [104]. The efficiency is variable and depends on the power output of the vehicles. Rewriting 5.14 results in Equation 5.15 which is the formula used to calculate the mass of the hydrogen required in each ISP ($m_{H_2,ISP}$). The summation over all the ISPs in one year results in the total mass of hydrogen used in one year.

$$E_{V2G,ISP} = E_{H_2,ISP} \cdot \eta_{CPPP,ISP} = m_{H_2,\mathrm{ISP}} \cdot HHV_{H_2} \cdot \eta_{CPPP,ISP} \tag{5.14}$$

$$m_{H_2,ISP} = \frac{E_{V2G,ISP}}{HHV_{H_2} \cdot \eta_{CPPP,ISP}} \tag{5.15}$$

$$m_{H_2} = \sum_{1}^{N} m_{H_2,ISP} \tag{5.16}$$

The produced electricity in one ISP is equal to the sum of the electricity produced for each product as shown in Equation 5.17. The amount of electricity production caused by the activation of the reserves depends on the frequency. To estimate the amount of activated aFRR, the available amount of the CPPP is compared with the actual amount of aFRR that was needed in 2016. This process is explained more in detail in Section 5.4 as it is also required to determine the revenues due to the energy payment.

$$E_{V2G,ISP} = E_{BL,ISP} + E_{FCR,ISP} + E_{aFRR,ISP} \tag{5.17}$$

The calculation of the electricity production caused by the activation of FCR can not be compared with historical data. There is no data available about the activated FCR because the BSP do not receive an energy payment but only a capacity payment. To estimate the energy used for FCR, the frequency of 2016 is considered. Measurements of the frequency were available with a time step of 10 seconds. The average frequency deviation is calculated for each ISP. This will result in moments of positive and moments of negative deviation. The positive deviation corresponds to moments that the frequency is too low and will result in extra costs and degradation because the power output needs to increase. The negative deviation, when the frequency is too high, will result in lower costs and less degradation because the CPPP will decrease its power output. Considering the droop settings for each ISP the average frequency deviation corresponds to a specific power output. This value is multiplied with the time of an ISP to find the electricity produced due to FCR contribution. In Appendix I a detailled explanation is given about the droop en the control setting for FCR.

To estimate the efficiency of the total CPPP ($\eta_{CPPP,ISP}$) an average power output per FCEV ($P_{FCEV,ISP}$) in V2G mode is calculated by dividing the total power output of the CPPP (P_{V2G}) by the amount of vehicles that is available in that specific ISP. The efficiency of the total CPPP is assumed equal to the Tank-To-Grid efficiency (η_{TTG}). It represents the efficiency that includes the transformation from hydrogen stored in the FCEV tank to the AC electricity that is delivered to the grid. This efficiency per vehicle, for a range from 1 kW to 10 kW, is expressed in Equation 5.19 and was determined by previous research [77].

$$P_{FCEV,ISP} = \frac{P_{V2G}}{nr_{vehicles,ISP}} \tag{5.18}$$

$$\eta_{CPPP,ISP} = \eta_{TTG} = \frac{47 \cdot P_{FCEV,ISP}}{0.7 + P_{FCEV,ISP}} \tag{5.19}$$

In Figure 5.5 it can be seen that the efficiency varies non linearly between circa 28% (1 kW) and 44% (10 kW) decreasing sharply at very low power outputs and increases, stabilising at higher power outputs. This non linear relation is mainly due to the fact that multiple mechanisms within the FCEV interfere. The efficiency of the FC stack is higher for lower V2G power outputs and decreases linearly for higher power output. The efficiency losses caused by the BOP contribution show, however, a double exponential behaviour. At lower power outputs the BOP contributions to the system efficiency loss are higher compared to higher power outputs. This is due to the fact that the required power of the cooling water pump, air compressor and hydrogen recirculation pump are relatively higher for lower power output.

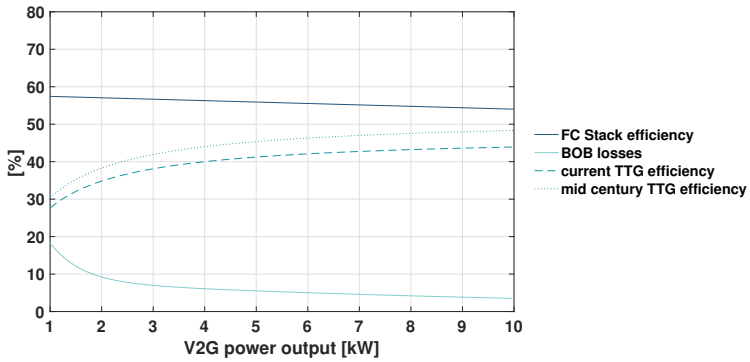

Figure 5.5: The fuel cell stack efficiency, BOP losses and TTG efficiency of a FCEV for a range from 1 to 10 kW in V2G mode.

It is expected that the efficiency of the CPPP will increase in the next years because the Tank-to-Wheel efficiency is also expected to increase [96]. The expectation is that the Tank-To-Wheel (TTW) efficiency will increase from 51.5% near future to 61.0% around mid century. All input variables of this model are based on expected values around mid century. For this reason the CPPP efficiency is increased linearly with the increase of the TTW efficiency. This implies that the used CPPP efficiency in the model is circa 10 percentage points higher respect to Equation 5.19. This efficiency is also indicated in Figure 5.5 with the dotted yellow line.

5.5.2. Degradation costs

The costs for degradation are calculated as wear for V2G due to extra running time on the fuel cell system. It is assumed that all the electricity is produced by the FC. The degradation of the battery is not taken into consideration. The cost per kWh is equal to the capital costs per kW of the fuel cell system (C_{FC}) divided by the lifetime in hours (L_h) as can be seen in Equation 5.20. When this value is multiplied with the total amount of electricity produced per year, it results into the total degradation costs per year. Using the cumulative produced energy, instead of power or voltage loss as degradation indicator for dynamic operated fuel cells, is in line with other research approaches [105].

$$C_d = \frac{C_{FC}}{L_h} \cdot E_{V2G} \tag{5.20}$$

The investment costs of a fuel cell system including maintenance are expected to be circa 26.9 euro per kW around mid century [96]. Lifetime, also referred to as durability, depends on the type of load. The lifetime for stationary load is almost 8 times larger than the load under cyclic driving conditions. The output of the FCEV that delivers balancing services will not be stationary but highly fluctuating. This can be seen from the dynamic behaviour of the frequency in Figure 5.6 which the FCEVs will

need to follow if delivering frequency reserves. In between the yellow lines the dead zone indicates an insensitivity range. Outside this line frequency reserves will be activated proportionally to the frequency deviation or based on the delta-setpoints send by TenneT.

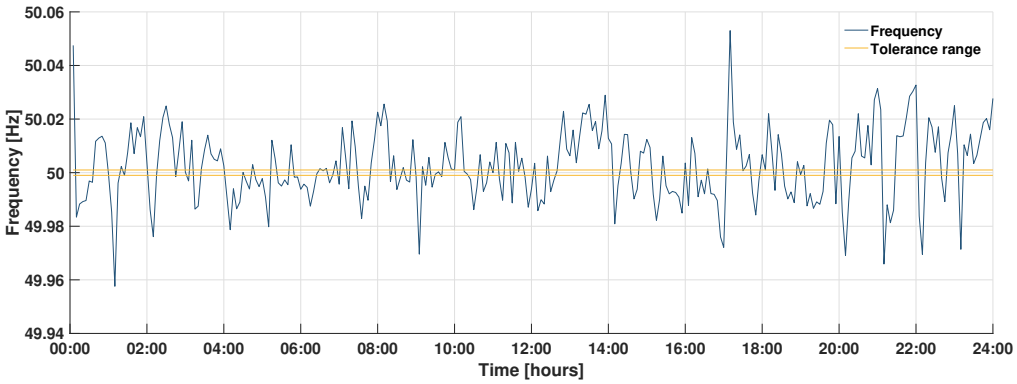

Figure 5.6: Grid frequency on 1-1-2016 with 5 minute average.

It is however too conservative to assume that the durability of a FC of a vehicle in driving mode is equal to the durability of a FC that offers frequency reserves. The ramp that the FCEV needs to cover for frequency control, is maximum 10% of what the ramp would be under driving conditions. When offering FCR the FCEVs must react proportionally to the frequency deviation. The average frequency deviation in 2016 is equal to 15.8 mHz. Considering that at a frequency deviation of 200 mHz the FCR must be fully activated, the ramp is on average only 8% of the maximum FCR output, which is only 0.8% of the maximum power of the FCEV. For the baseload and aFRR the ramp will be higher but still significantly low compared to the FCEV in driving mode.

In previous research it is assumed that every produced kWh for electricity balancing is causing 50% of the degradation as produced kWh in driving mode [96]. Therefore the degradation costs from formula 5.20, considering the lifetime of the FC in driving mode, are multiplied by 0.5. For mid century it is expected that the lifetime of the FC in driving condition is around 8000 hours [96, 106].

5.6. Investment costs

In the second part of the financial model the investment costs are considered to be able to evaluate the NPV and the payback time. It is assumed that the starting point is an existing car park to which several technical components need to be added. In Section 4.1 these components have been explained. The three main additions are the local hydrogen distribution system, the DC grid and the data communication system. As can be seen in Equation 5.21, the total investment costs (C_{ic}) are equal to the sum of the capital costs (CC_i) of each additional components (n).

$$C_{ic} = \sum_{1}^{n} CC_i \tag{5.21}$$

To calculate the payback time (t_{PB}), as shown in Equation 5.22, the investment costs (C_{ic}) are divided by the yearly cash flow (CF_{year}), which is assumed constant each year. The payback period does not take into consideration the time value of the cash flow and may not present the true picture when it comes to evaluating cash flows of a project. Therefore it is combined with the NPV which considers the discount rate.

$$t_{PB} = \frac{C_{ic}}{CF_{year}} \tag{5.22}$$

To determine the NPV, the cash flows (CF) of each year (t) over the lifetime (L) of the CPPP are discounted to its present value and summed up as can be seen in Equation 5.23. At t_0 the investment is done, afterwords the yearly cash flow is assumed constant and equal to the value determined in the first part of the financial model. These calculations will be done for the worst and best case marginal costs and for different expected lifetimes of the project. A discount rate (r) of 3% is assumed.

$$NPV = \sum_{1}^{L} \frac{CF}{(1+r)^t} \tag{5.23}$$

5.6.1. Local hydrogen distribution system

Every vehicle can be connected with a flexible hose to the local hydrogen network. Suitable piping material would be copper or stainless steel [107]. Estimating the costs of this system around mid century is not straightforward as it depends on many factors like the development of the required technologies and the development of the market. Average costs of the nozzle, hose and breakaway ensemble are not publicly available. Experts have been approached to give an estimation of the costs for these components but they vary too much to rely on this information. For this reason a plausible assumption has been made that, based on the advice of one of the experts, due to the characteristic of the transportation mechanism of hydrogen as a gas, it is similar to the transportation of natural gas in urban areas.

The assumption is made that around mid century the costs for low pressure hydrogen distributions systems will be approximately similar to the distribution systems of natural gas now [107, 108]. The costs for the car park will be translated into costs per parking place. The costs per parking place include all the costs related to the local hydrogen distribution system. The costs per parking place are assumed equal to the connection costs with the local gas network for a standard household. This is equal to approximately 900 euro per connection [109, 110].

5.6.2. DC grid

The DC grid represent the ensemble of the wires and all the converters (DC/DC and AC/DC) required to connect the vehicles to the national electricity grid. Also for this system it is difficult to estimate what the costs will be around mid century as low voltage DC equipment is currently not yet available on a large scale. There are also no standards yet, regarding low voltage DC networks which makes it difficult to estimate the exact settings of the required components.

It is however, expected that in the future the amount of DC grids on distribution level will increase considering the wide range of DC applications and higher efficiencies that can be obtained [111, 112]. A potential increase in the DC low voltage market will stimulate the development of the technology and cause a reduction in costs. The costs to connect the FCEVs to the national electricity grid are estimated equal to the current costs to make a V2G connection point in a car park. These costs are equal to 1750 euro per vehicle [113]. It is assumed that these costs include all the components required to operate the FCEV is V2G mode.

5.6.3. Data communication system

The costs of the physical installation of the current data communication system are highly dependent on the distance from a substation and the possible contract advantages with telecom providers. For this reason no exact value can be estimated. It is however expected that the costs for the data communication system will be significantly reduced in the future. It is expected that these costs will not be significant compared to the costs for the local hydrogen distribution system and the DC grid. For this reason the costs for the data communication system will be neglected.

The calculation of the total investment costs is a rough estimate based on the current costs of similar systems. The sum of the costs for the local hydrogen distribution system and the DC grid are equal to 2650 euro per connected parking place. This gives a total of 1,113,000 euro for 420 parking places. Due to the high uncertainty of this value, it is taken into consideration in the sensitivity analysis.

6

Analysis of a car park offering frequency reserves

During the conceptualisation of the CPPP design and specification of the financial model, it became clear that there are many changes in the market regulations and uncertainties about technical as well as economic parameters. For this reason, the impact of these aspects was analysed with the model to be able to draw more concise conclusions about the business case of the CPPP and evaluate what the best distribution is between the different products that could be offered. These analyses are explained before the final results are presented. At the end of this chapter, before an answer is given to the fourth subquestion, an evaluation of the effect of different input data and a sensitivity analysis can be found, which tests the robustness of the results of the financial model.

6.1. Relevant insights

Several analyses are done to gain insight in the mechanism of the CPPP. The analysis are related to the changing market mechanism and to the major assumptions done. Two market mechanisms are evaluated. The first one is the impact of the changing requirements like the bid size and the validity period. The second one is the effect of the position of the CPPP on the bid ladder, which as an implicit factor incorporates the effect of the hydrogen price. The major assumptions are the occupation pattern of the car park and the continuous fuelling of the cars with hydrogen.

6.1.1. Influence of market requirements

TenneT is adapting the market requirements to increase the flexibility and facilitate the possibility for a divers group of BSP to offer frequency reserves. The ongoing changes regarding the minimum bid size and validity period are summarised in Table 6.1 and named Stage 0, Stage 1 and Stage 2. The changing requirements have a large impact on the potential of the CPPP to offer balancing services. This can be seen in the Figures 6.1, 6.2, 6.3 and 6.4.

Table 6.1: Planned changes of the requirements for balancing reserves

	Stage 0		**Stage 1**		**Stage 2**	
	FCR	aFRR	FCR	aFRR	FCR	aFRR
minimum capacity [MW]	1	4	1	1	1	1
validity period [time]	week	ISP	week	ISP	4 h	ISP

In these four figures the x-axis contains the possible values that one vehicle can offer as baseload. The y-axis show the power that can be offered by the total aggregation. Only the maximum amount of FCR is graphically represented in these figures.The first figure (6.1) shows the summation over a year of the power that could be offered by one CPPP as baseload, FCR and aFRR when there would be no requirements at all. When a check is implemented to verify if the available power satisfies the current market requirements (Stage 0), it can be seen in Figure 6.2 that the moments that frequency reserves can be offered is nihil. Only a few moments in time aFRR can be offered in case of minimum (0 kW) or maximum (10 kW) baseload. This is caused by the fact that the available power is not large enough to satisfy the minimum bid size.

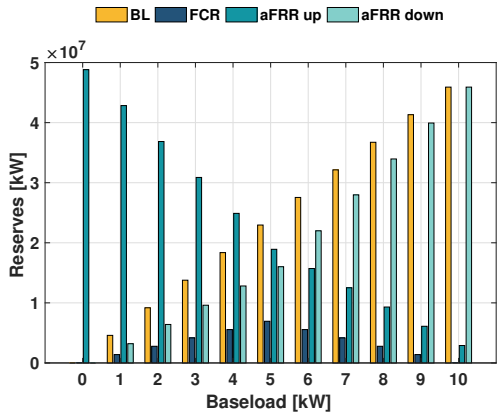

Figure 6.1: Summation over a year of reserves considering no market requirements.

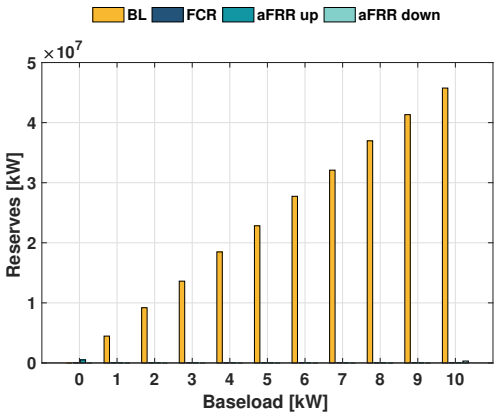

Figure 6.2: Summation over a year of reserves considering market requirements of Stage 0.

In Figure 6.3 the requirements of Stage 1 are implemented. It can be seen that by decreasing the minimum bid size from 4 MW to 1 MW, the amount of aFRR that can be offered increases significantly. The amount of FCR is however, still nihil. Only when the validity period for FCR is reduced from 1 week to 4 hours, which is the case in Stage 2, it becomes possible for the aggregator to offer FCR. This amount is still small compared to the potential shown in Figure 6.1. This is mainly caused by the fluctuating character of the occupation pattern.

The changes occur gradually in the occupation pattern of the city car park . Due to the fact that in each validity period the minimum amount of FCR that can be offered is assumed, this value stays rather small. A more constant occupation pattern or more steep occupation changes would increase the amount of FCR that can be offered.

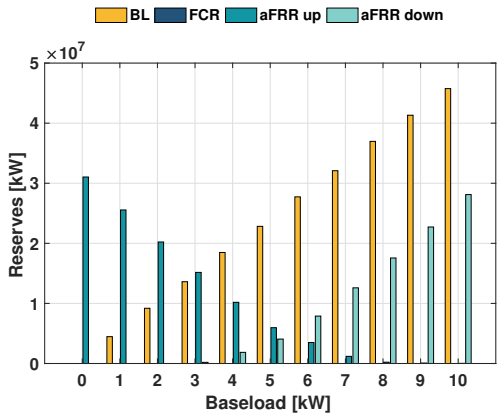

Figure 6.3: Summation over a year of reserves considering market requirements of Stage 1.

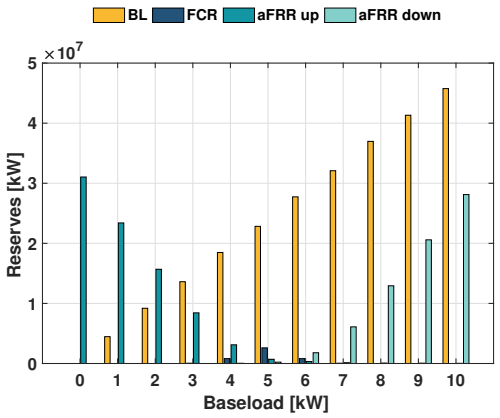

Figure 6.4: Summation over a year of reserves considering market requirements of Stage 2.

From this analysis it can be seen that the changes that are going on in the market for frequency reserves have a large impact on the amount of reserves that can be offered by BSP. These changes open the way towards a system where a larger share of new entrants can participate on the market for frequency reserves. Due to the fast changes, it is unsure what the requirements will be around mid century when the share of FCEVs is large enough to implement the CPPP concept. It can however be seen that the smaller the validity period and the minimum bid size, the larger the amount of reserves that can be offered by the aggregator. For further calculations the values of Stage 2 are used in the model.

6.1.2. Influence of the position on the bid ladder

The potential revenues without considering the order of the bid ladder and thus the effect of the marginal costs of the CPPP, would result in the values presented in the Figures 6.5 and 6.6. The first figure represents the total amount of revenues and the second the revenues per product on a yearly basis. The revenues for aFRR down are negative as this is an amount that the BSP pays the TSO. If the bid ladder is taken into consideration, there are moments that the CPPPs' bids will not be competitive enough to be accepted and thus will the revenues be lower.

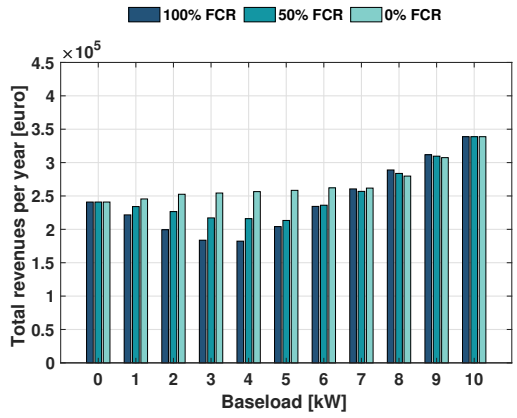

Figure 6.5: Total revenues without considering the bid order for three different amounts of FCR and different settings of the baseload.

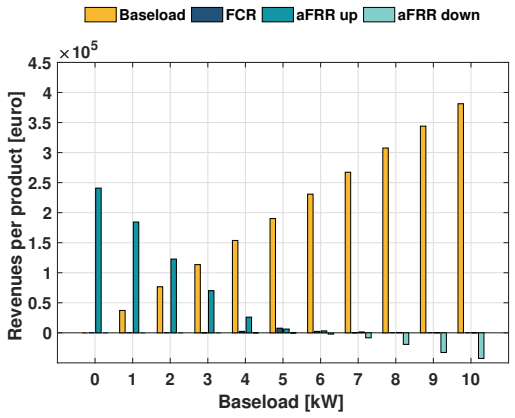

Figure 6.6: Yearly evenues per product without considering the bid order for minimum amount of FCR and different settings of the baseload.

For this reason the position of the CPPP on the bid ladder is checked. Due to the uncertainty about the marginal costs, a worst case and best case estimation is made. When comparing Figure 6.5 with 6.7, it can be seen that the revenues decrease significantly. This implies that considering the worst case for the marginal costs, large share of the time the CPPP is not competitive. It can also be noticed from Figure 6.8, that only on the market for aFRR up the CPPP is competitive. On the spot market the bids of the CPPP are not accepted and as a consequence FCR and aFRR down can not be offered. For this reason there are no revenues related the market for FCR and aFRR down.

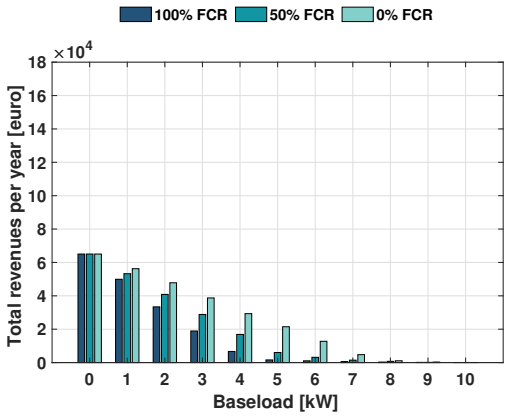

Figure 6.7: Total revenues with worst case marginal costs for three different amounts of FCR and different settings of the baseload.

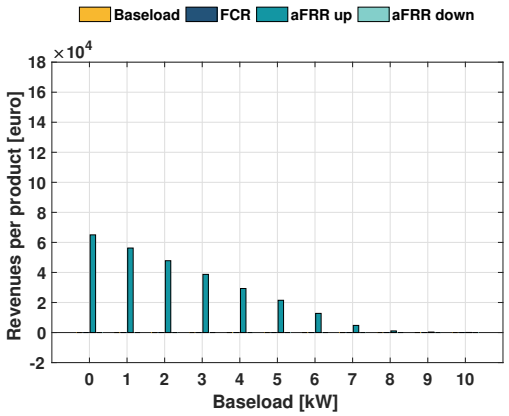

Figure 6.8: Yearly revenues per product with worst case marginal costs for minimum amount of FCR and different settings of the baseload.

When considering the best case for the marginal costs, the CPPP has more than double the amount of revenues compared to the worst case marginal costs. This can be seen in Figure 6.9. Interesting to see, is that, in this case the CPPP becomes competitive also on the spot market, which is indicated with the yellow color in Figure 6.10. Due to this fact, the CPPP can also offer aFRR down and FCR. The amount of FCR that can be offered is, however, to small to be significant and is not visible in the figure.

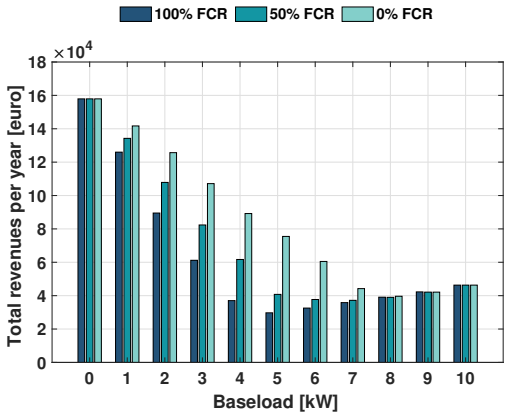

Figure 6.9: Total revenues with best case marginal costs for three different amounts of FCR and different settings of the baseload.

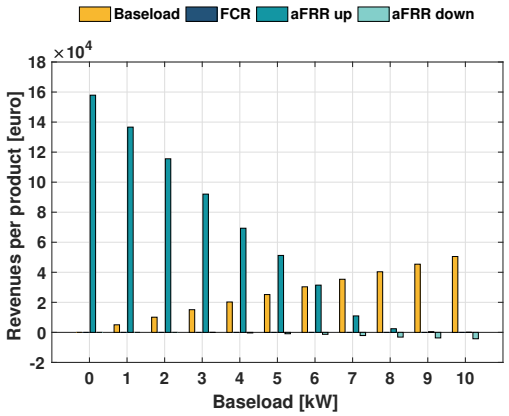

Figure 6.10: Yearly revenues per product with best case marginal costs for minimum amount of FCR and different settings of the baseload.

If more bids are accepted on the ladder, the CPPP has the possibility to offer more electricity and reserves. As a result, besides having more revenues, the CPPP has also more operational costs. The total operational costs for different FCR settings are shown in the Figures 6.11 and 6.12. In the Figures 6.13 and 6.14 a distinction is made between the operational costs for hydrogen and for the degradation of the FC. It can be seen that the largest share of the operational costs come from the purchased energy. On average only 6% of the operational costs come from degradation.

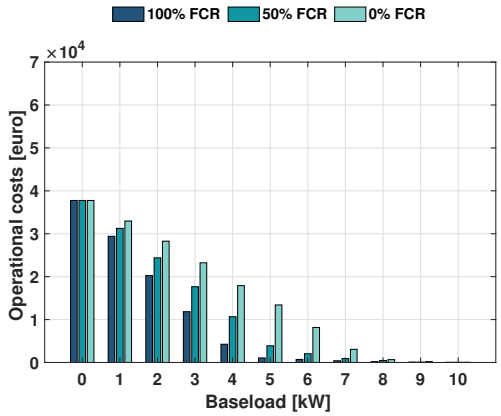

Figure 6.11: Total yearly operational costs with worst case marginal costs for all FCR settings and different settings of the baseload.

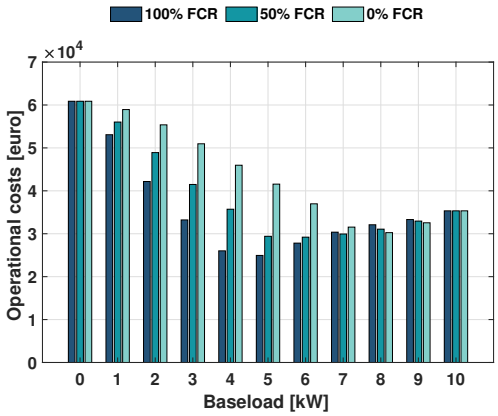

Figure 6.12: Total yearly operational costs with best case marginal costs for all FCR settings and different settings of the baseload.

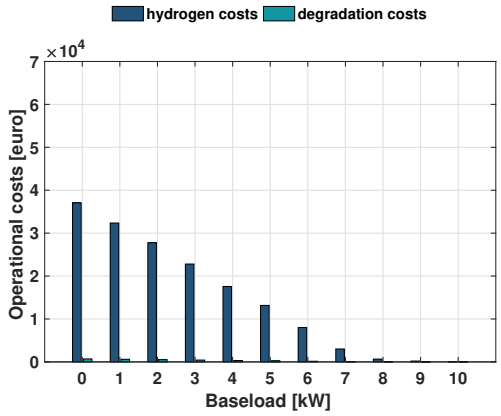

Figure 6.13: Distinct yearly operational costs with worst case marginal costs for minimum FCR and different settings of the baseload.

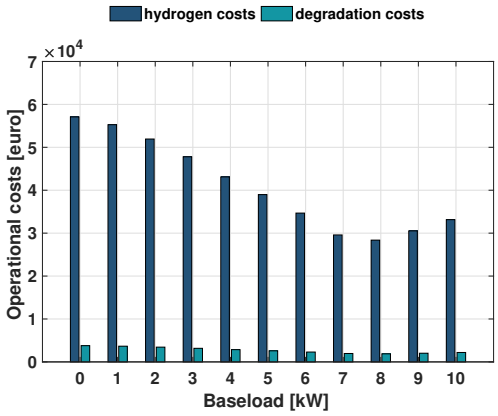

Figure 6.14: Distinct yearly operational costs with best case marginal costs for minimum FCR and different settings of the baseload.

From this analysis it can be concluded that the marginal costs of the CPPP have a large impact on the revenues of the aggregator. For high marginal costs, the CPPP is competitive only on the aFRR up market while for low marginal costs it becomes also competitive on the spot market. It can also be noticed that for both cases of the marginal costs, the operational mode of the CPPP with 0% FCR and no baseload is the most beneficial from a revenues point of view. In this case also the operational costs are higher due to the larger amount of electricity produced compared to the other operational modes.

The marginal costs are based only on the costs for hydrogen and the degradation due to the fact that it is assumed that the FC is the main and only power source. As a consequence to offer FCR and aFRR down, a baseload must be offered. If the CPPP is not competitive on the spot market, no FCR

and aFRR down can be offered, even if on those markets the CPPP would be competitive. If the battery would also have been considered as a power source, there would be more moments that the CPPP could offer FCR and aFRR down due to the fact that the battery can charge and discharge without the need to offer a baseload. The combined use of the FC and battery could increase the financial potential of the CPPP as BSP.

6.1.3. Influence of the occupation pattern

The occupation pattern gives an indication of how long a car is parked in the car park. Depending on the type of car park considered, this pattern changes. The main pattern considered in this research is the pattern of a city car park which is characterised by a gradually fluctuating pattern where cars are often parked not more than a couple of hours. An interesting insight is the effect of a different occupation pattern. Two types of company car parks are analysed and compared with the city car park of the main analysis. One park is considered where the cars are owned by the employees (Employee owned), the other park is a company car park with autonomous driving, company owned cars (Company owned).

Employee owned The first pattern, depicted in Figure 6.15 represents an 8 hour work day that starts around 9:00 and finishes around 17:00. Figure 6.16 shows what the weekly pattern would look like. A maximum value of 420 cars is assumed which is equal to the maximum amount of the city car park. This pattern is repeated 52 times to simulate a yearly pattern. Holidays or other factors that influence the occupation pattern are not taken into consideration.

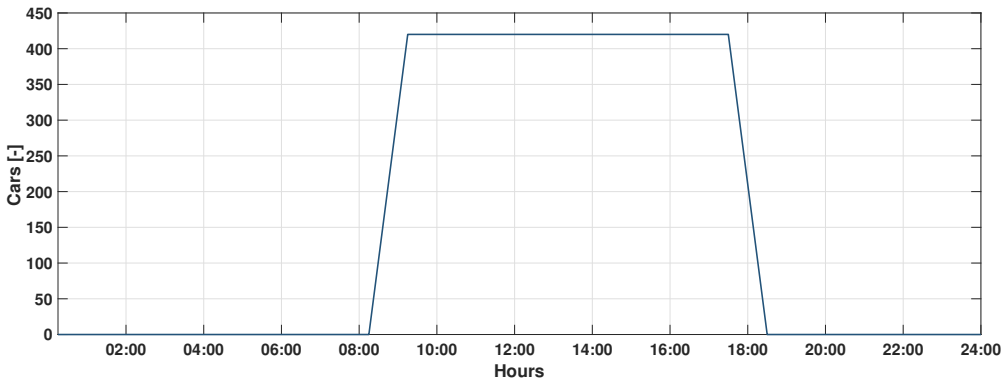

Figure 6.15: Assumed daily parking pattern of a company car park with vehicles owned by employees.

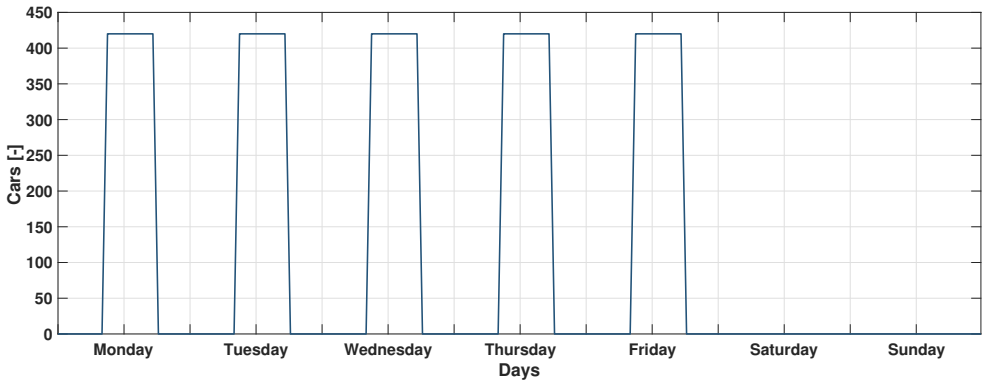

Figure 6.16: Assumed weekly parking pattern of a company car park with vehicles owned by the employees.

The comparison is made to evaluate what the effect is on the amount of reserves that can be offered and the yearly revenues. In the Figures 6.17 and 6.18 the summation over a year of the reserves that could be offered of respectively the city and company car park with cars owned by the employees, are shown. It can be seen that the latter has less capacity available that could be offered mainly due to the fact that the two day during the weekend no cars are available.

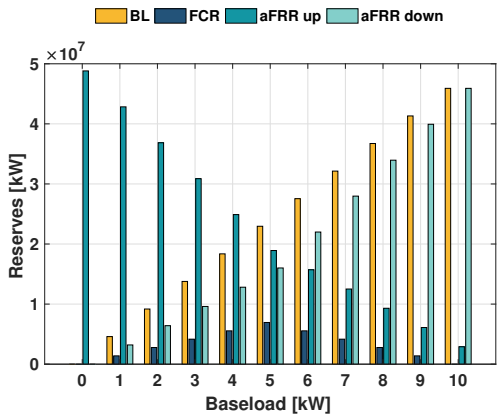

Figure 6.17: Reserves considering no market requirements for a city car park occupation pattern.

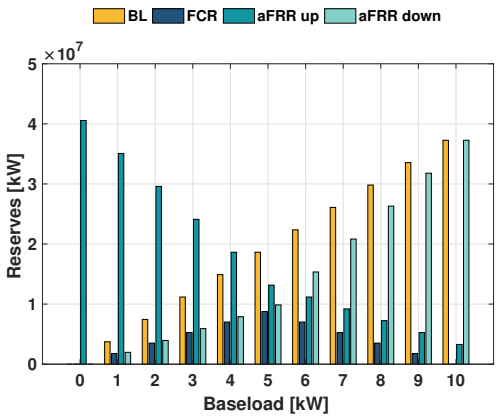

Figure 6.18: Reserves considering no market requirements for the employee owned occupation pattern.

However, when comparing the reserves after the market requirement check and the comparison with the moments that the reserves are actually needed, it can be seen in the Figures 6.19 and 6.20 that the company car park can offer more reserves. In the company park the total reserves available are less but there are more moments that the required reserves coincide with the availability of the reserves.

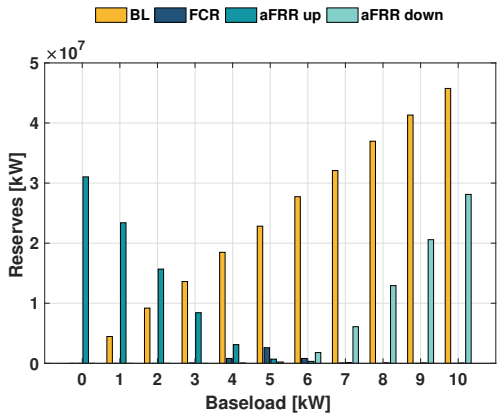

Figure 6.19: Reserves considering the market requirements for a city car park occupation pattern.

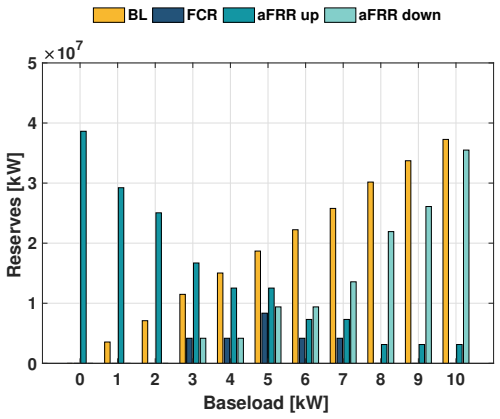

Figure 6.20: Reserves considering the market requirements for the employee owned occupation pattern.

When the position of the CPPP on the bid ladder is considered, the share of reserves and baseload that could be offered, is reduced in both cases. It is however interesting to highlight that in the worst case for the marginal costs, even if the amount of reserves that could be offered is higher, the revenues are lower compared to the revenues of the city car park. This can be seen by comparing Figure 6.7 and 6.21. This implies that for the time periods that the reserves are required and that they are available at the company car park, the prices for aFRR are lower and thus less bids will be accepted. When comparing the revenues on the best case marginal costs, the revenues of the company car park are

higher. This can be seen by looking at Figure 6.9 and 6.22. The financially most interesting combination of products, when looking at the revenues, is still the combination with 0% FCR, no baseload and all available reserves are offered as aFRR upwards.

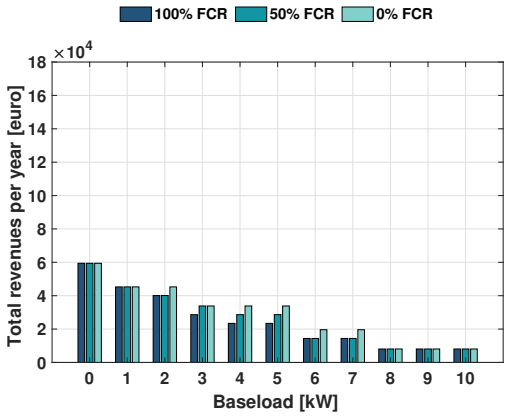

Figure 6.21: Revenues for the worst case marginal costs of the employee owned occupation pattern for three different amounts of FCR and different settings of the baseload.

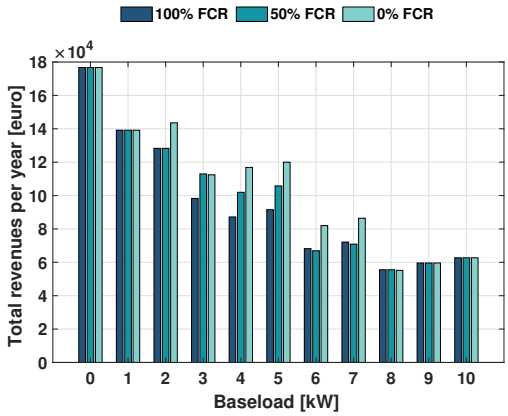

Figure 6.22: Revenues for the best case marginal costs of the employee owned occupation pattern for minimum amount of FCR and different settings of the baseload.

Higher revenues are proportional to the amount of operational hours of the FC system. The more hours the FC system is offering baseload or frequency reserves, the higher the degradation will be. In this model the degradation is translated into operational costs. It is therefore expected that the degradation costs will be higher for this occupation pattern. In the Figures 6.23 and 6.24 the total operational costs, split in hydrogen and degradation costs, can be seen for the worst and best case marginal costs. The costs are indeed proportional to the revenues.

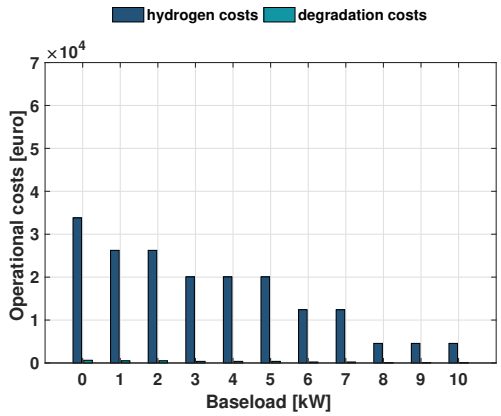

Figure 6.23: Distinct operational costs for the employee owned occupation pattern with worst case marginal costs.

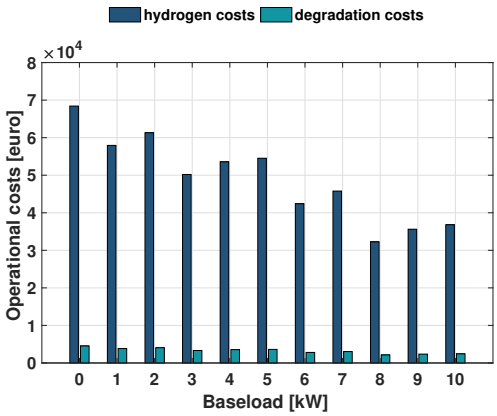

Figure 6.24: Distinct operational costs for the employee owned occupation pattern with best case marginal costs.

Company owned In a future system autonomous driving could become a realistic option. This occupation pattern assumes a different view about the ownership of company cars. Company cars would not be owned by the employees but used to function as a pick up service. This would make it possible to create a constant occupation pattern with a minimum only at the beginning and end of the day when employees need to be picked up an brought back home. With this pattern, shown in Figures 6.25 and 6.26, the occupation could be stabilised for the majority of the day.

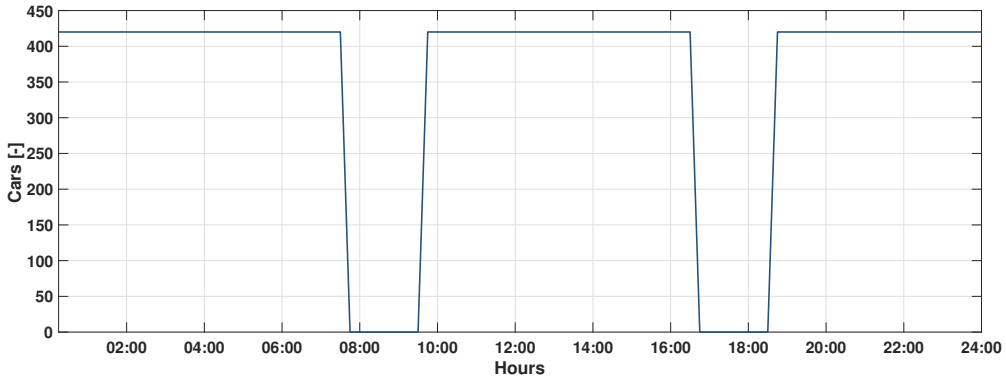

Figure 6.25: Assumed daily parking pattern of a company car park with autonomous driving vehicles.

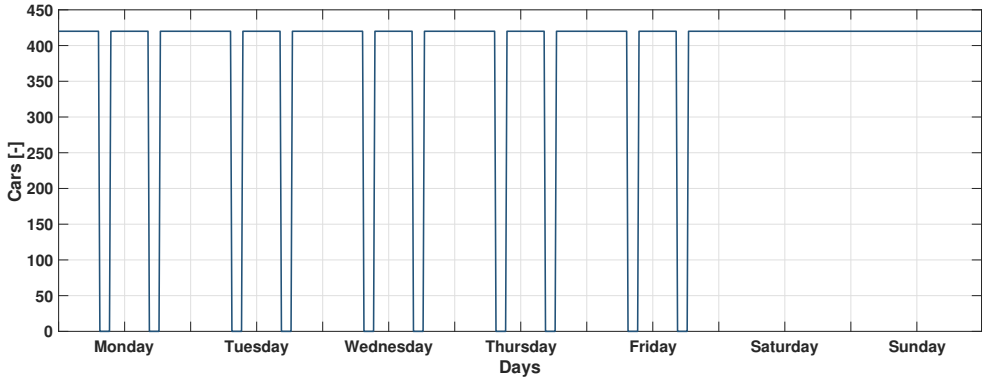

Figure 6.26: Assumed weekly parking pattern of a company car park with autonomous driving vehicles.

In Figure 6.27 it can be seen that the amount of reserves that can be offered is tripled and quadrupled compared to the reserves of the other occupation patterns (6.19 and 6.20). After checking the bid size of the products, the reserves that can be offered are significantly more compared to the other two. This can be seen by comparing the revenues in Figure 6.28 with Figures 6.9 and 6.22. The revenues of the autonomous driving occupation pattern are a factor ten higher. It must be kept in mind though, that by changing the car policy of a company, other changes in the cost flows of the aggregator occur. This is not taken into consideration in this research.

The operational costs, depicted in Figure 6.29 and 6.30, are proportional to the revenues just as for the other two parking patterns. The degradation costs remain only a small share of the total operational costs. The costs for the purchased hydrogen are the dominant expenditures.

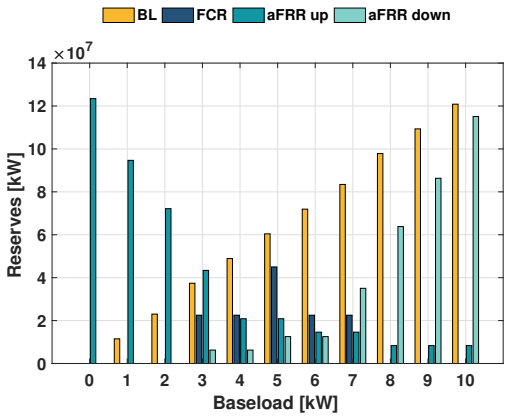

Figure 6.27: Reserves considering the market requirements for the company owned occupation pattern.

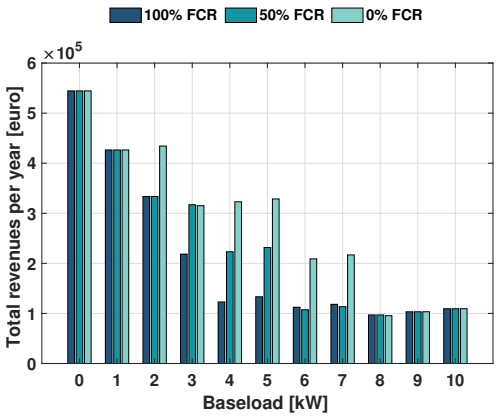

Figure 6.28: Revenues for the best case marginal costs of the company owned occupation pattern.

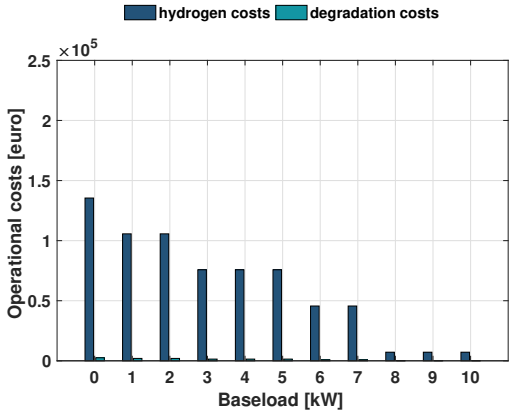

Figure 6.29: Distinct operational costs for the company owned occupation pattern with worst case marginal costs.

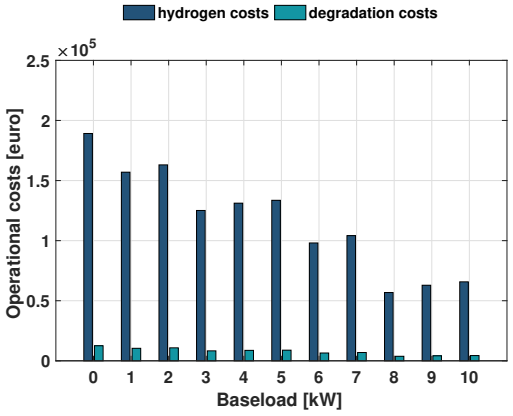

Figure 6.30: Distinct operational costs for the company owned occupation pattern with best case marginal costs.

The assumed parking patterns are rough estimations but they give an interesting insight in the impact of a more constant availability of the power source. Moments of constant occupation increase the probability that available reserves at the car park coincide with the moments that frequency reserves are actually needed. This implies that expanding the power sources of the car park to create a constant power output, would have a positive impact on the revenues of the aggregator. This could be done by adding additional components like electrolytic cells to produce hydrogen on site or by changing the behaviour of the car users. Also the amount of connections available in the car park could have an influence. An optimum amount of connections could be found considering the specific occupation pattern. The amount of vehicles will be taken into consideration during the sensitivity analysis to evaluate the impact on the payback time and the NPV.

6.1.4. Impact of limited hydrogen source

One of the largest assumptions made in the model is the ability to continuous fuel the FCEVs that are parked in the car park. This makes it possible to operate as a power plant without considering the limited amount of hydrogen stored in the fuel tanks of the vehicles. This assumption has a different impact depending on the parking pattern. For example, when the occupation pattern of a city car park is considered, the largest share of the vehicles is parked for not more than a couple of hours. When considering a company car park, most of the cars are parked for circa 8 hours straight. The time that the vehicles stay at the car park, has an influence on the need for a network that can continuously fuel the cars with hydrogen.

Around mid century a full tank is expected to store 6.5 kg of hydrogen. Considering a HHV of hydrogen equal to 39.41 kWh/kg and an efficiency of 50%, a full tank could deliver 128.08 kWh electricity to the grid. If the FCEV would operate at a maximum V2G power output of 10 kW, this would imply that it can deliver power for almost 13 hours. A tank that has only half of the maximum capacity could operate more than 6 hours.

If a short parking pattern is considered, a hydrogen connection would not be essential but does increase the certainty of availability. When considering a company car park with a parking pattern of 8 hours uninterrupted, a limited hydrogen source would not be desirable. Fuel in the storage tank could not be sufficient to generate power the whole parking duration. In this case a fuelling mechanism would be required.

It must also be kept in mind that the vehicles must not be left completely empty. A certain amount of hydrogen must be left in the storage tank of the vehicle to guarantee that the car owner is able to reach the next destination. What this optimum amount is, depends strongly on the hydrogen infrastructure and the available fuelling stations in the neighbourhood of the car park. The development of this infrastructure is still at a very early stage. No strong conclusions can be made regarding the recommended amount of remaining hydrogen in the fuel tank.

6.2. Financial analysis

The result of the first part of the financial model is the yearly cash flow. This serves as input for the second part of the model which, considering the investment costs, calculates the payback time and the NPV of the CPPP. The results are evaluated for the two cases of the marginal costs of the CPPP and the three types of occupation patterns: the city car park (Park 1), the company car park with cars owned by the employees (Park 2) and the company car park with autonomous driving cars that are owned by the company (Park 3).

6.2.1. Yearly cash flow

The yearly cash flow needs to be evaluated to calculate the NPV and the payback time of the investment of the aggregator to operate as a power plant. To calculate the yearly cash flow the operational costs are subtracted from the revenues. In the Figures 6.31 and 6.32 the yearly cash flow is shown for respectively worst and best case of the marginal costs and for variating settings for the baseload.

It can be seen that when comparing the results, the cash flow for the best case is almost three times as large as the cash flow of the worst case. This is interesting, as the best case for the marginal costs are more than four times lower compared to the high marginal costs. The fact that the yearly cash flow is not four times higher, is caused by the effect of the bid order and the marginal pricing which has a reducing effect on the revenues. It can also be seen that the difference between the car parks is smaller for a higher baseload output. This is caused by the fact that less aFRR down can be offered due to the limited competitiveness of the CPPP on the spot market.

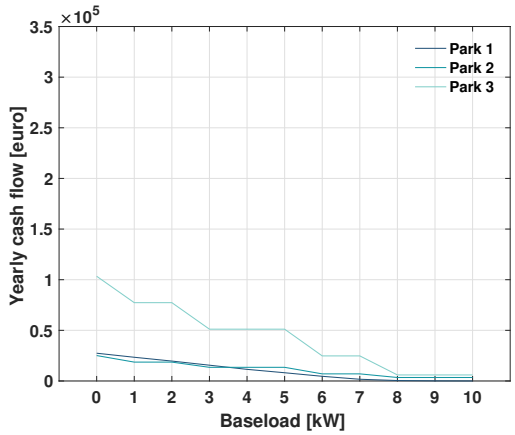

Figure 6.31: Yearly cash flow with the worst case marginal costs for the three types of occupation pattern and considering different values for the baseload.

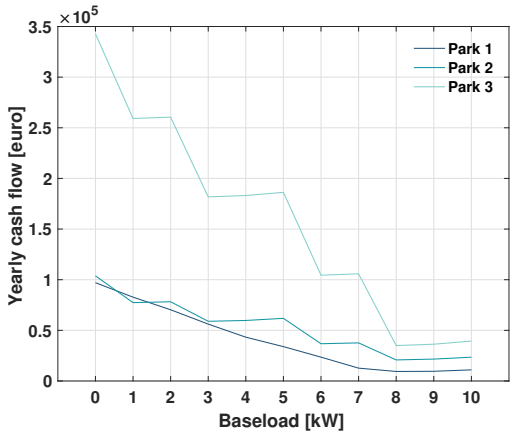

Figure 6.32: Yearly cash flow with the best case marginal costs for the three types of occupation pattern and considering different values for the baseload.

In case of the worst case marginal costs (6.31), the aggregator can compete only on the market for aFRR upwards as established in the previous sections. When considering the best case it can be seen that higher profit can be reached because of the fact that a baseload can be offered and thus also aFRR down. In all the cases a configuration where the CPPP offers no baseload and only aFRR upward would be financially the most attractive option.

As this option is the most profitable, this configuration is assumed for the calculation of the NPV and the payback time. The NPV and payback time are calculated for the worst and best case of the marginal costs and for the three occupation patterns. For the city car park a yearly cash flow range between 27,413 and 97,048 euro had been found. For the company car park where the employees own the cars, the range is between 25,104 and 103,780 euro. For the case with autonomous driving cars owned by the company the range is between 103,407 and 342,790 euro. These values are summarised in Table 6.2.

Table 6.2: The yearly cash flows of the three occupation patterns for the best and worst case marginal costs.

Yearly cash flow [€]	Worst case	Best case
Park 1	27,413	97,048
Park 2	25,104	103,780
Park 3	103,407	342,790

The uncertainty of the prices and the allocation of reserves are however very high. To decrease the uncertainty, it could be an option to spread the chances and offer multiple products, reducing the profit but increasing the possibility of bids being accepted. Another option is to offer passive contribution besides offering only aFRR. For this service there are no requirements and BRP can just increase or decrease their power output according to the needs of the power system. TenneT will compensate these BSP with the price for aFRR in that specific ISP. This is however also an uncertain activity as the imbalance can change during one ISP. If that happens, and the BSP contributes in the wrong direction, the BRP must pay the imbalance costs. The mechanism of passive contribution is explained in Section 4.3.4. How much could actually be earned using this mechanism is unknown and cannot be evaluated with the model .

6.2.2. Payback time

The investment costs per connected vehicle are assumed equal to 2,650 euro. This results in a total of 1,113,000 euro for 420 vehicles. There is a large difference between the payback time of the different type of car parks. It can be seen in Table 6.3 that the company car park with autonomous driving (Park 3) has a payback time that is four times shorter compared to the city car park (Park 1). The main reason is that there are more moments during the day that the vehicles are parked and can offer reserves. This results in higher revenues and thus a shorter payback time.

There is also a significant difference between the payback time of the two cases for marginal costs. In the worst case the payback time is almost four times longer than in the best case. The main reason is the lower competitiveness of the car park on the bid ladder.

Table 6.3: Payback time of the investment costs for the three type of occupation patterns and for the worst and best case of the marginal costs.

Payback time [years]	Worst case	Best case
Park 1	40.8	11.5
Park 2	44.5	10.7
Park 3	10 .8	3.2

Considering that the sectors are changing fast, the payback time for the worst case marginal costs are quite high for Park 1 and 2. All other values are within reasonable margins. It is, however, desirable, that, to obtain a shorter payback time, the occupation pattern of the car park is as constant as possible. This would increase the moments that the car park satisfies the minimum bid size requirement and would increase overall availability for V2G. For the different car parks considered, different incentives could be thought of to stimulate this constant occupation of the car park. This could be done by stimulating users to park longer times by reduced tariffs or offering discount for hydrogen refuelling of their cars.

6.2.3. Net present value

To take into account the discount rate of the cash flow, the NPV is calculated for the worst and best case of the marginal costs and also for the three different occupation patterns. This results in the NPVs shown in Figure 6.33 and 6.34. This is calculated for four different lifetimes of the CPPP project equal to 5, 10, 15 and 20 years. Negative values imply that it is not an interesting investment while positive values indicate there is business potential.

It can be seen that the car park with the autonomous driving pattern (Park 3), is the financially most interesting. This option is even more plausible when considering the current developments in the Netherlands regarding autonomous driving [114]. It must, however, be mentioned that the additional costs for this service, like operating the pick up service, that would be attributed to the aggregator, are not considered. This assumption might cause the results to be too optimistic. The other two car parks become financially interesting only when considering the best case for the marginal costs and a lifetime longer than 15 years.

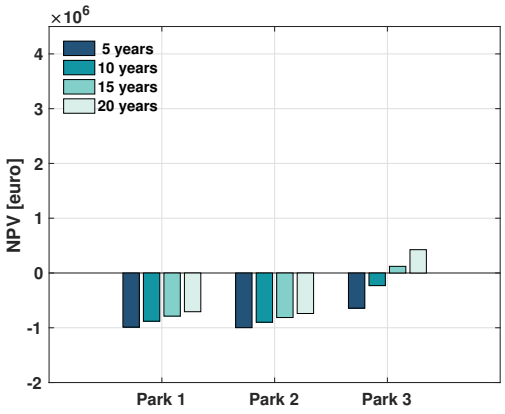

Figure 6.33: Net present value for the worst case for the marginal costs of the three car parks for different lifetimes.

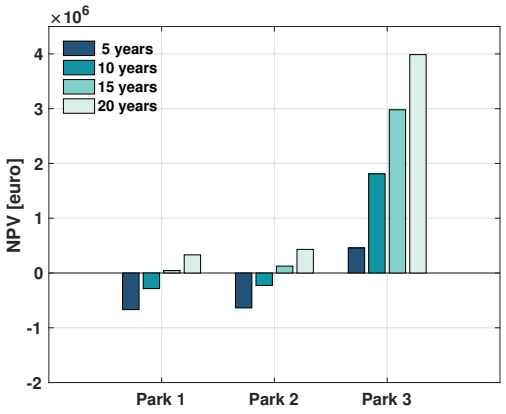

Figure 6.34: Net present value for the best case for the marginal costs of the three car parks for different lifetimes.

6.3. Comparison of different input data

To improve the robustness of the analysis, different data sets are used as input to evaluate if the results are comparable to the results of the used data set in the analysis. The by TenneT activated aFRR and the respective prices of the years 2014 and 2015 are used for the analysis. Based on this data, three aspects can be checkt: the share of aFRR that the CPPP can offer compared to the total amount of reserves required, the match between the moments that the reserves are actually required and the moments that the reserves of the CPPP are available and the impact of the bid order.

In Table 6.4 the results are shown. The three checks of the model are expressed as a percentage of the total sum of the reserves required that year. The check of the bid order is done for the worst and best case of the marginal cost of the CPPP. It can be seen that the total amount of aFRR upward which can be offered by the CPPP is between 3.07 and 4.04% of the total amount of reserves required in the years 2014, 2015 and 2016. The amount of aFRR down that can be offered by the CPPP is slightly lower and lies between between 2.77 and 2.94% of the total amount of aFRR down required in the considered years. This difference is mostly caused by the fact that in all the years the total amount of aFRR down required is larger compared to the amount of aFRR up required.

Table 6.4: Comparison of the reserves that can be offered as aFRR for the years 2014, 2015 and 2016 expressed as share of the total amount of reserves required that year.

		% aFRR up		% aFRR down	
Scenario marginal costs CPPP		worst	best	worst	best
$\frac{\text{Total available reserves CPPP}}{\text{Total required reserves in NL}}$	2016	4.04		2.77	
	2015	3.07		2.73	
	2014	3.50		2.94	
$\frac{\text{Matched reserves CPPP}}{\text{Total required reserves in NL}}$	2016	1.93		1.44	
	2015	1.75		1.51	
	2014	1.82		1.42	
$\frac{\text{Accepted reserves of CPPP on bid ladder}}{\text{Total required reserves in NL}}$	2016	0.11	0.57	0	0.001
	2015	0.001	0.77	0	0.001
	2014	0.001	0.88	0	0.18

When the model has filtered out the moments that no reserves are required and the moments that the CPPP does not have enough capacity to satisfy the market requirements, the share that can be offered is reduced to half of the size. The mismatch between the moments that the reserves are required and the moments that there are actually reserves available is a large loss caused by the fluctuating character of the available reserves and the unpredictability of the required reserves. By stabilising the available power in the CPPP, the share that could be offered, can be increased.

The third and most influential step is the check of the positions of the CPPP on the bid ladder. The share of reserves that can be offered is reduced far below 1%. It can be seen that for aFRR up there is a large difference between the worst and best case for marginal costs. In Figure 6.35 and 6.36 the prices for which the bids of the CPPP are accepted is indicated with the coloured area. It can also be seen that the share of activated bids in 2016 is relatively small compared to the years 2015 and 2014, which corresponds with the data in the table.

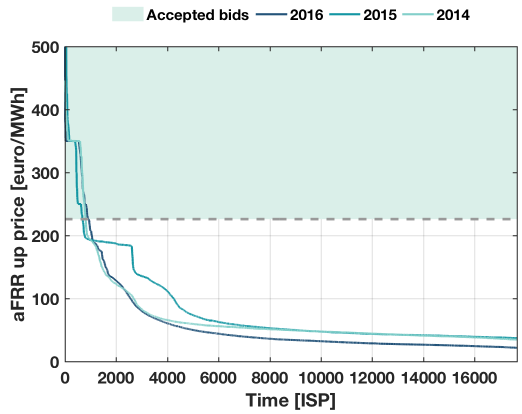

Figure 6.35: Price of aFRR up for the years 2014, 2015 and 2016 with the indication of the area of the worst case marginal costs accepted bids.

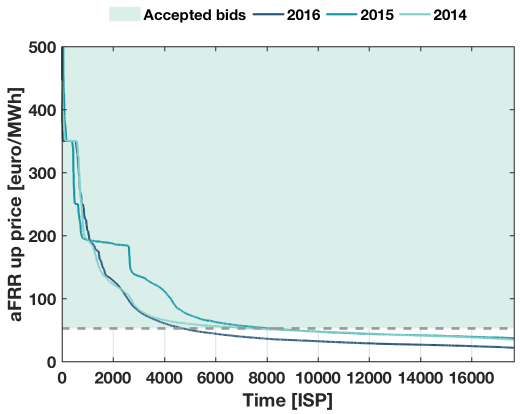

Figure 6.36: Price of aFRR up for the years 2014, 2015 and 2016 with the indication of the area of the best case marginal costs accepted bids.

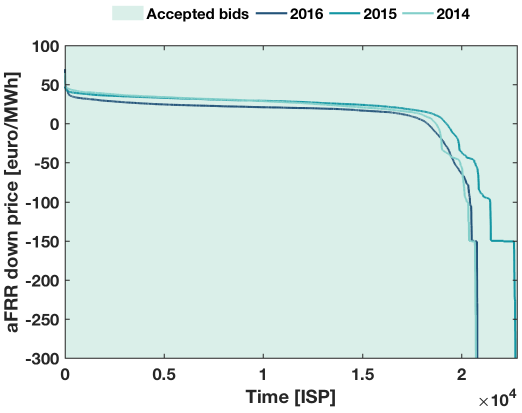

Figure 6.37: Price of aFRR down for the years 2014, 2015 and 2016 with the indication of the area of the worst case marginal costs accepted bids.

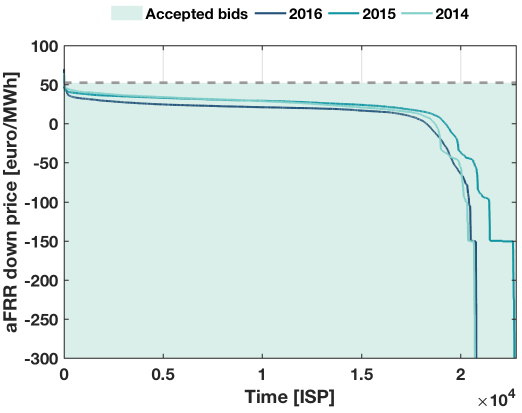

Figure 6.38: Price of aFRR down for the years 2014, 2015 and 2016 with the indication of the area of the best case marginal costs accepted bids.

The Figures 6.37 and 6.38 indicate that almost all the bids for aFRR down should be accepted in both cases. This is not the case. The fact that the share of activated aFRR down is low, is caused by the

relation between the aFRR down and the baseload. To be able to offer aFRR down, the CPPP must offer a baseload in that ISP.

The baseload, which is sold on the spot market, is not competitive for the worst case scenario (6.39) and only a few moments for the best case scenario (6.40). The amount of aFRR up does not depend on another product and the difference between the worst case and best case is purely caused by the bid order.

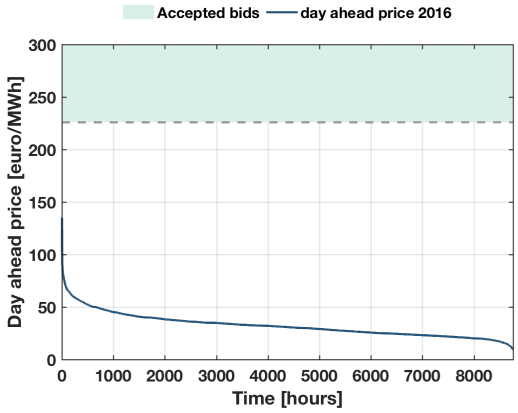

Figure 6.39: Price on spot market for the year 2016 with the indication of the area of the worst case marginal costs accepted bids.

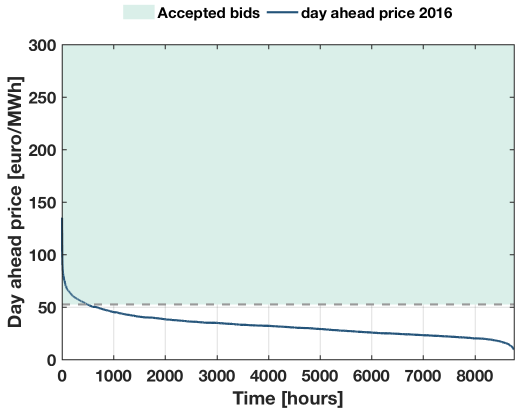

Figure 6.40: Price on spot market for the year 2016 with the indication of the area of the best case marginal costs accepted bids.

The results of the model are similar for different input data. The share of aFRR that can be offered by the CPPP decreases in the same proportions for different input data. The strong influence of the marginal costs and thus the hydrogen price is, however, emphasised by this analysis. For this reason the price of hydrogen will be taken into consideration in the sensitivity analysis.

6.4. Sensitivity analysis

A sensitivity analysis is performed to study how the uncertainty in the output of the financial model can be allocated to different inputs. Several input parameters are changed ±10% and the results are represented in this section. The input parameters that are adjusted are the hydrogen price, lifetime of the fuel cell system, investment costs per vehicle, day-ahead price, aFRR up price, aFRR down price, FCR price and the maximum amount of connected vehicles in the car park. These parameters are considered the most uncertain variables in the model or interesting parameters that could be adjusted to increase the NPV or decrease the payback time. The sensitivity analysis is performed for the city car park. To calculate the NPV a lifetime of 15 years is assumed. For both marginal costs cases the analysis is performed.

In Figure 6.41 the effect on the payback time is evaluated for the worst case marginal costs and in Figure 6.42 for the best case marginal costs. The 0% indicates the outcome with the original values of the parameters. It can be seen that the effect of the investment costs, the price for aFRR down, the price for FCR, the price on the spot market and the lifetime of the FC system, is nihil in both cases. The average deviation of the parameters that do influence the outcome is approximately 10%. These parameters are the connected vehicles, the price for hydrogen and the price for aFRR up.

The amount of connected vehicles is not an uncertainty but a variable that can be influenced by the aggregator. This is an interesting parameter to adjust to have an influence on the financial potential of the CPPP. It can be seen that by decreasing the amount of connected vehicles with 10%, also the

payback time decreases with 10%. The payback time reacts proportionally to the change of the amount of connected cars due to the fact that not all connections are always required. More connections do not directly cause more revenues. The occupation pattern stays unchanged during this analysis. The optimum value of the connected vehicles should be found because the amount must not decrease more than the minimum amount required to satisfy the minimum bid size.

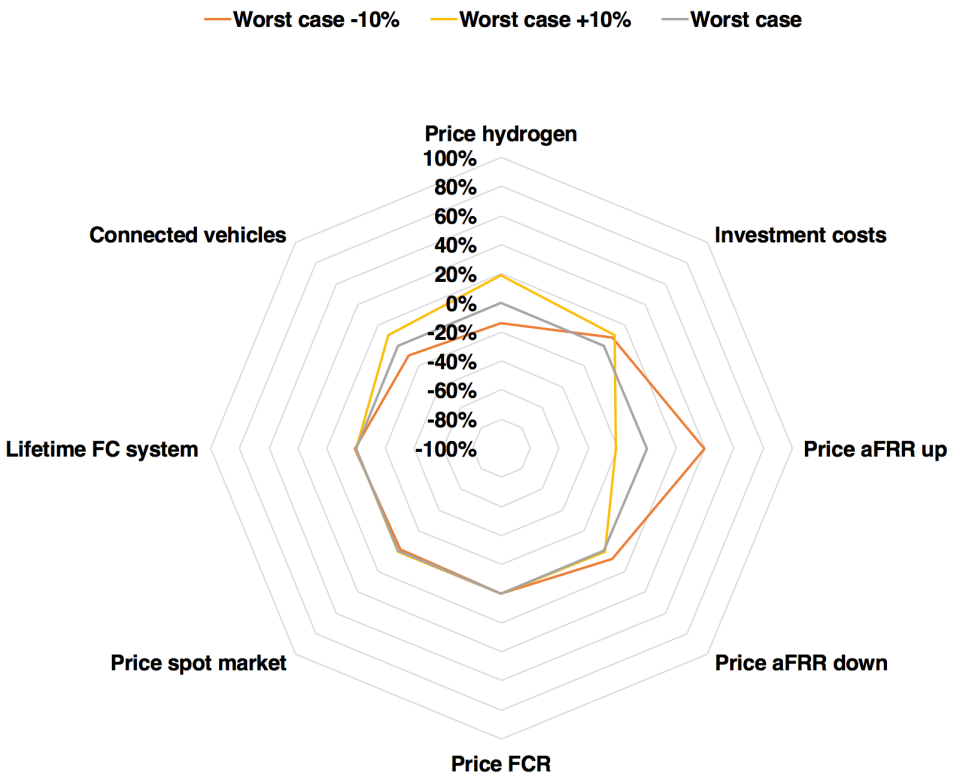

Figure 6.41: Sensitivity analysis of the city car park evaluating the payback time with ±10% worst case for marginal costs.

The other two input variables that cause a deviation in the output of the model, are the hydrogen price and the price for aFRR up. These input variables have a high uncertainty level and are also parameters that strongly influence the outcome of the model. The same behaviour can be seen when considering the NPV of the worst and best case for the marginal costs. This is represented respectively in Figure 6.43 and 6.44. The effect of the changes increases significantly when considering the NPV of the best case for marginal costs. While for all other situations the changes in the outcome are on average ±10%, for the best case marginal costs the changes are factor 10 higher. This is, however, not a completely surprising effect because the NPV is calculated over a period of 15 years. If the yearly cashflow increases or decreases with 10%, this effect will be added to the NPV each year.

In the Figures 6.45 and 6.46 a different graphical representation of the sensitivity analysis of the NPV is given. In these graphs it can be seen that the three variables that strongly influence the outcome of the model and are sensitive for change, are the price for hydrogen, the price of aFRR up and the amount of connected vehicles. All other variables trend lines coincide with the line for the lifetime of the FC systems and do not have a strong impact on the results.

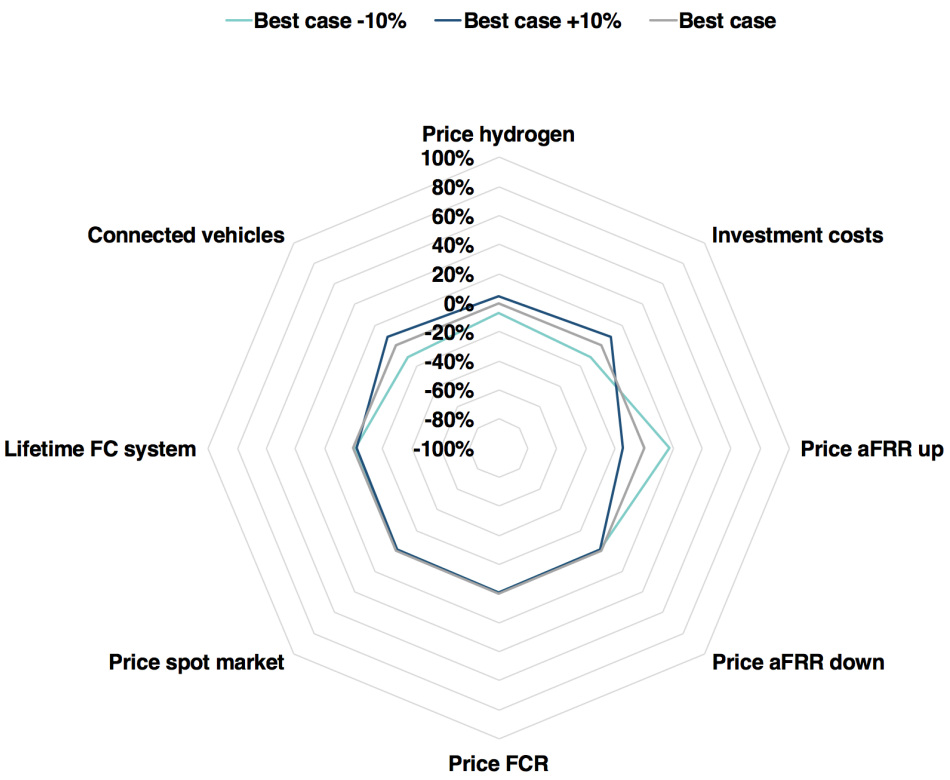

Figure 6.42: Sensitivity analysis of the city car park evaluating the payback time with ±10% best case for marginal costs.

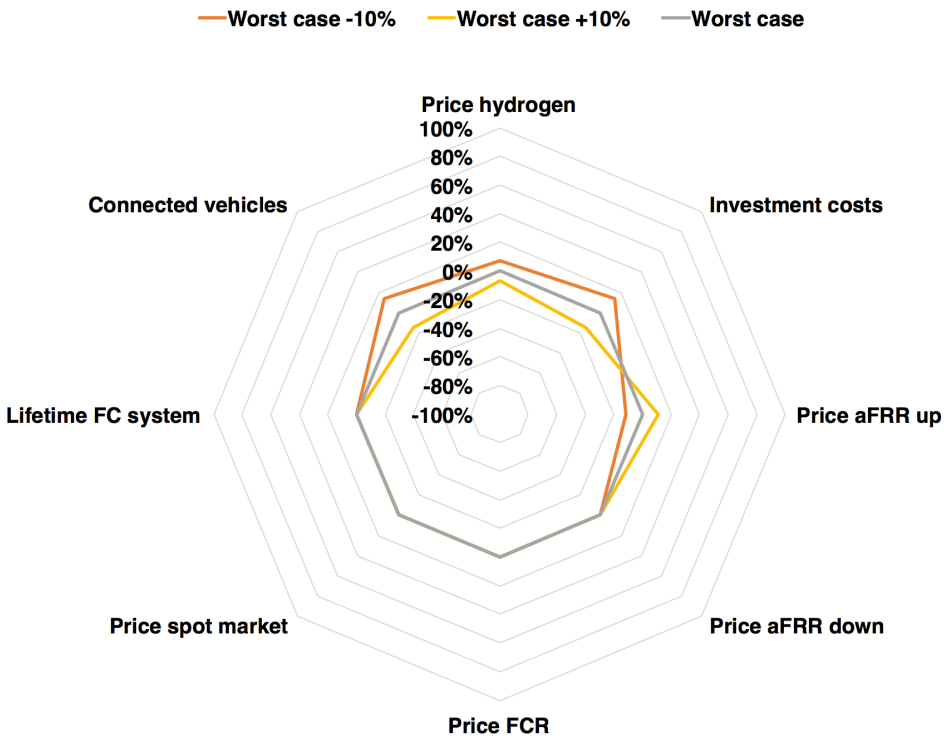

Figure 6.43: Sensitivity analysis of the city car park evaluating the NPV for a lifetime of 15 years with ±10% worst case for marginal costs.

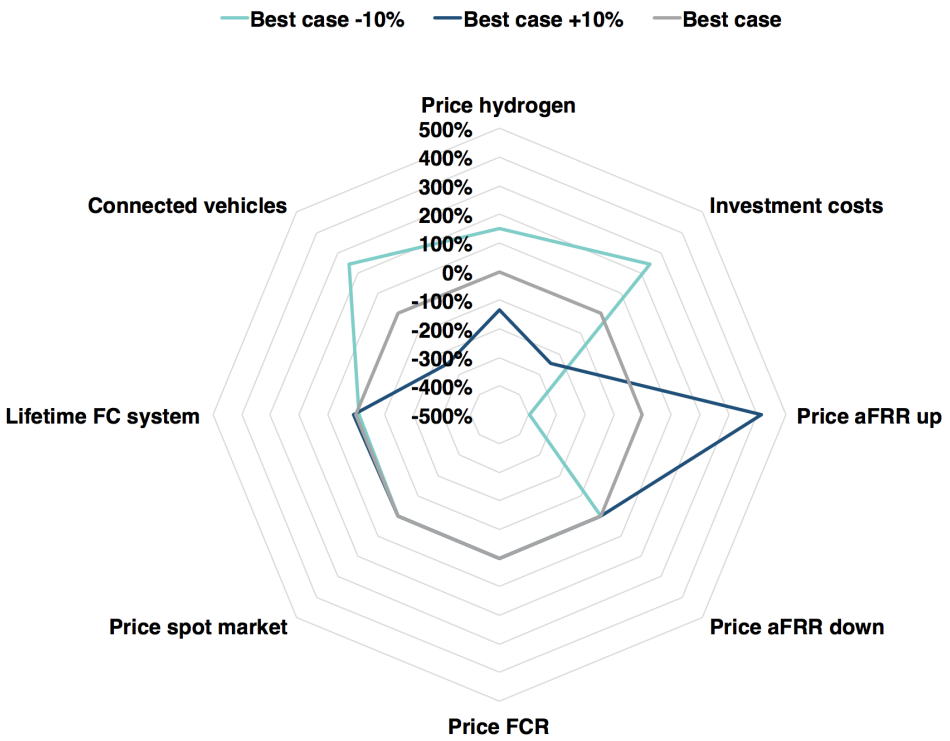

Figure 6.44: Sensitivity analysis of the city car park evaluating the NPV for a lifetime of 15 years with ±10% best case for marginal costs.

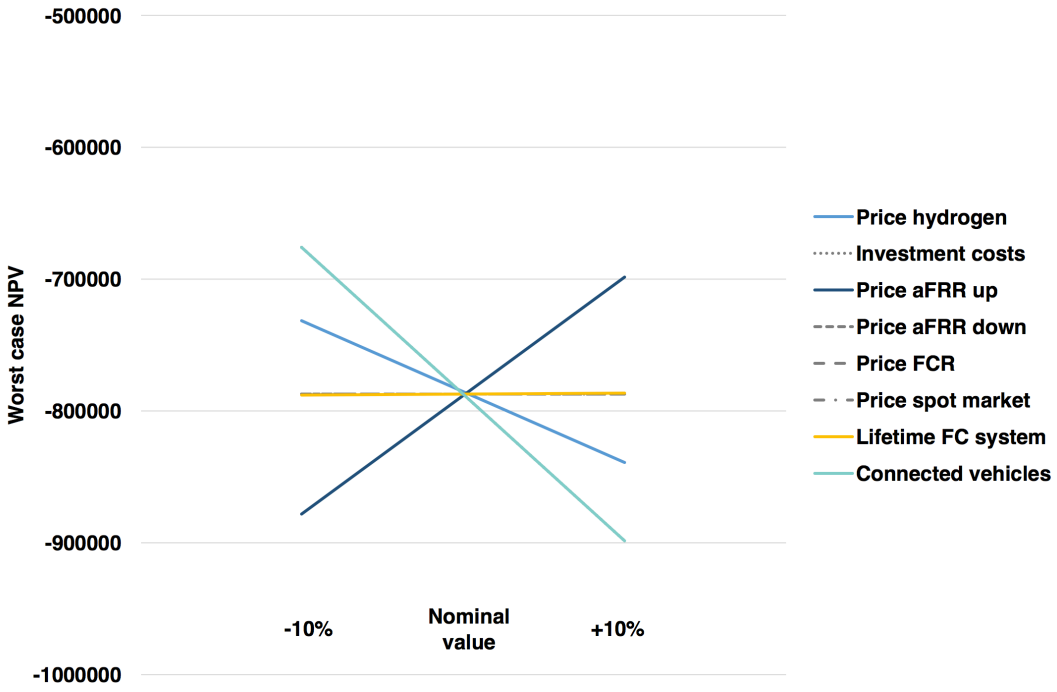

Figure 6.45: Detail of the sensitivity analysis of the city car park evaluating the NPV for a lifetime of 15 years with ±10% worst case for marginal costs.

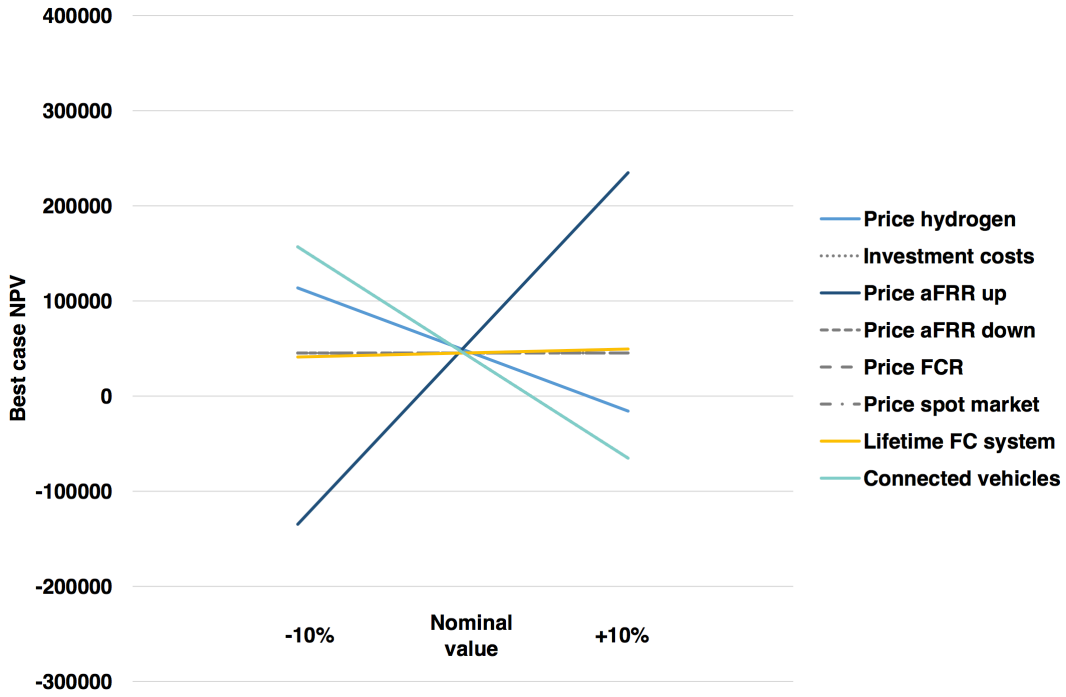

Figure 6.46: Detail of the sensitivity analysis of the city car park evaluating the NPV for a lifetime of 15 years with ±10% best case for marginal costs.

6.5. Conclusion

The fourth subquestions is formulated to investigate if there is a business case for the aggregator of the CPPP to offer frequency reserves and which reserves could be offered. The subquestion and answer are elaborated below.

Subquestion 4: What is the economic feasibility of the CPPP that offers frequency reserves?

When considering the market demand, the position of the CPPP on the bid ladder and the relation between the baseload and the frequency reserves, only a limited amount of reserves can be offered. Due to the fact that the FC is considered the only power source in the financial model, when the CPPP is not competitive on the spot market, no baselaod can be sold and as a consequence no FCR and aFRR can be offered. When also the battery of the FCEV would be considered as a power source, this interdependency could be reduced and FCR and aFRR down could be offered without the need to offer also a baseload. Also the marginal costs of the CPPP could be reduced by using the battery as additional power source. This could increase the competitiveness of the CPPP.

With the first part of the financial model the yearly cash flow of the CPPP was calculated. The highest yearly cash flow, considering the given assumptions, can be obtained by offering all the reserves as aFRR up. This implies that no baseload nor FCR or aFRR down are offered. The easiest way, however, to contribute to the stability of the power system, would be by offering passive contribution. This product can be offered without the need to bid and be activated by the TSO. It is however highly uncertain and unsure how much the yearly cash flow would be by offering this product. There is also the risk that within the ISP the imbalance and as a consequence the price signal changes direction, and the BRP, which in the case of this research corresponds with the aggregator and the BSP, will have to cover the costs related to the additional imbalance. These costs can rise to significant amounts nullifying the

earnings of previous ISPs.

With the second part of the financial model, for different type of car parks, the payback time and the NPV was calculated when only aFRR up is offered. The car park with the most constant occupation pattern, which is represented by the car park with the company owned autonomous driving cars, is financially most interesting. It has a relatively short payback time (3-10 years) and the high NPV compared to the other car parks. The payback time of the other car parks is long considering the fast changing energy market. The uncertainty about earning back the investment would be high. Only a car park with a rather constant occupation pattern would be an interesting investment. This does not necessarily need to be a car park with autonomous driving cars. It can also be a car park where it is stimulated to leave cars parked for longer periods. Another solution could be to extend the CPPP system with additional components like electrolysers or hydrogen storage facilities, which could also be used to offer frequency reserves.

IV

Part

7

Discussion, conclusion and recommendations

7.1. Discussion

The considered system design is limited: The evaluated design of the CPPP is limited. It considers only the cars as potential power sources. To increase the potential of the car park, the design could be extended with additional components like electrolysers that could produce on site hydrogen and local storage facilities. By adding these components there would be additional power components that could ramp up or down when it is economically interesting. Also other power sources like solar panels or wind turbines could be connected to the car park.

Another limitation is that in this research only frequency control of the electricity grid is considered. In a future energy system with more VRES, more moments of electricity surplus could occur. The relation between the hydrogen and electricity network could be integrated further. Systems like the CPPP could offer interesting services to both networks. It would be interesting to evaluate which additional services could be offered by the FCEV and the CPPP to support the grid.

Positive effect of flexibility: There are many changes going on in the balancing market on European level and on national level. TenneT is currently implementing changes to guarantee the flexibility of the market for frequency reserves. The lower minimum bid size and shorter validity period make it possible for other BSP than the conventional ones, to offer frequency reserves. If the amount of required reserves remains constant and a large share of new entries join the market, the market could become more competitive, which will cause the prices to decrease. This will result is lower profits for all the BSP.

While the increase of market participants could have a negative impact on the individual profits of aggregators, it could have a positive impact on the overall costs of the electricity system. The reduction of the price of frequency reserves enables a reduction of the costs related to the balance restoration. Eventually this will result in lower electricity prices which is beneficial for all the electricity consumers.

It must, however, be kept in mind that the increase of VRES could increase the amount of frequency reserves that need to be activated due to the faster and larger frequency deviations. It could cause an increase in costs for stabilising the frequency but there is no continuous function that describes the relation between VRES and required amount of frequency restauration reserves. Fast frequency

reserves, that can be offered by the CPPP, could offer a large contribution to the stability of the system, reducing the amount of aFRR that needs to be activated. Fast frequency reserves offer additional flexibility to the grid operator and could lower the overall costs.

Influence of uncertainties: To be able to make a model that estimates the financial potential of the CPPP that offers frequency reserves, assumptions have been made. With the assumed values, there could be an interesting business case for a car park with a specific occupation pattern. However, the used values neglect uncertainties of several variables and mechanisms. Parameters and mechanisms are changing fast and are highly unpredictable on the long term. In this research, there are two types of uncertainties, namely financial and human.

The financial uncertainties with the largest impact are the price of hydrogen and aFRR. The current hydrogen price depends on old production processes but the market for hydrogen production with renewable energies is developing fast. A lower hydrogen price would have a positive impact on the competitiveness of the CPPP due to the fact that it is the most dominant factor when determining the marginal costs. The closer the marginal costs of the CPPP are to the balancing energy price, the more interesting the concept becomes. The average of 2016 for aFRR up is equal to 0.0314 euro/kWh. Considering that the worst and best case for the marginal costs in this research were assumed equal to 0.2232 euro/kWh and 0.0507 euro/kWh. A reduction of the hydrogen price is necessary to improve the competitive position of the CPPP.

The price for aFRR is also one of the dominant variables in the model. The future value of the price for aFRR and the distribution of this parameter is uncertain due to the fast changing market. It is expected that it will change but in which direction is unknown. The potential increase of new market entries could increase the competition and thus decrease the price. Also by changing the requirements for frequency reserves, there could be a shift in the type of BSP that can offer reserves, which could influence the price.

The human uncertainties in this research are related to the fact that only the main actors are considered. The considered interactions of these actors are also limited to the minimum transactions required. For example, the payment of the car owners to cover the use of the vehicle for balancing services, is limited exclusively to the degradation costs while it could also be interesting to consider incentives to change the occupation pattern in the car park. Another example is the fact that penalties for erroneous bidding or costs related to the deviations from the E-program are not considered. It could for example be financially more interesting to deviate from the E-program and contribute passively to balance the system. The system of the CPPP is a complex social, technical and economical system where interactions between multiple aspects must be taken into account.

The CPPP as example for aggregators: In this thesis the CPPP is assumed as an example of an aggregation. With this analysis it is shown that a BSP with a power source of approximately 4 MW and a competitive price, is a plausible candidate to participate in the market for frequency reserves. The aggregation does not have to be made out of FCEVs. It can be an aggregation of a variety of power sources that can ramp up and down. A suitable market can be determined depending on the marginal costs and the flexibility of the power source. For example, batteries would be suitable power sources for FCR due to the symmetrical contribution which allows the battery to ramp up and down without being fully charged or depleted. Power sources with a larger storage capacity would be more suitable for aFRR up. Large industrial electricity consumers with a flexible power output could be a suitable source for aFRR down.

7.2. Conclusion

The amount of variable renewable energy sources will increase in the coming years, which will cause a reduction of the operational hours of the conventional power plants. These power plants are currently the primary sources of frequency reserves, which are required to guarantee the stability of the electricity grid. This is done by ramping up or down their power output depending on the difference between the electricity generation and load. If the operational hours of these power plants will reduce, there will be a need for other power sources that can offer frequency reserves. It is analysed if the Car Park as Power Plant would be a suitable concept to offer frequency reserves in a future power system. In this thesis the following research question is answered:

What is the technical and economic feasibility of a Car Park as Power Plant offering frequency reserves in a future power system with a low share of conventional power plants?

The future electricity grid will operate with a low share of conventional power plants which implies that there will be less inertia in the system. This causes the rate of change of frequency to increase. Moments that the frequency reaches the maximum instantaneous frequency deviation could occur when 75.6% of the electricity is produced with renewable energy sources. There are multiple options to safeguard the frequency of the power system if the rate of change of frequency will decrease. A possible solution is the reduction of the full activation time of frequency reserves. By changing this requirement the frequency deviation can be stopped earlier which can prevent the frequency from reaching the maximum instantaneous frequency deviation and thus keep the frequency within the standard frequency range.

Both power sources of the fuel cell electric vehicle, which are the fuel cell system and the battery, would be suitable to offer fast frequency reserves. The capacity of one single fuel cell electric vehicle is too small to participate in the market for frequency reserves, therefore an aggregation of a car park is considered.

The Car Park as Power Plant, from a technical point of view, would be a suitable balancing resource to offer FCR, aFRR up and aFRR down. If only the FC system would be used as a power source, from a financial point of view, the most interesting option would be to offer only aFRR upwards. If both power sources would operate simultaneously, there would be more moments that the CPPP could offer also FCR and aFRR downwards. This would increase the yearly cash flow of the CPPP.

The occupation pattern of the car park has a large influence on the payback time and the NPV of the aggregator. When considering a constant occupation pattern in the car park, the cash flow of the CPPP could be increased significantly which results in a shorter payback time and higher NPV. A constant occupation pattern that has a capacity of approximately 4 MW has, for both the worst and best case of the marginal costs of the CPPP and for variable lifetimes, a positive NPV.

This occupation pattern reflects a a company car park that has autonomous driving cars to transport their employees. For an occupation pattern that is more similar to the current use of vehicles, the results are less optimistic. The payback times are on average 4 times larger. The NPV is only positive when the best case for the marginal costs and a lifetime of at least 15 years, is considered.

7.3. Recommendations

The recommendations are divided into three parts. One part focusses on the recommendations for the aggregator, one on recommendations for the TSO and the last part are recommendations for further research.

7.3.1. Recommendations for the aggregator of the CPPP

Combine car parks with different occupation patterns: It would be beneficial to have a more constant power source which in case of a car park would mean that the occupation pattern has to be less fluctuating. Every car park has a specific occupation pattern depending on the location of the car park. By combining the capacity of different type of car parks, the total capacity could be increased and the fluctuations could be reduced. An ideal situation would be to combine the capacity of a car park where people park their car during working hours and a car park where people would park their car if they are at home. This would cover the largest time span off the day increasing the probability that the aggregator has enough power available to offer reserves.

Extend the system of the CPPP: In the discussion it was mentioned that the considered system design was limited. It would be useful for the aggregator to extend the system. A more constant power source would be beneficial for the revenues of the aggregator. It would be interesting to evaluate how the design could be extended to obtain a less variable power source and what impact this has on the business case of the aggregator.

It must be noticed that adding physical components like electrolysers or storage facilities for hydrogen is not the only option to obtain a constant power source. It can also be done by influencing the behaviour of the car owners and stimulating to leave the cars parked for longer periods. Incentives like reduced prices for hydrogen or cheaper parking prices are two examples of such incentives.

The system of the CPPP could also be extended by considering the products of the reaction in the FC. The produced water and heat could, for example, be used for heating purposes of surrounding buildings.

7.3.2. Recommendations for the TSO

Implementation of fast frequency reserves: With this research it has been indicated that faster frequency reserves could contribute to the stability of the frequency under conditions of low inertia. This research focussed on the adaptation of the requirements of existing frequency reserves. Another approach would be to develop a new product with a specific market for fast frequency reserves. Aspects like the minimum bid size, validity period, payment scheme and communication method should be determined. The development of a new product could increase the profitability of aggregators like the CPPP due to the fact that only a limited amount of BSP are in possession of power sources that can ramp up and down according to the requirements of fast reserves.

The reciprocal effect on the frequency of changing the requirements of several frequency reserves is not taken into consideration. Also the effect on other characteristics of the power system that are relevant for the stability of the grid are neglected in this research. Before adapting the requirements or developing a new type of frequency reserve, profound research should be carried out about the effect of shorter full activation times of frequency reserves.

7.3.3. Recommendation for further research

Take multiple power sources into consideration: The impact of the CPPP on the stability of the frequency in future systems, would be higher if it could offer fast FCR. In the financial model the FC was assumed the only power source which added the constraint that a baseload needed to be offered to be able to offer FCR. It would be interesting to quantitatively evaluate what the effect is if both power sources operate simultaneously. For example, the battery could offer FCR while the FC offers aFRR. By considering also the battery as a power source, different marginal costs could be calculated for different type of products. This could have a positive impact on the competitiveness of the CPPP and thus on the yearly cash flow.

The maximum V2G power output could be increased if the DC to AC conversion is adapted to higher power outputs. The FCEV can produce a higher power output and gradient if the FC and the battery operate simultaneously. While a lot of research has been done regarding the energy management system in driving mode, more research should be done regarding the specific optimisation between the power sources in the FCEV when operating in V2G mode [103]. This improvement of the energy management system in V2G mode could also be equipped with a smart interface that can take the market prices into account. This could enable the CPPP to chose a power source based also on financial parameters [38].

It would also be interesting, while designing the energy system of the vehicle, to consider more actively the possibilities of the car while operating in V2G mode. In the current Hyundai ix35 the total amount of energy that can be stored in the vehicle is stored for only 0.44% in the battery (0.95 kWh) and the remaining 99.56% in the hydrogen tank. The current tank can contain 5.5 kg of hydrogen. Multiplying this value with the HHV results in 217 kWh. When considering the capability of the FCEV to deliver frequency reserves, it would be interesting to evaluate this distribution taking into consideration the positive and negative aspects of both power sources and energy storage mechanisms. The battery would be a better source to offer FCR while the FC system would be more suitable to offer aFRR. This optimisation between the energy stored in the vehicles should of course be done taking into account also the main purpose of the car, which is driving, and the needs of the car owners [35, 115].

Evaluate the interaction between actors: The interaction between actors can be decisive in the development of the CPPP. It would be interesting to analyse how all these actors would interact in a CPPP and what the main obstacles are regarding the interaction between these actors. For example, the relation between the car manufacturer, the car park owner and the discharge unit owner is not straightforward. They could all become aggregators that offer power on the market for frequency reserves. However, technically only one will actually deliver the power. Collaborations between these parties would be very useful.

A good example of the complexity of the interactions can be given by comparing the activities of two companies. One is Jedlix, which functions as an aggregator of BEVs and collaborates with the car manufacturers. The software of the BEV is updated with the algorithm of Jedlix, which determines when the car should charge according to price incentives. The signals to start or stop charging are being send from inside the car. The company NewMotion is also an aggregator but in this case it owns and operates charging stations for battery electric vehicles, NewMotion sends signals from the charging station to the car. What will happen if a car that has the software of Jedlix, connects to a charging station that is operated by NewMotion, is still unclear.

V

Part

Bibliography

[1] R. Forrester. History of electricity. *Independent*, 2016. DOI: 10.2139/ssrn.2876929.

[2] N. Atkinson. Who discovered electricity?, December 2015, Webpage. URL: https://www.universetoday.com/82402/who-discovered-electricity/. Accessed: 2017-07-03.

[3] R. Ferguson, W. Wilkinson, and R. Hill. Electricity use and economic development. *Energy Policy*, 28(13):923 – 934, 2000. ISSN 0301-4215. DOI: https://doi.org/10.1016/S0301-4215(00)00081-1. URL: http://www.sciencedirect.com/science/article/pii/S0301421500000811.

[4] K. Rahman. Why grid failure occurs, causing a blackout, March 2015, Webpage. URL: http://www.thedailystar.net/op-ed/why-grid-failure-occurs-causing-blackout-3551. Accessed: 2017-02-02.

[5] M. van der Meijden. Grid architecture development. TU Delft University Lecture, 2014.

[6] Y. Rebours. A comprehensive assessment of markets for frequency and voltage control ancillary services. University of Manchester, School of Electrical and Electronic Engineering, 2008.

[7] Y. Rebours, D. Kirschen, M. Trotignon, and S. Rossignol. A survey of frequency and voltage control ancillary services. part i: Technical features. *IEEE Transactions on Power Systems*, 22 (1):350–357, Feb 2007. ISSN 0885-8950. DOI: 10.1109/TPWRS.2006.888963.

[8] D. Meadows, D. Meadows, J. Randers, and W. Behrens III. *The Limits to Growth*. Universe Books, 1972. ISBN 9780876639184.

[9] C. Morris and M. Pehnt. Energy transition - the german energiewende. Heinrich Boll Stiftung, 2012.

[10] J. Notenboom, P. Boot, R. Koelemeijer, and J. Ros. Climate and energy roadmaps towards 2050 in north-western europe. PBL, 2012.

[11] H. Kamp. Energieagenda, naar een CO_2 -arme energievoorziening. Ministerie van Economische Zaken, 2016.

[12] C. Hewicker, O. Werner, and H. Ziegler. Qualitative analysis of cross-border exchange of balancing energy and operational reserves between netherlands and belgium. DNV KEMA Energy and Sustainability, 2013.

[13] B. Hebb. Res integration in the belgian balancing market. In *Symposium on European Grid Service Markets*. Elia, July 2017. URL: http://www.efcf.com/fileadmin/content/GSMpresentations/02_Hebb.pdf.

[14] P. Kundur, J. Paserba, V. Ajjarapu, G. Andersson, A. Bose, C. Canizares, N. Hatziargyriou, D. Hill, A. Stankovic, C. Taylor, and et al. Definition and classification of power system stability ieee/cigre joint task force on stability terms and definitions. *IEEE Transactions on Power Systems*, 19:1387 – 1401, 2004. DOI: 10.1109/TPWRS.2004.825981.

[15] G. Andersson. Modelling and analysis of electric power systems. power flow analysis fault analysis power systems dynamics and stability. ETH Zurich, 2008.

[16] B.S. Abdulraheem and C.K. Gan. Power system frequency stability and control: Survey. *International Journal of Applied Engineering Research*, 11(8):5688–5695, 2016. ISSN 0973-4562.

[17] R. Dugan, M. McGranaghan, S. Santoso, and H. Wayne Beaty. *Electrical Power Systems Quality*. McGraw-Hill Companies, Inc., 2014. ISBN 0-07-138622-X.

[18] P. Kundur, N. Balu, and M. Lauby. *Power System Stability and Control.* McGraw-Hill, Inc., 1994.

[19] P. Kundur and G.K. Morison. A review of definitions and classification of stability problems in today?s power systems. In *Panel Session on Stability Terms and Definitions, IEEE PES Winter Meeting, New York*, 1997.

[20] H. Bevrani. *Power System Control: An Overview*, pages 1–17. Springer International Publishing, Cham, 2014. ISBN 978-3-319-07278-4. DOI: 10.1007/978-3-319-07278-4_1. URL: https://doi.org/10.1007/978-3-319-07278-4_1.

[21] D. Schweer, A. Maaz, and A. Moser. Optimization of frequency containment reserve provision in m5bat hybrid battery storage. In *2016 13th International Conference on the European Energy Market (EEM)*, pages 1–5, June 2016. DOI: 10.1109/EEM.2016.7521335.

[22] K. Mahbubur Rahman. Synchronous grid of continental europe, Webpage. URL: https://www.revolvy.com. Accessed: 2017-02-28.

[23] ENTSO-e. Supporting document for the network code on load-frequency control and reserves. European Network of Transmission System Operators, 2013.

[24] ENTSO-e. Guideline on electricity transmission system operation. European Network of Transmission System Operators, 2016.

[25] R. van der Veen and R. Hakvoort. Balance responsibility and imbalance settlement in northern-europe? an evaluation. In *2009 6th International Conference on the European Energy Market*, 2009.

[26] I. Lampropoulos, J. Frunt, F. Nobel, A. Virag, P. van den Bosch, and W. Kling. Analysis of the market-based service provision for operating reserves in the netherlands. pages 1–8, May 2012. ISSN 2165-4077. DOI: 10.1109/EEM.2012.6254735.

[27] F. Nobel. *On balancing market design*. PhD thesis, PhD Thesis, Technical University Eindhoven, May 2016.

[28] U. Baran Baloglu and Y. Demir. Economic analysis of hybrid renewable energy systems with {V2G} integration considering battery life. *Energy Procedia*, 107:242 – 247, 2017. ISSN 1876-6102. DOI: https://doi.org/10.1016/j.egypro.2016.12.140. 3rd International Conference on Energy and Environment Research, {ICEER} 2016, 7-11 September 2016, Barcelona, Spain.

[29] Z. Lukszo and E. Park Lee. Demand side and dispatchable power plants with electric mobility. *Smart Grids from a Global Perspective*, 2(163-177), 2016. DOI: 10.1007/978-3-319-28077-6_11.

[30] Willett Kempton and Jasna Tomić. Vehicle-to-grid power fundamentals: Calculating capacity and net revenue. *Journal of Power Sources*, 144(1):268 – 279, 2005. ISSN 0378-7753. DOI: http://doi.org/10.1016/j.jpowsour.2004.12.025.

[31] A. van Wijk and L. Verhoef. *Our Car as Power Plant*. IOS Press BV, 2014.

[32] P. Codani, M.Petit, and Y. Perez. Missing money for evs: economics impacts of tso market designs. *SSRN*, page 19, November 2014.

[33] M. Sarker, Y. Dvorkin, and M. Ortega-Vazquez. Optimal participation of an electric vehicle aggregator in day-ahead energy and reserve markets. *IEEE Transactions on Power Systems*, 31 (5):3506–3515, 2016.

[34] T. Lipman, J. Edwards, and D. Kammen. Fuel cell system economics: comparing the costs of generating power with stationary and motor vehicle {PEM} fuel cell systems. *Energy Policy*, 32 (1):101 – 125, 2004. ISSN 0301-4215. DOI: https://doi.org/10.1016/S0301-4215(02)00286-0.

[35] F. Alavi, E. Park Lee, N. van de Wouw, B. De Schutter, and Z. Lukszo. Fuel cell cars in a microgrid for synergies between hydrogen and electricity networks. *Applied Energy*, 192:296 – 304, 2017. ISSN 0306-2619. DOI: https://doi.org/10.1016/j.apenergy.2016.10.084.

[36] J. de Haan. *Cross-border balancing in Europe : ensuring frequency quality within the constraints of the interconnected transmission systemy*. PhD thesis, PhD Thesis, Technical University Eindhoven, 2016.

[37] R. Fonteijn. Non-conventional inertia in a res dominated power system. MSc thesis, Eindhoven University of Technology, 2015.

[38] G. Xiao, C. Li, Z. Yu, Y. Cao, and B. Fang. Review of the impact of electric vehicles participating in frequency regulation on power grid. pages 75–80, Nov 2013. DOI: 10.1109/CAC.2013.6775705.

[39] R. Raustad. The role of v2g in the smart grid of the future. The Electrochemical Society Interface, 2015.

[40] D. Newbery, G. Strbac, and I. Viehof. The benefits of integrating european electricity markets. *Energy Policys*, 94:253 – 263, 2016. DOI: http://dx.doi.org/10.1016/j.enpol.2016.03.047.

[41] L.de Vries, A. Correlje, and H. Knops. Electricity: Market design and policy choices (spm4520). System Engineering, Policy Analysis and Management, Technical University of Delft, 2016.

[42] B. Bhandari, K. Tae Lee, C. Sunyong Lee, C. Song, R. K. Maskey, and S.H. Ahn. A novel off-grid hybrid power system comprised of solar photovoltaic, wind, and hydro energy sources. *Applied Energy*, 133:236 – 242, 2014. ISSN 0306-2619. DOI: https://doi.org/10.1016/j.apenergy.2014.07.033.

[43] ENTSO-e. Operational reserve ad hoc team report. European Network of Transmission System Operators, 2012.

[44] ENTSO-e. Supporting document for the network code on electricity balancing. European Network of Transmission System Operator, 2014.

[45] ENTSO-e. Frequency stability evaluation criteria for the synchronous zone of continental europe. European Network of Transmission System Operators, 2016.

[46] J. Frunt. Analysis of balancing requirements in future sustainable and reliable power systems. PhD thesis, Eindhoven University of Technology, 2011.

[47] H. Shayeghi, H.A. Shayanfar, and A. Jalili. Load frequency control strategies: A state-of-the-art survey for the researcher. *Energy Conversion and Management*, 50(2):344 – 353, 2009. ISSN 0196-8904. DOI: http://dx.doi.org/10.1016/j.enconman.2008.09.014. URL: http://www.sciencedirect.com/science/article/pii/S0196890408003567.

[48] M. Godfried, R. Hakvoort, C. Meeuwis, G. Noordzij, F. Rijkers, and G. Zwart. Transparantie voor onbalanssystematiek. Dienst Uitvoering en toezicht Energie, 2004.

[49] Y. Schaber, F. Steinke, and T. Hamache. Transmission grid extensions for the integration of variable renewable energies in europe: Who benefits where? *Energy Policy*, 43:123–135, April 2012. ISSN 0301-4215. DOI: http://doi.org/10.1016/j.enpol.2011.12.040.

[50] CBS. Elektriciteit en warmte; productie en inzet naar energiedrager elektriciteit en warmte; productie en inzet naar energiedrager, May 2017, Webpage. URL: http://statline.cbs.nl/Statweb/publication/?DM=SLNL&PA=80030ned&D1=0-1&D2=a&D3=0,6&D4=2-18&HDR=T&STB=G1,G2,G3&VW=T. Accessed: 2017-05-29.

[51] CBS. Hernieuwbare elektriciteit; productie en vermogen, May 2017, Webpage. URL: http://statline.cbs.nl/Statweb/publication/?DM=SLNL&PA=82610ned&D1=3&D2=0-2,5-10&D3=20-26&HDR=T&STB=G1,G2&VW=T. Accessed: 2017-05-29.

[52] T. Jensen. The role of demand side management in scandinavia and the baltics. In *European Grid Service Markets Symposium*. Energi Danmark, July 2017. URL: http://www.efcf.com/fileadmin/content/GSMpresentations/05_Jensen.pdf.

[53] L Bird, M Milligan, and D Lew. Integrating Variable Renewable Energy: Challenges and Solutions. *Nrel/Tp-6a20-60451*, (September):14, 2013. DOI: NREL/TP-6A20-60451. URL: http://www.nrel.gov/docs/fy13osti/60451.pdf.

[54] Y. Wang, V. Silva, and M. Lopez-Botet-Zulueta. Impact of high penetration of variable renewable generation on frequency dynamics in the continental europe interconnected system. *IET Renewable Power Generation*, 10(1):10–16, 2016. ISSN 1752-1416. DOI: 10.1049/iet-rpg.2015.0141.

[55] G. Papaefthymiou, K. Grave, and K. Dragoon. Flexibility options in electricity systems. Ecofys, European Copper Institute, 2014.

[56] H. Thiesen, C. Jauch, and A. Gloe. Design of a system substituting today?s inherent inertia in the european continental synchronous area. *Energies*, 9, 2016. DOI: 10.3390/en9080582.

[57] A. Ulbig, T. Borsche, and G. Andersson. Impact of low rotational inertia on power system stability and operation. *IFAC Proceedings Volumes*, 47(3):7290 – 7297, 2014. ISSN 1474-6670. DOI: http://dx.doi.org/10.3182/20140824-6-ZA-1003.02615.

[58] P. Tielens and D. Van Hertem. The relevance of inertia in power systems. *Renewable and Sustainable Energy Reviews*, 55:999 – 1009, 2016. DOI: http://dx.doi.org/10.1016/j.rser.2015.11.016.

[59] I. Erlich and M. Wilch. Primary frequency control by wind turbines. pages 1–8, July 2010. ISSN 1932-5517. DOI: 10.1109/PES.2010.5589911.

[60] I. Margaris, S. Papathanassiou, N. Hatziargyriou, A. Hansen, and P. Sorensen. Frequency control in autonomous power systems with high wind power penetration. *IEEE Transactions on Sustainable Energy*, 3(2):189–199, April 2012. ISSN 1949-3029. DOI: 10.1109/TSTE.2011.2174660.

[61] F. Diaz-Gonzaleza, M. Sumpera, and O. Gomis-Bellmunta. Participation of wind power plants in system frequency control: Review of grid code requirements and control methods. *Renewable and Sustainable Energy Reviews*, 34:551?564, June 2014. DOI: 10.1016/j.rser.2014.03.040.

[62] J. Morren, S. de Haan, W. Kling, and J. Ferreira. Wind turbines emulating inertia and supporting primary frequency control. *IEEE Transactions on Power Systems*, 21(1):433–434, Feb 2006. ISSN 0885-8950. DOI: 10.1109/TPWRS.2005.861956.

[63] R. Suryana and W. Hofmann. Wind farm contribution to primary frequency control. pages 1–10, Sept 2015. DOI: 10.1109/EPE.2015.7309447.

[64] M. Rezkalla, A. Zecchino, S. Martinenas, A. Prostejovsky, and M. Marinelli. Comparison between synthetic inertia and fast frequency containment control based on single phase evs in a microgrid. *Applied Energy*, 2017. ISSN 0306-2619. DOI: http://dx.doi.org/10.1016/j.apenergy.2017.06.051. URL: http://www.sciencedirect.com/science/article/pii/S0306261917308024.

[65] NationalGrid. Enhanced frequency response. intivation to tender for pre-qualified parties. NationalGrid, July 2016.

[66] C. Morris. German power prices negative over weekend, May 2014, Webpage. URL: https://energytransition.org/2014/05/german-power-prices-negative-over-weekend/. Accessed: 2017-08-24.

[67] EPEX. Negative prices, Webpage. URL: https://www.epexspot.com/en/company-info/basics_of_the_power_market/negative_prices. Accessed: 2017-08-24.

[68] Rijksoverheid. Windenergie op zee, 2017, Webpage. URL: https://www.rijksoverheid.nl/onderwerpen/duurzame-energie/windenergie-op-zee. Accessed: 2017-08-24.

[69] J. Vis. Wordt komende 7 jaar meer zon en wind capaciteit gerealiseerd dan fossiel in periode 2000-2023?, 2016, Webpage. URL: https://jaspervis.wordpress.com/2016/04/17/komende-7-jaar-meer-zonwind-capaciteit-dan-fossiel-in-2000-2023/. Accessed: 2017-08-24.

[70] ECN. Nationale energieverkenning 2016, Webpage. URL: https://www.ecn.nl/nl/energieverkenning/. Accessed: 2017-08-24.

[71] ENTSO-e. Future system inertia. Entso-e, 2016.

[72] Hyundai. Tuscon fuel cell emergeny response guide. Hyundai, 2014.

[73] Hyundai. Technical specifications hyundai i x 35 fuel cell. Hyundai, 2016.

[74] Toyota. Technical specifications toyota mirai. Toyota, 2015.

[75] Honda. Technical specifications honda fcv. Honda, 2016.

[76] V. Oldenbroek, V. Hamoen, S. Alva, C. Robledo, L. Verhoef, and A. van Wijk. Fuel cell electric vehicle-to-grid: Experimental feasibility and operational performance. 6th European PEFC and Electrolyser Forum, July 2017.

[77] C. Robledo, V. Oldenbroek, F. Abruzzesse, and A. van Wijk. Case study of integrating a hydrogen fuel cell electric vehicle with vehicle-to-grid technology, photovoltaic power and a residential building case study of integrating a hydrogen fuel cell electric vehicle with vehicle-to-grid technology, photovoltaic power and a residential buidling. *In preparation for Applied Energy*, 2017.

[78] S. Kwon, N. Lee, J. Ko, and W. Sung. Method for shutting down fuel cell system, February 17 2015. URL: `http://www.google.mk/patents/US8956774`. US Patent 8,956,774.

[79] T. van Keulen, B. de Jager, J. Kessels, and M. Steinbuch. Energy management in hybrid electric vehicles: Benefit of prediction. *Proc. IFAC Symp. Adv. Automot. Control*, 2010.

[80] Department of Energy. Fuel cell technologies office (fcto). U.S. Department of Energy, 2016.

[81] J. Wishart. Fuel cells vs batteries in the automotive sector. Intertek, 2017.

[82] Richtek. Understanding the characteristics of li-ion batteries and richtek power management solutions. Richtek, 2014.

[83] M. Winter and R. Brod. What are batteries, fuel cells, and supercapacitors? Published on Web 09/28/2004 American Chemical Society, 2004.

[84] FERC. Frequency regulation compensation in the iso/rto markets, May 2010, Webpage. URL: `https://www.ferc.gov/EventCalendar/Files/20100526085637-Judson,%20Beacon%20Power.pdf`. Accessed: 2017-08-16.

[85] M. Lazarewicz. Flywheel technology energy storage for grid services, September 2011. URL: `https://www.uml.edu/docs/15_Energy_M_Lazarewicz_tcm18-48972.pdf`.

[86] Ecofys. Energy storage opportunities and challenges. Ecofys, April 2014. URL: `http://www.ecofys.com/files/files/ecofys-2014-energy-storage-white-paper.pdf`.

[87] Spark. Parkeren in nederland. Spark parkeren, 2014.

[88] K. van de Schaaf. Interview: Big data voor verkeerskundige analyses, Webpage. URL: `http://www.kxa.nl/pages/verkeer.html`. Accessed: 2017-07-14.

[89] Z. Lukszo. Engineering optimisation and integrating renewables in electricity markets. In *Forecasts essential to the integration of RES in electricity market operation*, number 7, 2017.

[90] EPEX. Day-ahead auction, 2017, Webpage. URL: `https://www.epexspot.com/en/product-info/auction`. Accessed: 2017-07-14.

[91] EPEX. Epex spot intraday in the netherlands, 2017, Webpage. URL: `https://www.epexspot.com/en/product-info/intradaycontinuous/the_netherlands`. Accessed: 2017-07-14.

[92] ENTSO-e. Guideline on electricity balancing. European Commission, 2017.

[93] ELaadNL. De waarde van flexibel laden. verkenning van de waarde van demand response bij het laden van elektrische voortuigen. Movares Adviseurs & Ingenieurs, 2016.

[94] E. Koliou, C. Eid, J. Pablo Chaves-Ávila, and R. A. Hakvoort. Demand response in liberalized electricity markets: Analysis of aggregated load participation in the german balancing mechanism. *Energy*, 71:245 – 254, 2014. ISSN 0360-5442. DOI: https://doi.org/10.1016/j.energy.2014.04.067. URL: http://www.sciencedirect.com/science/article/pii/S0360544214004800.

[95] TenneT SON-SY. Productinformatie regelvermogen. TenneT, 2016.

[96] V. Oldenbroek, L. Verhoef, and A. van Wijk. Fuel cell electric vehicle as a power plant: Fully renewable integrated transport and energy system design and analysis for smart city areas. *International Journal of Hydrogen Energy*, 42(12):8166 – 8196, 2017. ISSN 0360-3199. DOI: https://doi.org/10.1016/j.ijhydene.2017.01.155. URL: http://www.sciencedirect.com/science/article/pii/S036031991730321X.

[97] J. Eichman, A. Townsend, and M. Melaina. Economic assessment of hydrogen technologies participating in california electricity markets. NREL, February 2016.

[98] J. Aartsen, A. van Wijk, R. Goossens, E. Dirkse, and J. Buining. Green hydrogen economy in the northern netherlands. Noordelijke Innovation Board, 2016.

[99] Tractebel. Study on early business cases for h2 in energy storage and more broadly power to h2 applications. Tractebel, Engie, Hinicio, 2017.

[100] International Energy Agency. Technology roadmap hydrogen and fuel cells. International Energy Agency, 2015.

[101] Energy Renaissance. Hydrogen generator, 2015. URL: http://www.h2energyrenaissance.com.

[102] S. Dillich, T. Ramsden, and M. Melaina. Doe hydrogen and fuel cells program record. Department of Energy, 2012.

[103] N. Sulaiman, M. Hannan, A. Mohamed, E. Majlan, and W. Wan Daud. A review on energy management system for fuel cell hybrid electric vehicle: Issues and challenges. *Renewable and Sustainable Energy Reviews*, 52:802 – 814, 2015. ISSN 1364-0321. DOI: http://dx.doi.org/10.1016/j.rser.2015.07.132. URL: http://www.sciencedirect.com/science/article/pii/S1364032115007790.

[104] Ludwig-Bölkow-Systemtechnik GmbH. Wasserstoff daten - hydrogen data, 2017, Webpage. URL: http://www.h2data.de. Accessed: 2017-10-11.

[105] M. Jouin, M. Bressel, S. Morando, R. Gouriveau, D. Hissel, Marie-Cécile Péra, N. Zerhouni, S. Jemei, M. Hilairet, and B. Ould Bouamama. Estimating the end-of-life of {PEM} fuel cells: Guidelines and metrics. *Applied Energy*, 177:87 – 97, 2016. ISSN 0306-2619. DOI: https://doi.org/10.1016/j.apenergy.2016.05.076. URL: http://www.sciencedirect.com/science/article/pii/S0306261916306729.

[106] Department of Energy. Office of energy efficiency and renewable energy, July 2017, Webpage. URL: https://energy.gov/eere/fuelcells/fuel-cells. Accessed: 2017-07-18.

[107] B. Fumey. Interview: Hydrogen distribution systems, 2017.

[108] U. Cabalzar. Interview: Hydrogen distribution systems, 2017.

[109] Liander. Tarieven 2017 voor consumenten, 2017, Webpage. URL: https://www.liander.nl/consument/aansluitingen/tarieven2017/?ref=14389. Accessed: 2017-08-06.

[110] Enexis. Kosten werkzaamheden kleinzakelijk aansluiting of meter, 2017, Webpage. URL: https://www.enexis.nl/zakelijk/facturen-en-tarieven/tarieven/kleinzakelijke-tarieven/kosten-werkzaamheden-aansluiting?stap=Kosten-werkzaamheden-aansluiting-of-meter_1_1. Accessed: 2017-08-06.

[111] A. Elsayed, A. Mohamed, and O. Mohammed. Dc microgrids and distribution systems: An overview. *Electric Power Systems Research*, 119:407 – 417, 2015. ISSN 0378-7796. DOI: http://dx.doi.org/10.1016/j.epsr.2014.10.017. URL: http://www.sciencedirect.com/science/article/pii/S0378779614003885.

[112] E. Planas, J. Andreu, J. Ignacio Gárate, I. Martínez de Alegría, and E. Ibarra. Ac and dc technology in microgrids: A review. *Renewable and Sustainable Energy Reviews*, 43:726 – 749, 2015. ISSN 1364-0321. DOI: http://dx.doi.org/10.1016/j.rser.2014.11.067. URL: http://www.sciencedirect.com/science/article/pii/S1364032114010065.

[113] Pieter Vliex. Interview: Costs for adapting a car park to offer v2g services. *QPark*, 2017.

[114] NOS. Nederland loopt voorop bij ontwikkeling zelfrijdende auto's, 2017, Webpage. URL: https://nos.nl/artikel/2192878-nederland-loopt-voorop-bij-ontwikkeling-zelfrijdende-auto-s.html. Accessed: 2017-09-28.

[115] T. Hoogvliet, G.Litjens, and W. van Sark. Provision of regulating- and reserve power by electric vehicle owners in the dutch market. *Applied Energy*, 190:1008 – 1019, 2017. ISSN 0306-2619. DOI: http://doi.org/10.1016/j.apenergy.2017.01.006.

[116] B. Ummels. *Power System Operation with Large-Scale Wind Power in Liberalised Environments*. PhD thesis, Technical University Delft, February 2009.

[117] NewMotion. Newmotion. URL: https://newmotion.com/nl_NL.

[118] Peeeks. Flexibility is the future, 2015. URL: http://www.peeekspower.com/#readmore.

[119] Vandebron. Tennet opent de balanceringsmarkt voor batterijen via blockchain, 2017. URL: https://www.tennet.eu/nl/nieuws/nieuws/tennet-opent-de-balanceringsmarkt-voor-batterijen-via-blockchain/.

[120] Jedlix. Start smart charging at home, 2017, Webpage. URL: https://jedlix.com. Accessed: 2017-09-12.

[121] CBS. Motorvoertuigenpark; type, leeftijdsklasse, 1 januari, May 2017, Webpage. URL: http://statline.cbs.nl/statweb/publication/?dm=slnl&pa=82044ned. Accessed: 2017-05-08.

[122] Rijksdienst. Cijfers elektrisch vervoer. Rijksdienst voor Ondernemend Nederland, 2017.

[123] McKinsey. Evolution. electric vehicles in europe: gearing up for a new phase? McKinsey & Company and Amsterdam Round Tables, 2016.

[124] C. Bach. Future mobility demonstration. EMPA, Dübendorf, 2017.

[125] European Comission. Reducing co2 emissions from passenger cars, June 2017, Webpage. URL: https://ec.europa.eu/clima/policies/transport/vehicles/cars_en. Accessed: 2017-07-03.

[126] M. Traa, J. Van Meerkerk, and G. Geilenkirchen. Autopark in beweging. trends in omvang en samenstelling van het personenautopark. Planbureau voor de Leefomgeving, 2016.

[127] ElementEnergy. Hydrogen refueling and storage infrastructure. E4tech, 2017.

[128] J. Pratt, D. Terlip, C. Ainscough, J. Kurtz, and A. Elgowainy. H2first reference station design task. NREL, 2015.

[129] N. Takeichi, H. Senoh, T. Yokota, H. Tsuruta, K. Hamada, H. Takeshita, H. Tanaka, T. Kiyobayashi, T. Takano, and N. Kuriyama. "hybrid hydrogen storage vessel", a novel high-pressure hydrogen storage vessel combined with hydrogen storage material. *International Journal of Hydrogen Energy*, 28(10):1121 – 1129, 2003. ISSN 0360-3199. DOI: https://doi.org/10.1016/S0360-3199(02)00216-1. URL: http://www.sciencedirect.com/science/article/pii/S0360319902002161.

[130] G. Parks, R. Boyd, J. Cornish, and R. Remick. Hydrogen station compression, storage and dispensing. technical status and costs. NREL, 2014.

[131] Department of Energy. Hydrogen pipelines, July 2017, Webpage. URL: https://energy.gov/eere/fuelcells/hydrogen-pipelines. Accessed: 2017-07-21.

[132] Air Liquide. Waterstofnet congres-mobiliteit, July 2017. URL: http://www.waterstofnet.eu/_asset/_public/Presentatie-Air-Liquide-Christian-Nachtergaele.pdf.

[133] Air Liquide. Europe hydrogen pipelines.

[134] R. Gupta. *Hydrogen fuel. Production, transportation and storage.* CRC PRess, 2009.

[135] W. Leighty, J. Holloway, R. Merer, B. Somerday, and G. Keith. Compressorless hydrogen transmission pipelines deliver large-scale stranded renewable energy at competitive cost. 23rd World Gas Conference, 2006.

[136] P. Bolat and C. Thiel. Hydrogen supply chain architecture for bottom-up energy systems models. part 1: Developing pathways. *International Journal of Hydrogen Energy*, 39(17):8881 – 8897, 2014. ISSN 0360-3199. DOI: https://doi.org/10.1016/j.ijhydene.2014.03.176. URL: http://www.sciencedirect.com/science/article/pii/S0360319914008684.

[137] S. Baufume, F. Gruger, T. Grube, D. Krieg, J. Linssen, M. Weber, J. Friedrich Hake, and D. Stolten. Gis-based scenario calculations for a nationwide german hydrogen pipeline infrastructure. *International Journal of Hydrogen Energy*, 38(10):3813 – 3829, 2013. ISSN 0360-3199. DOI: http://dx.doi.org/10.1016/j.ijhydene.2012.12.147. URL: http://www.sciencedirect.com/science/article/pii/S0360319913000670.

[138] J. Andre, S. Auray, D. De Wolf, M. Memmah, and A. Simonnet. Time development of new hydrogen transmission pipeline networks for france. *International Journal of Hydrogen Energy*, 39(20):10323 – 10337, 2014. ISSN 0360-3199. DOI: http://dx.doi.org/10.1016/j.ijhydene.2014.04.190. URL: http://www.sciencedirect.com/science/article/pii/S0360319914012804.

[139] J. Andre, S. Auray, J. Brac, D. De Wolf, G. Maisonnier, M. Ould-Sidi, and A. Simonnet. Design and dimensioning of hydrogen transmission pipeline networks. *European Journal of Operational Research*, 229(1):239 – 251, 2013. ISSN 0377-2217. DOI: http://dx.doi.org/10.1016/j.ejor.2013.02.036. URL: http://www.sciencedirect.com/science/article/pii/S0377221713001690.

[140] P. Dodds and S. Demoullin. Conversion of the uk gas system to transport hydrogen. *International Journal of Hydrogen Energy*, 38(18):7189 – 7200, 2013. ISSN 0360-3199. DOI: http://dx.doi.org/10.1016/j.ijhydene.2013.03.070. URL: http://www.sciencedirect.com/science/article/pii/S0360319913006800.

[141] V. Tietze and D. Stolten. Comparison of hydrogen and methane storage by means of a thermodynamic analysis. *International Journal of Hydrogen Energy*, 40(35):11530 – 11537, 2015. ISSN 0360-3199. DOI: http://dx.doi.org/10.1016/j.ijhydene.2015.04.154. URL: http://www.sciencedirect.com/science/article/pii/S0360319915010927.

[142] B. Balasubramanian, F. Barbir, and J. Neutzler. Optimal operating temperature and pressure of pem fuel cell system in automotive applications. Energy Partners.

[143] D. Feroldi and M. Basualdo. *Description of PEM Fuel Cells System*. Springer-Verlag, 2012.

[144] I. Patrao, E. Figueres, G. Garcerá, and R. González-Medina. Microgrid architectures for low voltage distributed generation. *Renewable and Sustainable Energy Reviews*, 43:415 – 424, 2015. ISSN 1364-0321. DOI: http://dx.doi.org/10.1016/j.rser.2014.11.054. URL: http://www.sciencedirect.com/science/article/pii/S1364032114009939.

[145] Energypedia. Dc mini-grids, Webpage. URL: https://energypedia.info/wiki/DC_Mini-grids. Accessed: 2017-08-03.

[146] P. Madduri, J. Rosa, S. Sanders, E. Brewer, and M. Podolsky. Design and verification of smart and scalable dc microgrids for emerging regions. Department of Electrical Engineering and Computer Science University of California, Berkeley, 2013.

[147] G. Laudani and P. Mitcheson. Comparison of cost and efficiency of dc versus ac in office buildings. Imperial College, 2011.

List of AppendixFigures

List of AppendixTables

A

Derivation RoCoF

The derivation from the relation between the RoCoF and the inertia constant is taken from the dissertation of Ummels [116]. The power system is considered as a large, single rotating mass. The relation between the mechanical torque (T_m) and the electrical torque (T_e) is expressed by the swing equation A.1. An imbalance between the mechanical and electrical torque results in the accelerating torque (T_a). All torques are expressed in [N·m].

$$T_a = T_m - T_e \tag{A.1}$$

In case T_a is not equal to zero, the mass will experience an angular acceleration which can be described with Newton's second law for rotational motion. This relation, described in Equation A.2, relates the imbalance to a rate of change of the rotational speed of the mass. The constant J expresses the mass' rotational inertia [kg·m^2].

$$T_a = J\frac{d\,\omega}{d\,t} \tag{A.2}$$

Considering the relation P = ω T for the mechanical and electrical torque, Equation A.2 can be rewritten as Equation A.3. This gives the relation between the mechanical and electrical power expressed in [W] and the acceleration [rad/s^2].

$$\frac{d\,\omega}{d\,t} = \frac{P_m - P_e}{J\omega_m} \tag{A.3}$$

The rotational speed (ω) can be rewritten as $2\,\pi\,f$. Replacing P_m with the mechanical power input of all generators of the system (P_G) and P_e with the load (P_L), Equation A.3 can be reformulated as Equation A.4. This equation gives the relation between the inertia of the system and the RoCoF [37]. Using the relation of aggregated moment of inertia M = 4 π^2 J f_m [Ws/Hz] the equation can be rewritten in its final form.

$$\frac{d\,f}{d\,t} = \frac{P_G - P_L}{4\,\pi^2\,J\,f_m} = \frac{\Delta P}{M} \tag{A.4}$$

B

Measurements with the FCEV

During the experiment the power gradient of the FCEV in V2G mode is calculated. The average power gradient is calculated using only the moments that the EMS switches between the battery and the FCEV. This is due to the fact that the power output of both the battery and the FC are fluctuating. If the average of all the power gradients was calculated, this would not represent the real capability of the power sources.

The required data points are selected by choosing a threshold that filters out all the small power gradients that are not relevant for the analysis. Once the irrelevant power gradients are filtered out, a limited amount of data points are available. This amount should correspond with the amount of switches between the battery and the FC. The measurements per setting should be around 10 because of the 10 repeated cycles. If the number is higher, this implies that there have been switches between the battery and the FC during the operation that were not caused by the switching on/off of the discharge unit. If the number is less than 10 it is caused by the EMS that minimises the switching on/off of the FC. Table B.1 shows the amount of considered measurements. The respective standard deviations per dataset are shown in Table B.2.

Table B.1: Number of considered measurements of the data sets for power gradients up- and downwards.

St. Dev.	**FC**		**Battery**	
	↑	↓	↑	↓
5 kW	11	8	8	18
10 kW	11	10	9	13

Table B.2: Standard deviations of the data sets for power gradients up- and downward.

St. Dev.	**FC**		**Battery**	
	↑	↓	↑	↓
5 kW	8.3	1.1	0.4	5.6
10 kW	10	2.8	2.2	8.6

C

Overview of pilots

This appendix contains a brief description of the pilots that are currently experimenting with the delivery of frequency reserves. Not all information of the pilots can be shared due to confidentiality agreements. For this reason some descriptions are more extensive than others and no specific quantities can be provided.

FCR Pilot

- **NewMotion** NewMotion is the operator of a charging infrastructure for EVs made out of charge points sold by NewMotion itself or third parties. They issue charge cards for customers to charge their EVs. NewMotion is participating in the pilot with 10,000+ chargers each with MID certified meter, live connection and live control. They offer FCR by increasing or decreasing the charging speed in the chargers [117].
- **KPN** KPN is a well known Dutch telecom company. KPN has an overcapacity of backup batteries available at the technical buildings that can be used for other purposes like the delivery of frequency reserves.
- **Peeks** Peeeks is a company that ”finds, accesses and unlocks flexibility in energy portfolios of electric companies, providing them with greater control over their flexibility” [118]. It collaborates with Green Choice which operates several CHP installations running on biogas that can ramp up or down to offer FCR.
- **Senfal** Senfal is a company of which the main focus is demand respons of the various assets throughout the Netherlands such as coldstores, waterpumps and heatpumps. With advanced forecasting software, based on self regulating algorithms, Senfal is able to predict market prices, energy demand and available flexibility form the assets.
- **Engie** Engie has a variety of assets that could be used to offer FCR such as batteries, turbines and residential assets. Engie has an integrated portfolio and partnerships which make it possible to offer frequency reserves.

aFRR - Signal communication Pilot

TenneT has just initialised a new pilot regarding the communication system. This is a collaboration between Vandebron and IBM. It tries to use blockchain as a tool to elaborate all the bids for frequ ency reserves. Where previously the bids were done by circa seven large conventional power plants, in the

future there could be hundreds of market participants that can bid. This requires a different system. This pilot is the first of a series that tries to find the best way to elaborate the bids of BRPs [119].

Passive contribution
Currently there are also several companies that contribute to the stability of the grid by contributing passively. An example is Jedlix, a startup of Eneco. They use a software installed in BEVs to increase or decrease the charging speed. They already have a collaboration with Tesla, Renault and BMW [120].

Energinet - TSO Denkmark
Also in Denmark the TSO is testing pilot projects for emerging technologies in the ancillary service markets. The main reason is to reduce the barriers for market participation and improve the competition. They have pilot projects with batteries, EVs, service industries and heat pumps. The project framework covers various barriers: online measurements, verification and third party aggregators. In this pilot the participants cover their own costs but in return they get a first mover experience and can participate under temporarily relaxed conditions.

- EnergyCool and EConGrid: Delivery of regulating power from a pool of batteries from telesites, including the calculation of baselines. This pilot includes 4 telesites with approximately 300 kW battery capacity.
- Insero and NeoGrid: Delivery of regulating power from a pool of heat pumps, including the delivery of consumption data from a submeter into the DataHub, with the purpose of billing. The setup includes 9 heat pumps located at public institutions with a capacity of approximately 300 kW.
- EnergiDanmark: The purpose of the project is to demonstrate the effects of delivering demand response from service industries to the ancillary services market. The pilot setup includes a shopping mall, a cooling company, a wastewater treatment plant and a nursery. KiwiPower delivers the software for aggregation.

The overall findings and recommendations of the pilots are enlisted below:

- Qualification of the assets should be standardised. It is time consuming to test every asset of a pool. It would be advised to make classes of assets that are pre-qualified and do not need to be tested separately. This would save the BSP as well as TenneT a lot of time.
- New data communication and elaboration methods are required.
- Algorithms and the software are the key of the functioning of an aggregation. Sharing these algorithms between companies would increase the ability to improve the service.
- These pilots open the doors to innovative entrants but an additional stimulans could be created by actively getting incumbents to stop dominating the market.
- The pilots are operational but not yet ready to fully participate in the real market. It would be desirable to adapt a transition period between the pilot and the official participation in the market.
- Frequency measurements can be done locally or centrally. It has not been determined yet what is the best option for the safety of the system. This should be determined.
- Costumers or owners of the assets are not really interested in the support of frequency or simply don't understand it. They only want to know what it does for the pocket. They also have the fear to lose the control of their assets especially for residential components.

D

Summary of modelling assumptions

The assumptions summarised in this appendix are extendedly described in the chapters of Part III.

Model assumptions regarding the design of the car park

- Occupation pattern is known
- Infinite source of hydrogen directly fuelled to the cars with a low pressure distribution network
- National electricity grid is AC and requires the use of frequency reserves
- Local electricity grid in the car park is DC

Model assumptions regarding the relation between relevant parties

- Aggregator compensates the owner of the vehicle by paying the degradation costs
- Only revenues/costs of activities related to the function as power plant of the car park are considered

Model assumptions regarding the FCEV

- FC system is the only power source

Model assumptions regarding the market

- Bid of the CPPP is equal to the marginal costs
- Spot market price is based on values of 2016
- aFRR price price is based on values of 2016
- FCR price is taken the average price of 2017
- For aFRR only energy payments are considered
- Financial penalties are not taken into account
- The settlement for created imbalance is not considered
- The aggregator will sell any desired quantity of baseload

E

Moment of application of the CPPP concept

Currently the fleet of FCEVs is to small to form an aggregation that can make a car park operate as a power plant. For this reason the increase of the share of FCEVs on the basis of scenarios is considered to evaluate in how many years the concept of CPPP could become interesting.

The current fleet of passenger cars in the Netherlands is equal to 8,222,974 of which only 31 are FCEVs [121, 122]. Considering the policy of the Dutch government, Green Deal Elektrisch Vervoer 2016-2020, there is the outspoken ambition to increase the share of EVs in the coming years. The goal is to increase the share of newly bought passenger cars that is electric to 10% in 2020 and 50% in 2025 and at least 30% of those must be fully electric. No explicit distinction is made for the type of EV.

The growth of different types of EVs has been evaluated by the technical report of McKinsey [123]. According to this report, the Netherlands is one of the frontrunners within Europe. Taking the average European prognosis is a realistic, slightly conservative, estimation for the future fleet of FCEVs in the Netherlands. The technical report considers three scenarios related to the maximum amount of CO_2 that can be emitted per kilometer in 2050 referred to as cap. A high CO_2-cap goes together with a low penetration level of EV. The first has a cap of 95 g CO_2/km, the second of 40 g CO_2/km and the last one of 10 g CO_2/km.

The EU has already announced the target to reduce the emission cap for passenger cars from 130 g CO_2/km in 2015 to 95 g CO_2/km in 2021 and 70 g CO_2/km in 2025 [124, 125]. Severe penalty payments are related to higher emission rates and regulation gives manufacturers additional financial incentives to produce vehicles with extremely low emissions. These regulations stimulate car manufacturers to invest in the development of EVs, which as a consequence increases the affordability of EVs. Assuming that the targets set by the EU are realistic and achievable, also the scenario's of the technical report for 2050 are plausible since the target of the EU assumes higher change rates.

In this research, the CO_2 emissions for passenger vehicle scenarios of the technical report are translated to the share of FCEVs of the total fleet of the Netherlands. Four scenarios are created: the reference scenario is a scenario where no penetration of FCEV is considered, low-scenario considers an increase of the share of FCEVs with 5% of the total fleet of vehicles every 10 years, the mid-scenario considers an increase of 10% every 10 years and the high-scenario an increase of 15% every 10 years. A growth rate of 0.09% for the total fleet of passenger vehicles has been considered [126]. This trend is compared with fitting curves for the historical data of the Dutch fleet from Centraal Bureau Statistiek

(CBS) [121]. The 0.09% growth seems a good estimation as it represents the average value between the polynomial and power function. The yellow line in Figure E.1 shows growth rate of 0.09% of the total amount of vehicles within the Netherlands. The histogram indicates the amount of FCEVs in the different scenarios for the years 2020, 2030, 2040 and 2050.

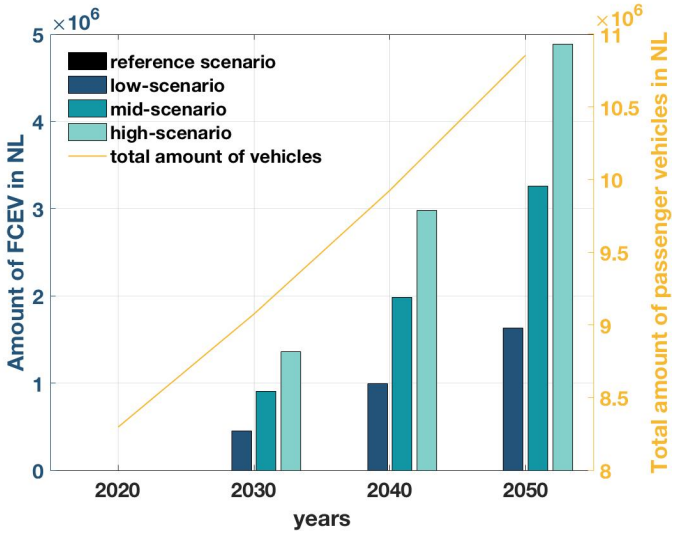

Figure E.1: Amount of total vehicles and FCEVs based on different scenarios.

It is difficult to estimate how large the fleet of FCEVs needs to be, before there is potential for a CPPP. The optimum relation between the construction of a CPPP and the number of FCEVs is not known and is not considered within the scope of this research. It depends not only on the amount of FCEVs but also on the location where the FCEVs are used, urban development, development of hydrogen economy, hydrogen storage locations, hydrogen production locations and many more factors. Therefore the total available V2G capacity from FCEVs is used as an indication of the potential of the CPPP concept.

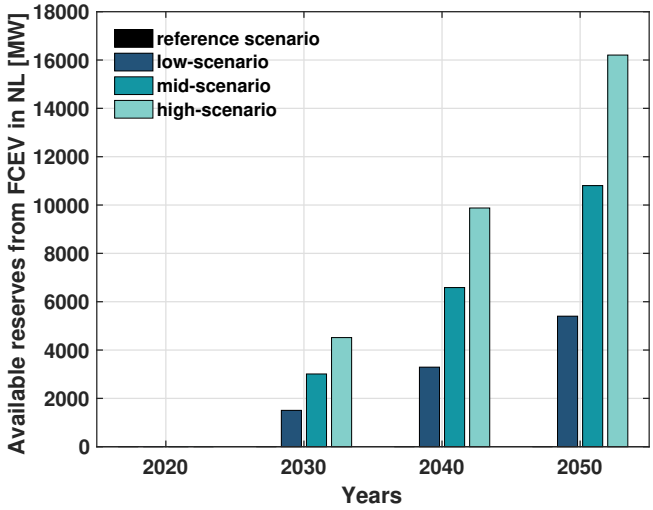

Figure E.2: Capacity available for reserves if all FCEVs operate at 10 kW power output.

In Figure E.2 the total available capacity of the fleet of FCEVs that could be offered as frequency reserves is graphically represented. The amount of available FCEVs per scenario is multiplied with the

maximum V2G power output of 10 kW. It can be seen that from 2040 onwards the fleet of FCEVs in the Netherlands has, even for the low-scenario, a larger capacity than the reference incident, which is equal to 3000 MW. Between 2040 and 2050, which will be referred to as mid century, the fleet of FCEVs is expected to be large enough to offer significant amounts of power and reserves.

F

CPPP design

In this appendix, assumptions about the required components are given and explained. In the original concept of CaPP described in [31], the parking of the car and the connection to the electricity, water and hydrogen network happens in a fully automated manner. To be able to simulate such a concept some simplifications needed to be made. Only the essential technical components that are required for delivering electricity and balancing services are taken into consideration. The automatisation of the actual parking of the car and the automatic connection of the car to the hydrogen and electricity network ,is left out of scope. The proces products, heat and water, are also not taken into consideration.

F.1. Hydrogen network

A car park to operate as a power plant, needs to be connected to a source that can continuously deliver hydrogen. In the CPPP design it is assumed that all the vehicles in the car park are connected to a hydrogen source, which is considered the main input of the system. Hydrogen can be delivered either in a liquefied form by tanker truck, as a compressed gas in cylinders or through a hydrogen network. The advantage of liquefied hydrogen is the high density compared to compressed gas. This implies that more energy can be contained in a given volume which is beneficial for transportation of hydrogen. Liquefied hydrogen tends only to be delivered in large volumes whereas compressed gas is far more scalable and can be supplied in small quantities. If hydrogen is delivered as a liquid, it requires cooling to a temperature of -253 °C. Liquefaction is an energy intensive process and can consume up to 35% of the energy in the stored hydrogen. Afterwards it needs to be stored in cryogenic storage vessels. For this reasons, it is plausible that around mid century the distribution of hydrogen will occur by means of compressed gas in cylinders or through a hydrogen network [127]. Most hydrogen vehicles are also being developed with compressed gas onboard storage in stead of liquid gas.

When hydrogen is delivered as a compressed gas, the storage vessel is usually dropped off at the site by a truck and then replaced when empty. For large volumes of hydrogen, a tube trailer will be delivered on which is mounted a bundle of pressurised tubes. The initial pressure in the tubes is around 200 to 250 bar and contains circa 300 kg of hydrogen. This hydrogen source could fuel circa 41 FCEVs considering that around mid century the storage stank of a FCEV could contain circa 6.5 kg of hydrogen. Considering that one tube trailer is already small to fuel the total car park, smaller volumes delivered in cylinders are not considered as a plausible option to deliver hydrogen to the car park.

As hydrogen is consumed the pressure in the trailer will drop. A high-pressure compressor is used to compress hydrogen from the tube trailers into the high-pressure stationary storage [128]. This com-

pressor is required to operate for a wide range of suction pressures (and thus mass flows), since when tube trailers become more and more empty, the pressure in the tubes falls [129]. Hydrogen to refuel the vehicles will be taken from the high-pressure stationary storage. The compressors comprise 55% to 65% of total costs of this compression, storage and dispensing system [130]. The initial investment costs of the aggregator would be very high if the use of tube trailers with on site storage would be considered.

The last option to deliver the hydrogen to the CPPP, is to connect the car park to a hydrogen network. Gaseous hydrogen can be transported through pipelines similar to the way natural gas is transported [131]. Currently there already is a hydrogen network in the Netherlands operated mainly by Air Liquide and a small part by Air Products [132]. This network is situated around Rotterdam as the industry that currently uses large amounts of hydrogen is situated in that area. The Northern European hydrogen network, which is the longest hydrogen pipeline network in the world, is circa 1598 km of which 237 km is located in the Netherlands [133].

If the use of hydrogen would penetrate further in different sectors and hydrogen would become a primary energy carrier, the transportation of the fuel through pipelines would be considered the best option. This way of transportation is considered the most efficient and also the most economical option in a hydrogen energy environment [134, 135]. It could significantly reduce the costs of hydrogen storage at the location of the CPPP. Considering the perspective of the CPPP aggregator, this system would be preferred as transportation system due to the low costs for storage facilities. This concept would require a national hydrogen network, referred to as transmission network, that reaches until the location of the car park [136]. Structures for a transmission network are already being investigated for UK, France and Germany [98, 137–140]. From the point of view of thermodynamics, no obstacles exist in transporting and storing hydrogen in a supply infrastructure similar to the existing one for natural gas [141].

There are some technical concerns related to pipeline transmission that still need to be overcome. Current research focusses therefore on the potential for hydrogen to embrittle the steel and welds used to fabricate the pipelines, the need to control hydrogen permeation and leaks and the need for lower cost, more reliable, and more durable hydrogen compression technology [131]. A possible solution is the use of fiber reinforced polymer pipelines for the hydrogen distribution. These pipelines can be obtained in sections that are longer than steel pipelines which minimises the welding requirements which results in a 20% installation costs reduction [131].

F.2. Fuelling of the FCEVs

At the location of the car park a metering system needs to be implemented and a local small scale hydrogen network should cover the distribution in the car park to fuel the vehicles. The local hydrogen network, referred to as distribution network, is designed in such a way that it is similar to a local gas network [136]. The hydrogen can be distributed through the whole car park and dispensed to the vehicle through a flexible hose which can be connected to the vehicle.

The current FCEV that are available on the market all have a homologised fuelling socket (SAE J2799) to which a data interface can be added. If the vehicles would be connected to the hydrogen network through this socket, the hydrogen would be stored in the tank of the vehicle before it reaches the fuel cell stack. In passenger vehicles the hydrogen is stored at 700 bar. This would imply that compressors are required at the location of the car park which result in additional high investment costs. The mechanism hydrogen storage and consumption in an automotive application can be seen in Figure F.1. It can be seen that from the hydrogen tank the hydrogen flows through a pressure-reduction valve and a pressure-controlled valve, before it enters the humidifier, heater and eventually the fuel cell stack. The pressure must be reduced from 700 bar until the operational pressure of the

fuel cell stack which is between 1 and 6 bar [142].

It would be more efficient to connect the hydrogen network, which is already at a lower pressure, directly to the pressure valve in stead of storing it in the hydrogen tank first. Using an external hydrogen connection also prevents that car owners are faced with empty tanks. This connection would require additions to the car but could be seen as an additional manufacturing package, just like the DC output socket. A specific socket would be build in the car to which the hydrogen network could be connected. This is a concept that still needs to be developed by car manufacturers but is estimated around 300 to 500 euro by the research group at EMPA[1], the Swiss Federal Laboratories for Materials Testing and Research [108]. Considering that in this research a future scenario is evaluated, it would be a plausible solution. The costs for this addition are not considered as it is part of the car. Only the costs of the hydrogen network and the fuelling hoses in the car park would be attributed to the aggregator. When this fuelling method is used, no additional hydrogen is stored in the tank for which the car owner should pay. Therefore there are no financial transactions between the car owner and the aggregator regarding hydrogen fuelling.

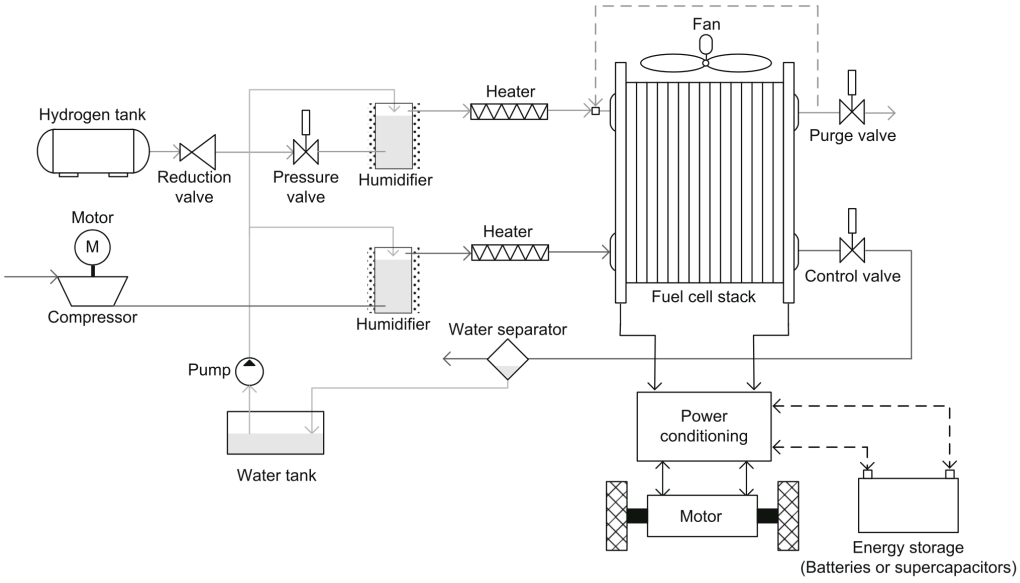

Figure F.1: General scheme of hydrogen storage and consumption of a fuel cell stack oriented to automotive applications. [143]

F.3. Vehicle-to-Grid connection

The FCEVs need to be connected to the electricity grid to be able to deliver balancing services. The main obstacle of this connection is that the DC current that is generated in the FCEV needs to be converted to AC for which a inverter is required. At The Green Village a Vehicle-to-Grid DC-AC discharge unit is used to do experiments and evaluate the capabilities of one FCEV. This discharge unit contains a 10 kW DC/AC 3 phase inverter to which only one FCEV can be connected. It would not be an economical option to install such an inverter for each car in the car park.

The CPPP design in this research is considered as a distributed generator with a DC microgrid [144]. The FCEVs plug in to the DC grid with for example a type 1 SAE J1772 socket and a DC/DC converter. The presence of the DC/DC converters depends on the voltage at which the DC microgrid operates and the output voltag of the FCEV. The DC microgrid is connected through an AC/DC converter to

[1]EMPA: Eidgen*ö*ssische Materialpr*ü*fungs- und ForschungsAnstalt

the national electricity grid. Only one large DC/AC converter station that can cover the capacity of the total car park, is used in stead of small individual inverters. It is desired that the microgrid exports the generated power, which implies that the power electronic interface must be bi-directional. When the car park operates as a power plant, the inverter's input is the summation of the DC from all the FCEVs and the output is the AC that will be delivered to the grid.

The DC microgrid presents a DC-bus with a regulated voltage. The AC loads in the car park require a DC/AC converter. The other DC loads besides the FCEVs, could be connected directly to the DC bus or may need a DC/DC converter, depending on the bus voltage. Generally speaking, DC mini-grids tend to be simpler in system architecture and operation than AC systems. This is primarily a result of their limited requirements in terms of power control and management. A DC grid can increase in the end-to-end-efficiency between 17 and 25% with 380 V DC transmission and DC loads [145, 146]. A positive side effect is that it would result in lower electricity costs for the aggregator and fast charging possibilities for BEVs.

The development and production costs for customised DC components are however still higher than AC technology due to the lower level of development of the concept. The total costs of the network are however, strongly related to the connected elements. For example DC grids lead to lower installation costs in locations that tend to have more DC loads [147]. For a car park, this would be an interesting advantage as most components that are located in the car park are DC loads.

F.4. Requirements for data communication

For the delivery of aFRR special requirements are set by TenneT regarding data communication and monitoring. To be able to guarantee the security, velocity and reliability of the communication system an end-to-end connection is required. For the BSP that are currently delivering frequency reserves, this connection has been installed in the time of SEP. For new entries, this connection would be a large investment.

A remote terminal unit (RTU) at the location of the data collection point of the aggregator must be installed and connected with the RTU at a substation of TenneT. The substations of TenneT are spread over the whole country and depending on the location of the CPPP and the distance from a substation, the investment costs will diversity. The substations are shown on the map in Appendix J.

The substations represent the information transfer point (IOP[2]). This is the physical point were information is transferred. The BSP is responsible for the data transfer between its own system and the IOP. TenneT takes over the responsibility from the IOP until the TSOs EMS. Each party bears its own expenses for the realisation and maintenance of the agreed information exchange. It is even required to have a redundant communication connection to limit the risk of interruptions to the signal transfer due to failures or maintenance. One connection is active and one serves as backup. The setpoints are sent via the active connection. The passive connection is scanned by the EMS of TenneT to check whether the connection is still working correctly.

Data exchange between the BSP and TenneT is required for the real-time control of aFRR and the monitoring of the control performance afterwards.The safety requirements for this connection are so high because of the direct connection with the EMS of TenneT. The EMS monitors the electricity production and demand of the whole country, calculates the ACE and sends setpoints to the relevant parties. If data connections fail, wrong calculations will be done, risking the stability of the power system.

This system data exchange mechanism is currently reevaluated by TenneT as it is an old and maybe outdated system. The investment costs for new entries are expected to be too high to enter in the

[2]IOP: Informatie Overdrachts Punt

market for frequency reserves. A pilot is being done with blockchain to evaluate if this mechanism of exchanging data satisfies the safety, velocity and reliability requirements of TenneT. In the near future other pilots with other data exchange mechanisms will be tested. It is still highly uncertain what the data communication mechanism will be in a few year. This makes it impossible to estimate what the requirements will be around mid century.

It is, however, certain that a trade off is being made between the safety, velocity and reliability requirements and the investment costs and technical feasibility for the BSP. TenneT has the ambition to open the reserves market for more participants and the data communication requirements is one of the barriers that need to be reduced.

G

Distribution of the delta-setpoints

To evaluate if the CPPP is competitive on the market for aFRR, the amount of activated aFRR was analysed. TenneT must be able to activate a maximum of 340 MW aFRR but most of the time the activated amount is much smaller than this maximum. The aFRR is activated based on the bid order. The lowest bids, are activated first. This implies that if the marginal costs of the CPPP are not on the lowest part of the bid ladder, the reserves will not be activated.

Figure G.1 shows the cumulative probability of the total amount of activated bids per ISP. It can be seen that only a few moments per year the total amount of aFRR is activated. Circa 90% of the time the activated amount is 100 MW. This implies that the bid of the CPPP should belong to the lowest 30% to be activated.

These findings were decisive to implement check if the marginal costs of the CPPP are lower or equal to the price of aFRR as that determines if the reserves are activated or not. This check results into more realistic findings about the financial potential of the CPPP. If the bid order wasn't considered the revenues of the CPPP would have been too high compared to a realistic scenario.

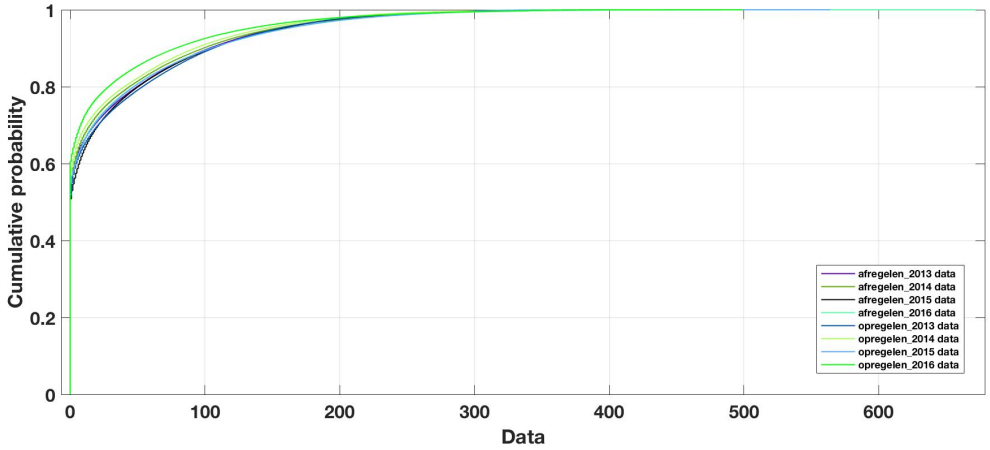

Figure G.1: Cumulative probability of the amount of activated aFRR per ISP.

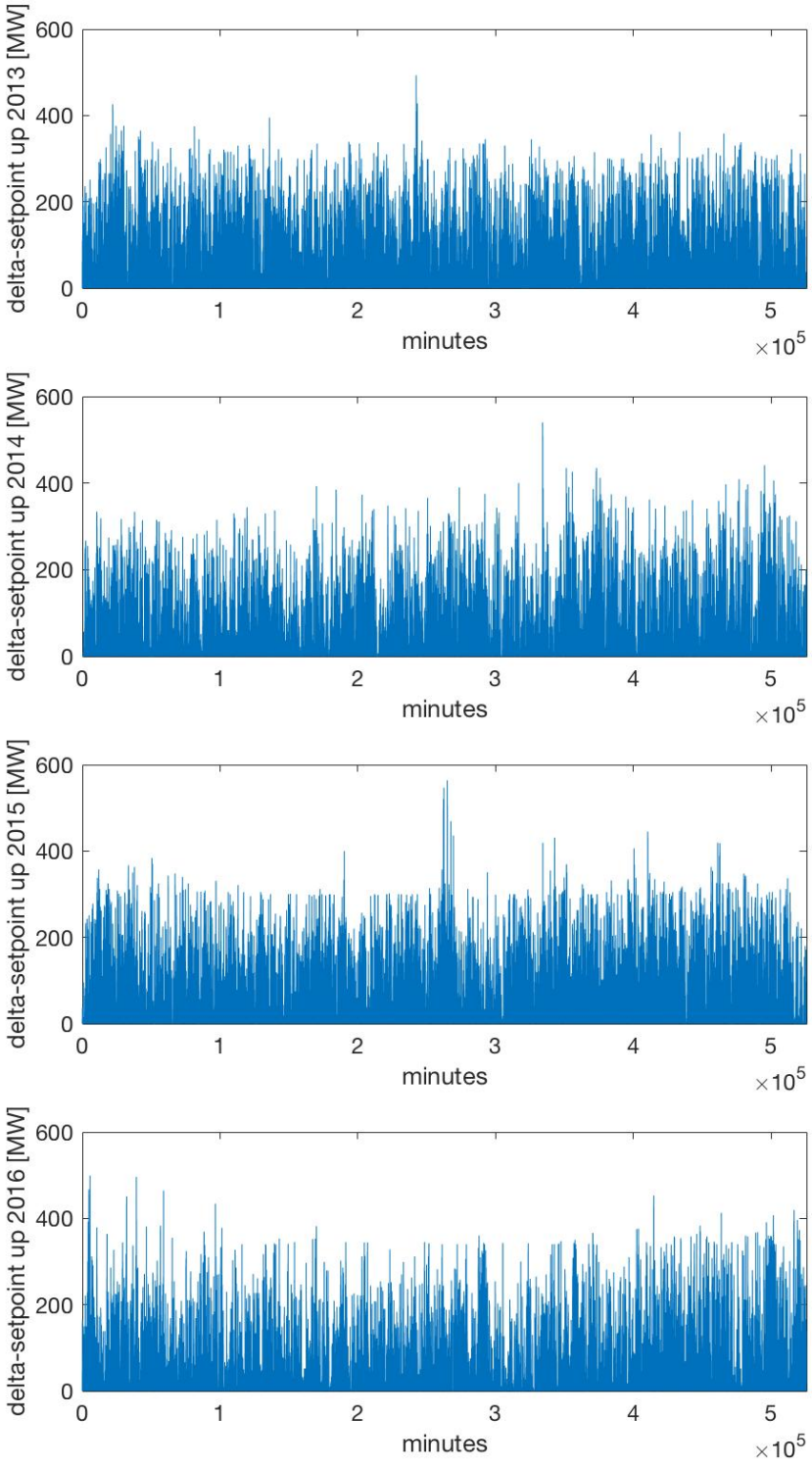

Figure G.2: Cumulative delta-setpoints per ISP for aFRR up measured each minute for 2013-2016.

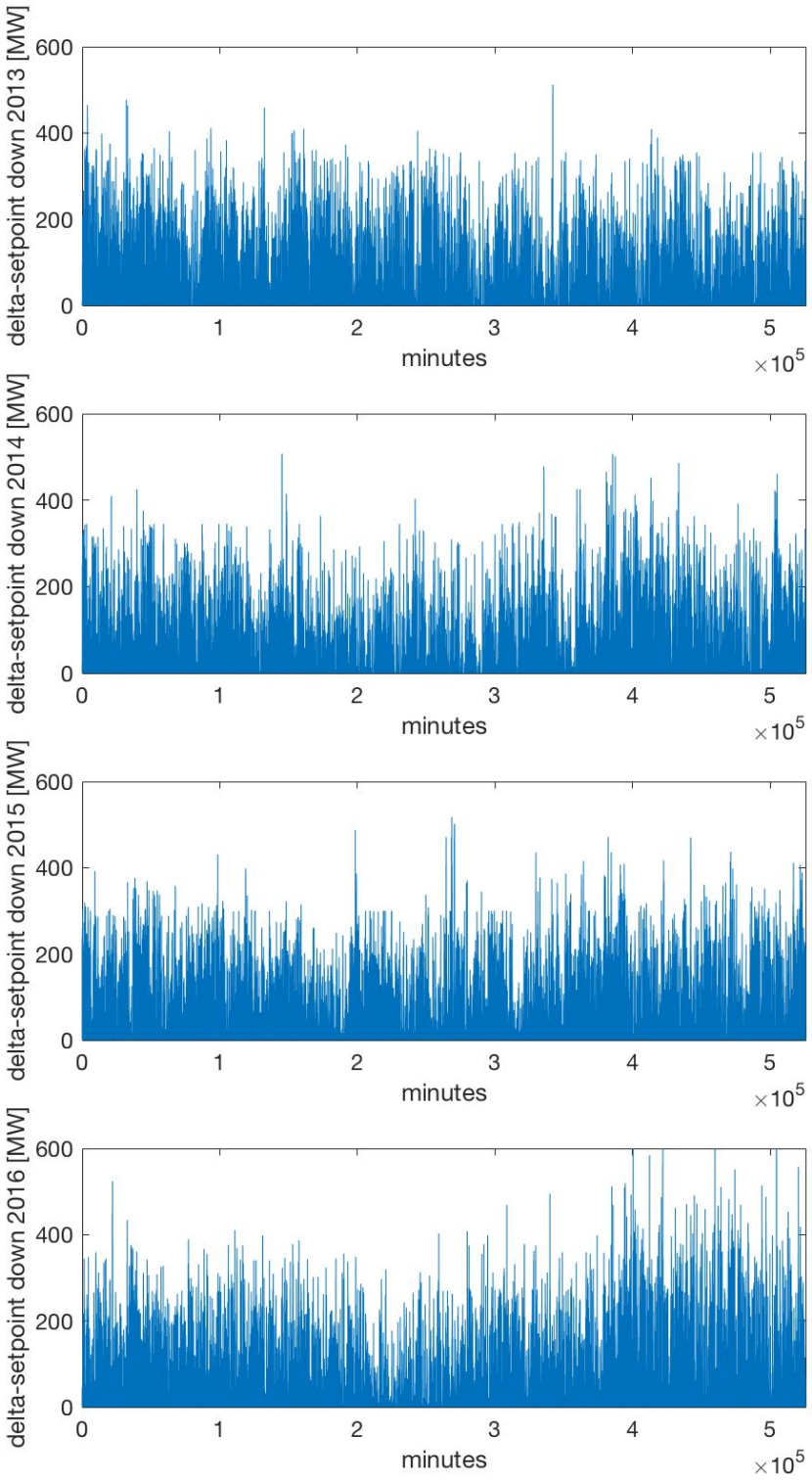

Figure G.3: Cumulative delta-setpoints per ISP for aFRR down measured each minute for 2013-2016.

H

Marginal costs of the CPPP

The bid price of a power plant is assumed equal to the marginal costs. In the CPPP the total marginal costs are assumed as the sum of the costs of the required hydrogen and the degradation costs to produce one kWh of electricity. During the analysis with the financial model two cases for the marginal costs of the CPPP are considered which represent a worst case and a best case based on the expected hydrogen price and the efficiency of the CPPP system. The lowest and highest price for hydrogen are expected to be respectively equal to 1 and 3.52 euro. This is broadly explained in Section 5.5.1.

In the worst case for the marginal costs of the CPPP the highest price for hydrogen and an efficiency of 40% is assumed. This efficiency is based on the current efficiency of a FCEV operating between 1 and 10 kW in V2G mode [77]. This results in a price of 0.2232 euro per kWh for the required hydrogen per kWh electricity produced.

The best case for marginal costs assumes an efficiency of 50% and a hydrogen price of 1 euro per kilogram, which is a slightly lower price than the current price of reformed hydrogen from natural gas sold on an industrial scale [101][102][103]. This is assumed the best case for a potential hydrogen price when ignoring the production method of hydrogen. Ideally the CPPP would use renewable hydrogen which is hydrogen made with renewable energies. In this research it is assumed that in the future the cost of renewable hydrogen will be the same as the current cost of reformed hydrogen. The best case for the hydrogen costs is 0.0507 euro per kWh of electricity produced. Both cases are based on the HHV of hydrogen which is equal to 39.41 kWh/kg.

The degradation costs per kWh are calculated by dividing the investment costs of the FC system per kW by the lifetime of the FC in driving mode and multiplying that value times 0.5 to correct the value for degradation of the vehicle in balancing mode which has a lower degradation level with respect to driving mode. This results in a value of 0.0017 euro per kWh.

The sum of the price for hydrogen and the costs of degradation constitute the marginal costs of the CPPP. The best and worst case are respectively 0.0524 and 0.226 euro per kWh electricity and will be used during the analysis with the financial model.

Table H.1: Overview of the used variables to calculate the marginal costs

	Hydrogen price [euro/kg]	Efficieny [%]	Degradation costs [euro/kWh]	Total marginal costs [euro/kWh]
Worst case	1	40	0.0017	0.226
Best case	3.52	50	0.0017	0.0524

Proportional controller for FCR

Frequency containment control is achieved by a joint action of FCR providing units within the whole synchronous area with respect to the frequency deviation. FCR is locally activated and the BSP needs to measure the frequency deviation itself without any input from the TSO. Generally, it is achieved using droop controllers, so that governors operating in parallel can share the load variation according to their rated power. The droop of the generator represents the ratio of frequency deviation to change in power output.

For the CPPP to deliver FCR the droop needs to be determined. The droop is a value expressed in percentage that indicates the deviation of the nominal frequency value for which the power delivering unit goes from 0 to 100% power output. This relation is determined according to Equation I.1. The nominal value of the power ($Pnom$) is the maximum power output of the installation. For the CPPP this changes every ISP and is equal to the maximum V2G power output multiplied with the available amount of vehicles in that ISP. The nominal frequency ($Fnom$) is equal to 50 Hz. The ΔF and ΔP are respectively the maximum steady-state frequency deviation equal to 200 mHz and the maximum amount of FCR that the unit offers. Also this factor changes for every ISP as the maximum amount FCR depends on the baseload, which is a degree of freedom and changes every ISP.

$$\%\, droop = \left(\frac{\Delta F}{Fnom} \cdot \frac{Pnom}{\Delta P}\right) \tag{I.1}$$

By expressing the droop in Hz, Equation I.2 can be written to relate the deviation of the frequency to the additional power (P_{FCR}) that needs to be delivered by the unit. This relation is called the characteristic of the power delivering unit.

$$dP = P_{FCR} = \frac{dF \cdot Pnom}{Hz\, droop} \tag{I.2}$$

The smaller the droop, the more sensitive the power reacts to frequency deviations, which can be seen in Figure I.1. The impact of changing the baseload is shown in Figure I.2. Depending on the baseload and the nominal power for each ISP, a new droop is calculated.

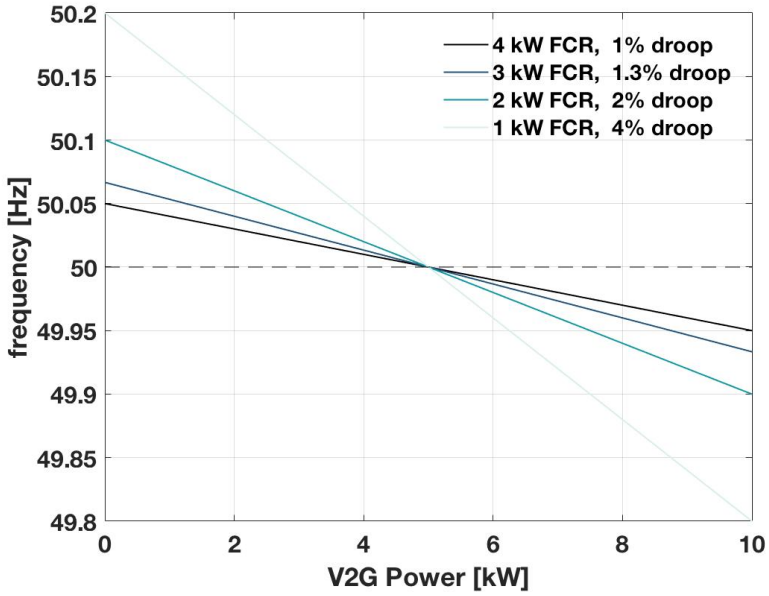

Figure I.1: Characteristics for fixed baseload of 5 kW with different amount available for FCR and thus different droop settings.

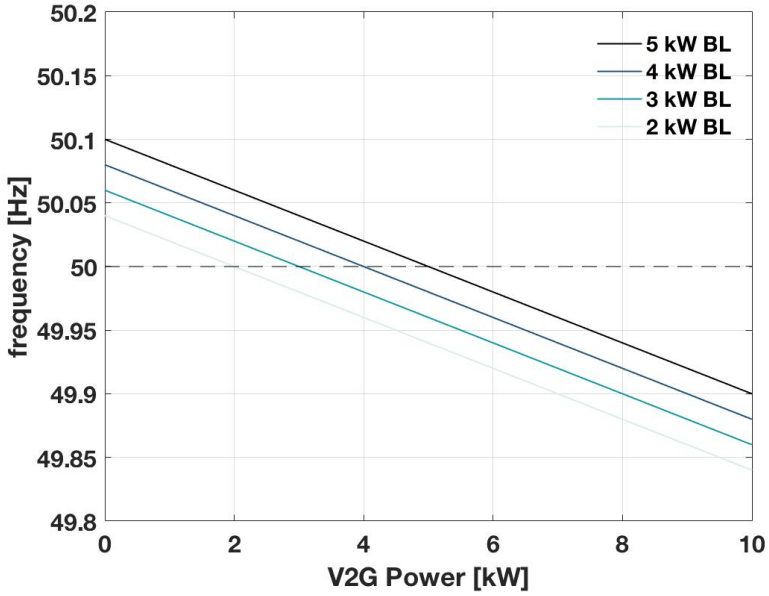

Figure I.2: Characteristics of a FCEV for variable baseloads and a droop of 2%.

In Figure I.3 the characteristic of one FCEV with a baseload of 5 kW and a droop of 4 % is shown. For a frequency deviation 0.1 Hz the power of the FCEV will have to shift from 5 kW to circa 2.5 kW. The FCR contribution will be 2.5 kW downwards. For each ISP the FCR contribution of the whole CPPP is calculated based on the FCR that can be offered and the maximum V2G power output of the aggregation.

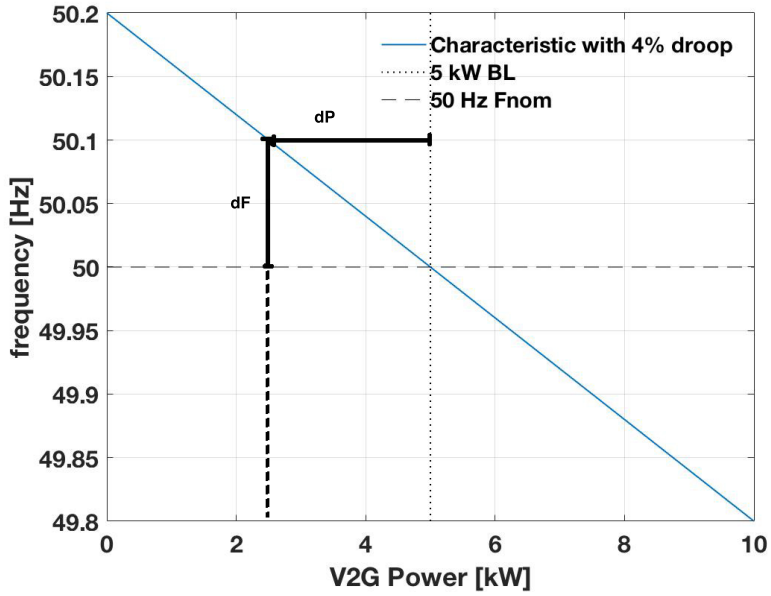

Figure I.3: Characteristic with indication of operating point for frequency deviation of 0.1 Hz

J

Substations of TenneT

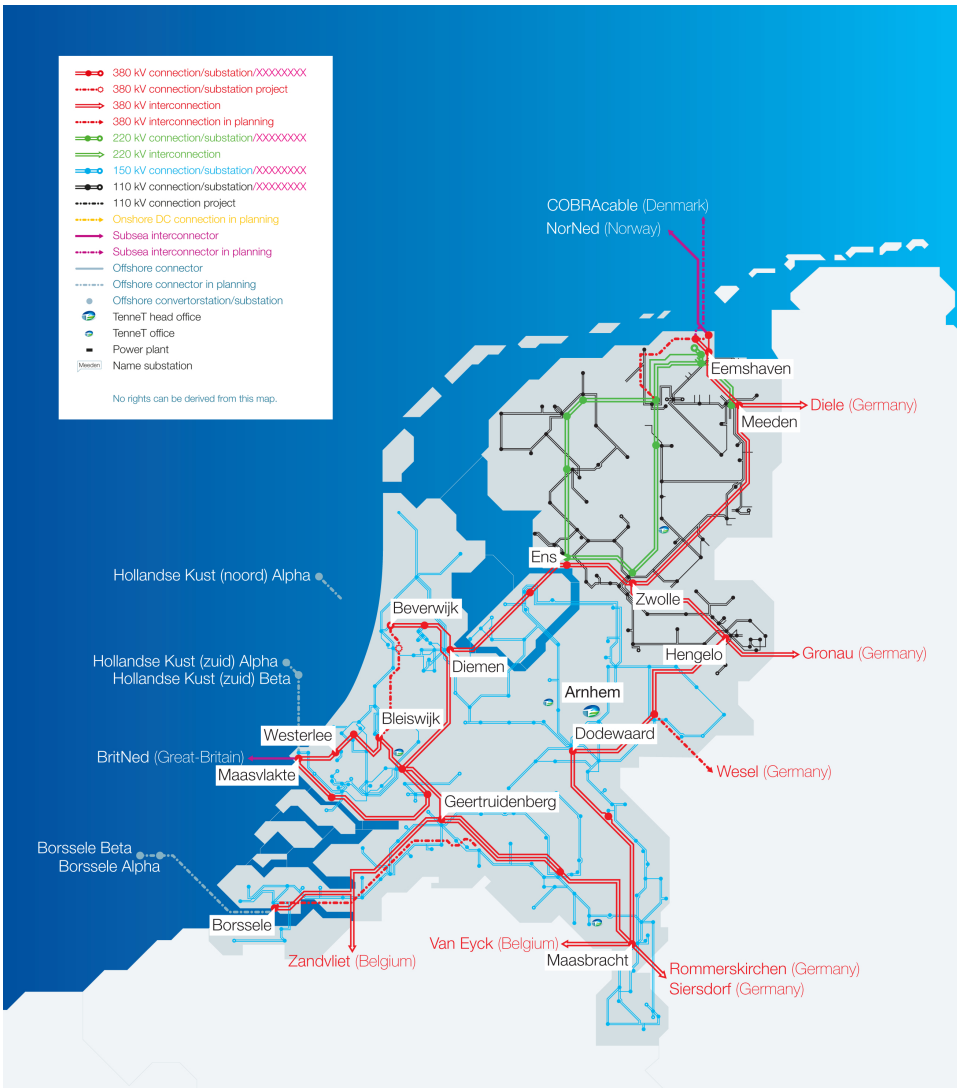

Figure J.1: Indication of the network and the substations of TenneT.